Mechanisms of presynaptic release and postsynaptic development in cortical neurons

by

Oliver Prange

Dipl. Biol., Christian Albrechts Universität Kiel, Germany, 1995

A THESIS SUBMITTED IN PARTIAL FULFILMENT OF THE REQUIREMENTS

FOR THE DEGREE OF

DOCTOR OF PHILOSOPHY

THE FACULTY OF GRADUATE STUDIES

(Department of Psychiatry; Faculty of Medicine; Neuroscience Program)

(Graduate Program in Neuroscience)

We accept this thesis as conforming to the required standard

THE UNIVERSITY OF BRITISH COLUMBIA

MAY 2001

In presenting this thesis in partial fulfilment of the requirements for an advanced degree at the University of British Columbia, I agree that the Library shall make it freely available for reference and study. I further agree that permission for extensive copying of this thesis for scholarly purposes may be granted by the head of my department or by his or her representatives. It is understood that copying or publication of this thesis for financial gain shall not be allowed without my written permission.

Department of PSYCHIATRY

The University of British Columbia
Vancouver, Canada

Date Aug. 8th, 2001

DE-6 (2/88)

ABSTRACT

Electrophysiology and imaging techniques have been applied to study presynaptic vesicle release and postsynaptic development *in vitro* at cortical synapses. The amphiphilic dye FM1-43 was used to evaluate vesicle turnover at synaptic terminals in response to action potential (AP) stimulus evoked- and spontaneous miniature synaptic activity. Loading and unloading of FM1-43 into and out of synaptic vesicles was visualized in real-time using laser scanning confocal microscopy. Under conditions that maximized release probability at synapses, we found that the amounts of AP-evoked vesicular FM1-43 release could not be described by a normal distribution, but were positively skewed. A significant, albeit relatively small, fraction of all synapses (13 - 17 %) released FM1-43 amounts that could be attributed to the release of more than one vesicle per AP stimulus. When utilizing miniature synaptic activity for FM1-43 uptake, we found a large variability in the amount of FM1-43 loading among presynaptic terminals, indicating a non-uniform probability for miniature release among synapses. Imaging of AP-stimulated vesicle release showed that release rates were significantly elevated at synapses with high rates of miniature activity compared to control synapses. In addition, we found a significant correlation between miniature activity and AP-evoked release probability at single synaptic sites. Lastly, real-time confocal imaging of filopodial postsynaptic spine precursors was employed in cortical neurons during two stages of early *in vitro* development. Particle mediated gene transfer was used to overexpress a green fluorescent protein (GFP)-labeled form of the postsynaptic density protein PSD-95, which can mediate the clustering of postsynaptic receptors and signal transduction proteins. Neurons overexpressing PSD-95/GFP were additionally labeled with the red dye sulforhodamine and two-channel confocal data acquisition was used. We found that preformed PSD-95 clusters could be rapidly translocated into and out of filopodia and spines. Moreover, filopodia and spines that were associated with clusters of PSD-95 were significantly more stable (i.e. less likely to turn-over) during 1 hour of imaging than filopodia and spines without PSD-95 clusters. In summary, these findings suggest the occurrence of multivesicular release at cortical synapses, indicate a physiological association between spontaneous miniature and evoked synaptic release, and implicate PSD-95 in the stabilization of filopodial spines during early development of cortical neurons.

TABLE OF CONTENTS

TABLE OF FIGURES

ABBREVIATIONS

2-Amino-5-Phosphono-Valeric Acid (D,L-APV)

6-Cyano-7-Nitroquinoxaline-2,3-Dione (CNQX)

Acetylcholine (ACh)

Action potential (AP)

Brain-derived neurotrophic factor (BDNF)

Calcium/calmodulin dependent protein kinase II (CamKII)

cAMP response element (CRE)

cAMP response element-binding protein (CREB)

cAMP-dependent protein kinase A (PKA)

Coefficient of variation (CV)

Diaglycerol (DAG)

Excitatory postsynaptic current (EPSC)

Green fluorescent protein (GFP)

Guanine nucleotide exchange factor (GEF)

Guanylate kinase associated protein (GKAP)

Hours (h)

Long-term depression (LTD)

Long-term potentiation (LTP)

Mitogen activated protein kinase (MAPK)

Milliosmol (mosm)

Millisecond (ms)

N-ethylmaleimide-sensitive fusion protein (NSF)

Neuromuscular junction (NMJ)

Nitric oxide synthase (NOS)

Paired pulse facilitation (PPF)

Paired pulse modulation (PPM)

PDZ (PSD-95, ZO1/2, Disklarge)

Plasma membrane (PM)

Postsynaptic density (PSD)

Protein kinase C (PKC)

Receptor tyrosine kinase (RTK)

Release probability ($P_{rel.}$)

Rho-associated kinase (ROCK)

Seconds (sec)

Short-term synaptic enhancement (STE)

SNAP receptor (SNARE)

Soluble NSF attachment protein (SNAP)

Standard deviation (SD)

Standard error of the mean (SEM)

Synaptic protein interaction (Synprint)

Synaptophysin (SynPh)

Tetrodotoxin (TTX)

ACKNOWLEDGEMENTS

My thanks go to Dr. Timothy H. Murphy for his excellent supervision during my years in the laboratory. Furthermore, I would like to thank Dr. Kerry R. Delaney, Dr. Timothy P. O'Connor, and Dr. Steven R. Vincent of my supervisory committee for always helpful and reasonable suggestions. Of many helpful co-students and lab-mates I want to give special thanks to Dr. Paul J. Mackenzie and to Dr. Carolyn Isbister with whom I shared a significant portion of my graduate student years and who helped me with advice and a lasting friendship. Furthermore, Dr. Sabrina Wang was very helpful in many experiments and cell culture procedures. Lastly, I deeply want to thank my friends and family for their continuing support.

During my dissertation I was supported by grants from the following institutions:

Deutscher Akademischer Austauschdienst

Heinrich-Hertz Stiftung des Landes Nordrhein-Westfalen

Theodore E. Arnold Fellowship

University Graduate Fellowship (UBC)

Vancouver Foundation

I. INTRODUCTION

CENTURY OF THE SYNAPSE

The concept of the synapse started to emerge in the last two decades of the 19th century pioneered by the work of anatomist Santiago Ramón y Cajal and physiologist Charles Sherrington (review in Shepherd and Erulkar, 1997). Cajal - and his many un-named coworkers - used a just newly developed staining technique by Camillo Golgi ("Golgi-impregnation") to anatomically characterize the architecture of the cerebellum, cortex, and neuromuscular junction (NMJ). Cajal documented sub-cellular specializations (Raymon y Cajal, 1888) that would later be unambiguously identified as synapses. In doing so he provided the first evidence to disprove the "reticular" theory of the nervous system (NS) - ironically developed by Golgi -, stating that the NS is a capillary network of syncitial nerve cells (Golgi, 1873). Only a few years later Charles Sherrington, studying spinal reflexes, introduced the term "synapse". He concluded that nerve cells are not continuous but "*[...] merely in contact [...]*" with one another by special connections, and proposed "*[...] such a special connection [...] might be called a synapse*" (Sherrington, 1897).

Examining the effect of adrenalin on the NMJ, in 1904 Thomas Elliott formulated, for the first time, a theory of chemical synaptic transmission. He suggested "*[...] the chemical excitant* (adrenalin) *[...] may cause the change of tension of the muscle fiber [...] in response to its union with the synapsing sympathetic fiber [...]*" (Ellitot, 1904). It took almost another half century until Bernard Katz and Paul Fatt introduced intracellular electrophysiological recording methods to the NMJ. Using this approach they found that changes in the resting potential of the muscle end plate membrane could be induced by stimulation of the corresponding presynaptic nerve terminals, and that it was acetylcholine (Ach) which acted to depolarize the postsynaptic membrane (Fatt and Katz, 1950). In another groundbreaking study Fatt and Katz showed that spontaneously occurring so-called "miniature" endplate potentials (EPPs) were of the same amplitude as the smallest EPPs evoked by presynaptic stimulation (Fatt and Katz, 1952). Moreover, they found that the amplitude of larger EPPs was an integer multiple of this initial "quantal" (unitary) size

(Fatt and Katz, 1952). The hypothesis of "quantal synaptic transmission" was born. Soon, electron microscopic evidence would emerge that revealed highly intricate and feature-rich pre- and postsynaptic structures, and most relevantly, a homogenous population of small, densely packed vesicles at the presynaptic membrane (Palay, 1956). These vesicles - if evenly filled with a neurotransmitter - could provide the anatomical basis for the discretely quantal postsynaptic potentials (Fatt and Katz, 1952).

We now, indeed, know that the presynaptic vesicles hold neurotransmitter, that they undergo a continuous cycle of transmitter release and re-filling (review in Betz and Angleson, 1998), and that a highly complex machinery of structural and signal transducing proteins controls every step of this process (review in Brunger, 2001). Moreover, we have begun to uncover the molecular components and pathways that are involved in initializing, building and maintaining the pre- and postsynaptic elements during development and maturation of the nervous system (review in Scannevin and Huganir, 2000; Brunger, 2001). In **Chapter II** and **III** of this thesis I will present an experimental approach to directly visualize release and uptake of synaptic vesicles in presynaptic terminals using the amphiphilic dye FM1-43 (Betz et al., 1992) which provides a tool for measuring activity-dependent vesicle turnover. In **Chapter IV** I have used a green-fluorescent protein (GFP) labeled form of the postsynaptic density (PSD) protein PSD-95 and time-lapse confocal microscopy during early development of cortical neurons to study the potential role of PSD-95 in formation and maturation of synaptic contacts.

THE SYNAPSE AND LEARNING

Soon after the discovery of chemical synaptic transmission it was hypothesized that the computational power of the brain may be encoded in the regulation of synaptic function and synaptic connectivity itself. Cortical leisoning studies in animals, pioneered by Karl Lashley (Lashley, 1929), showed that the magnitude of the memory impairment was dependent on the total size of the lesion, rather than the specific area where the lesion had been applied, indicating that memory storage was distributed throughout larger cortical areas, rather than linked to specific regions (Milner et al., 1998). This data, as well as emerging evidence for recurrent connections in the cortex, led Donald Hebb 1949 to postulate a set of fundamental

rules necessary and sufficient to acquire and store information in the brain. In his classical book "The Organization of Behavior" Hebb hypothesized that information is not stored in neurons themselves, but rather in the spatio-temporal activity pattern of groups ("assemblies") of neurons (Hebb, 1949). Most importantly, he reasoned that learning and forgetting could be encoded in the strengthening and weakening, respectively, of synaptic contacts within these neuronal circuits. He originally stated that *"When an axon of cell A is near enough to excite cell B and repeatedly or persistently takes part in firing it, some growth process or metabolic change takes place in one or both cells such that A's efficiency, as one of the cells firing B, is increased"* (Hebb, 1949). Additionally, he suggested that unused synaptic connection would weaken, and eventually decay. Most commonly, Hebb's statements have been interpreted that coincident activity in the pre- and postsynaptic neuron will strengthen a synaptic connection while asynchronous activity will weaken it (Goodman and Shatz, 1993; Sejnowski, 1999; Tsien, 2000). Hebb's theory delivered a model for information storage in the brain, which, in its simplicity, was not only powerful, but also experimentally well testable. The rapid progress in cell stimulation and recording techniques (Hamill et al., 1981) as well as in neuropharmacology (Olney et al., 1981) since the 1980's has enabled neuroscientists to examine Hebb's prediction by independently manipulating pre- and postsynaptic activity (Harris et al., 1984; Herron et al., 1985; Herron et al., 1986; Morris et al., 1986; Thomson, 1986; Wigstrom and Gustafsson, 1986). Furthermore, improved imaging techniques (Helmchen et al., 1999; Mainen et al., 1999a) now allow study of coincident pre- and postsynaptic activity on the level of single synapses in intact brain tissue (Yuste et al., 1999; Wang et al., 2000).

As it turned out, Hebb's postulate stood the test of time: coincident pre- and postsynaptic activity is a fundamental requirement for eliciting long-lasting changes in synaptic efficacy (review in Tsien, 2000). The most prominent long-lasting form of synaptic plasticity is called long-term potentiation (LTP). Since first described by Bliss and Lomo in 1973 (Bliss and Lomo, 1973), LTP still represents the best candidate for a physiological mechanism underlying learning & memory formation (review in Stevens, 1998; Malenka and Nicoll, 1999; McGaugh, 2000; Thompson, 2000; Tsien, 2000).

SYNAPTIC PLASTICITY: SHORT- TO LONG-LASTING

As a nerve impulse in the form of an AP advances through a series of neuronal connections, it undergoes a repeated translation from an electrical into a chemical signal at chemical synapses. Since the process of synaptic transmission can be highly regulated, this mechanism of signal propagation provides a powerful means to alter the nerve impulse along its cellular pathway. As originally described for the NMJ (Eccles et al., 1941) a constant electrical stimulus at the presynaptic nerve can result in a variable amplitude of the induced postsynaptic current, indicating that synaptic transmission is not constant, but variable or plastic. (The quantal nature of this "amplitude-stepping" suggested a pre-synaptic locus of the variance). Ever since this original finding, the number of reported forms of synaptic plasticity has grown extensively (review in Stevens and Sullivan, 1998a); synaptic plasticity is generally categorized by the locus of its expression, pre- and/or postsynaptic, and by the longevity of the phenomenon, short- or long-lasting.

More remarkable than the original and somewhat paradoxical observation that the ratio of presynaptic input to postsynaptic output could vary in a seemingly unpredictable way was the discovery that certain physiological manipulations could alter the behavior of synaptic transmission predictably, and reproducibly.

Short-term plasticity

Eccles, Katz, and Kuffler showed for the toad NMJ that when applying two presynaptic stimuli within a short interval (< 50ms), the postsynaptic amplitude response to the second pulse applied would by greater than that to the first pulse (Eccles et al., 1941). Additionally, longer-lasting (> 10 s), high frequency (10 Hz) train stimulation of the presynaptic fiber would significantly elevate the postsynaptic response to subsequently applied stimuli for up to 10 min (Eccles et al., 1941). These forms of short-term synaptic enhancement (STE) have since been repeated in many vertebrate systems, including mammals (review in Fisher et al., 1997). From shorter- to longer lasting phenomena they have been termed paired pulse facilitation (PPF, lasting < 100 ms), augmentation (Aug; lasting < 10 s), and post-tetanic potentiation (PTP, lasting < 15 min). All forms of STE found so far are presynaptic mechanisms, and linearly related to $[Ca^{2+}]_i$ (review in Fisher et al., 1997). Most evidence suggests that

STE is mediated by accumulation of $[Ca^{2+}]_i$ acting either on local microdomains of $[Ca^{2+}]_i$ near the vesicle release site (for PPF) (Katz and Miledi, 1968; Delaney and Tank, 1994), or (for Aug, PTP) on secondary targets away from the release site (Fisher et al., 1997; Tang and Zucker, 1997; Zucker, 1999). For either category, the direct (PPF) or indirect (Aug, PTP) consequence of this $[Ca^{2+}]_i$ accumulation is an enhancement in the probability of neurotransmitter release, and therefore in the reliability of synaptic transmission (Stevens and Wesseling, 1999a; Zucker, 1999).

As simultaneous activity in the postsynaptic neuron is not required for either the induction, or for the expression of STE, this form of synaptic plasticity is often categorized as "non-Hebbian". However, STE may play an important role in tuning synaptic network properties and ensuring reliable information propagation (Lisman, 1997). In addition, STE can be effectively exploited experimentally to evaluate and manipulate release probability at synapses. In **Chapter II** of this thesis I have used a PPF protocol as a means to classify synaptic populations with regard to their release probabilities.

Long-term plasticity

As originally suggested by Hebb, the induction of most forms of long-lasting synaptic changes requires a coinciding activity of the pre- and postsynaptic neuron. The most widely studied cellular forms of long-term plasticity are long-term potentiation (LTP) (review in Stevens and Sullivan, 1998a; Malenka and Nicoll, 1999; Paulsen and Sejnowski, 2000) and, somewhat in its shadow, long-term depression (LTD) (review in Bear and Malenka, 1994; Daniel et al., 1998; Bear, 1999). There is compelling evidence that at least certain forms of LTP (review in Stevens, 1998; Malenka and Nicoll, 1999; Martin et al., 2000; McGaugh, 2000; Tsien, 2000) and LTD (review in Daniel et al., 1998; Bear, 1999; Martin et al., 2000) are cellular correlates necessary (Tsien, 2000; Hansel et al., 2001) and/or sufficient (Stevens, 1998; Jones et al., 2001) for learning and memory formation. Standard protocols to experimentally elicit these synaptic modifications are, for LTP, a short lasting (0.5 - 1 sec) high-frequency (50 - 100 Hz) synaptic stimulus, and for LTD, a longer lasting (6 - 10 min) lower frequency (1 - 2 Hz) synaptic stimulus (Bear and Malenka, 1994; Connor et al., 1999). These stimulus protocols lead in the postsynaptic compartment to a brief and high elevation in $[Ca^{2+}]_i$ (> 540 nM) for LTP, and to a longer lasting lower elevation in

$[Ca^{2+}]_i$ (180 - 500 nM) for LTD (Ngezahayo et al., 2000; Cormier et al., 2001). Consequently, both forms of plasticity can also reliably be induced by manipulation, such as photolytic uncaging of postsynaptic $[Ca^{2+}]_i$ (Yang et al., 1999). The $[Ca^{2+}]_i$ elevation will trigger the activation of differential sets of kinases and/or phosphatases as well as the activation of nuclear transcription factors (see below), depending on the magnitude and longevity of the $[Ca^{2+}]_i$ signal (Bear and Malenka, 1994; Soderling and Derkach, 2000). The physiological consequence of the LTP and LTD inducing stimulus protocols is a long-lasting (up to days) increase (for LTP) or decrease (for LTD) in the postsynaptic response amplitude to a presynaptic stimulus (Bear and Malenka, 1994; Malenka and Nicoll, 1999). In addition to experimentally induced LTP and LTD, both forms of plasticity have also been shown to occur in freely moving animals associated with learning behavior (Skelton et al., 1987; Garcia et al., 1993; Mitsuno et al., 1994; Xu et al., 1998; Manahan-Vaughan and Braunewell, 1999; Froc et al., 2000; Frey et al., 2001).

As proposed by Hebb, a sensor for coincident pre- and postsynaptic activity is necessary to induce most forms of long-lasting synaptic changes. For both, LTP and LTD, the N-methyl-D-aspartate (NMDA) glutamate receptor serves as the coincidence detector (Herron et al., 1986; Morris et al., 1986; Wigstrom and Gustafsson, 1986; review in Tsien, 2000). When open, the NMDA receptor channel is permeable to calcium ions which upon entering into the cytoplasm can trigger diverse second messenger responses, ultimately leading to synaptic strengthening (Heemskerk et al., 1987; Connor et al., 1988; Kauer et al., 1988; Malinow et al., 1988; review in Soderling and Derkach, 2000). However, the NMDA channel will conduct ions only if presynaptically released glutamate is bound to it and its channel pore blocking Mg^{2+} ions are simultaneously removed by coincident postsynaptic depolarization (Mayer et al., 1984; Nowak et al., 1984). Thus, another important proposal of Hebb has been realized in the NMDA receptor properties: pre- and postsynaptic activity has to be temporally precisely coordinated; paired stimulation of connected neurons can lead to either LTP or LTD in connecting synapses depending on small differences in the temporal relationship of pre- to postsynaptic activation (review in Paulsen and Sejnowski, 2000; Bi and Poo, 2001). The essential role of the NMDA receptor in mediating synaptic plasticity through the controlled entry of Ca^{2+} into the cell has been impressively documented using transgenic animal models; genetic impairment of

NMDA receptor function or downstream targets of Ca^{2+} influx dramatically decreases LTP expression, and corollary learning performance (review in Tsien, 2000). Conversely, overexpression of a more Ca^{2+} permeable NMDA receptor sub-unit (NR2B) in forebrains of mice leads to a significant enhancement in both, LTP expression and learning task performance (Tang et al., 1999).

Even though there is evidence that presynaptic changes can occur during the expression and maintenance of long-lasting synaptic plasticity (Stevens and Wang, 1994; Ryan et al., 1996) more attention has recently been drawn to LTP- and LTD-associated changes on the postsynaptic site (review in Malinow, 1998; Malenka and Nicoll, 1999; Malinow et al., 2000). In the initial phase of LTP expression, $[Ca^{2+}]_i$ mediated activation of the of protein kinases results in phosphorylation of AMPA type glutamate receptors and subsequent enhancement of postsynaptic conductivity (i.e. AMPA response amplitude) (review in Soderling and Derkach, 2000). Specifically, after LTP induction the calcium/calmodulin dependent protein kinase II (CamKII) has been shown *in situ* to phosphorylate the AMPA subunit GluR1 on residue Ser^{831} and resulting in a subsequent enhancement of the single channel conductivity (Derkach et al., 1999; review in Soderling and Derkach, 2000). These findings make CaMKII the foremost candidate in directly mediating early LTP. In addition, very recent data shows that rapid insertion and extrusion of AMPA receptors into and out of postsynaptic membranes significantly contributes to changes in synaptic conductance after the induction of long-term plasticity (Malinow et al., 2000; Lu et al., 2001). The modulation of AMPA receptor properties and distribution can last for 1 - 3 hours, but eventually cease. Longer lasting changes associated with LTP rely on gene-transcription, which is triggered by Ca^{2+} influx trough NMDA receptors during the LTP inducing stimulus (review in Mayford and Kandel, 1999). Rapidly elevated $[Ca^{2+}]_i$ will activate protein kinase pathways including the cyclic AMP (cAMP) dependent protein kinase (PKA) (review in Mayford and Kandel, 1999; Walton et al., 1999) and the mitogen activated protein kinase (MAPK) (Davis et al., 2000) pathways which converge onto a nuclear signaling mechanism that leads to the phosphorylation of a family of transcription factors called cAMP response element-binding protein (CREB). CREB phosphorylation leads to the activation of CRE (cAMP Responsive Element) and the transcription of a set of immediate early genes (IEGs) of which the identified ones also represent transcription factors (Bartsch et al., 2000; Hardingham et al., 2001; Jones et

al., 2001). Importantly, expression of long-lasting LTP and memory in the hippocampus has been shown to be dependent on CREB activation (review in Mayford and Kandel, 1999; Walton et al., 1999) and expression of the IEG Zif286 - a zinc-finger transcription factor (Jones et al., 2001). Furthermore, transgenic mice overexpressing CREB in the basolateral amygdala (BLA) display an enhanced learning response in a BLA-dependent fear-conditioning paradigm (Josselyn et al., 2001).

What the ultimate protein-expression mediated synaptic modifications are is still unknown. These may involve a lasting upregulation of AMPA receptor presence and/or subtype composition in potentiated synapses (Malinow et al., 2000). Insertion of AMPA receptor into formerly AMPA-lacking (so-called "silent") synapses furthermore provides an explanation for the LTP-associated elevation in "release probability" (Atwood and Wojtowicz, 1999; Malenka and Nicoll, 1999) which, even though postsynaptically measured, had long been interpreted as an indication for a presynaptic locus of LTP expression (Malgaroli and Tsien, 1992; Leahy et al., 1993; Stevens and Wang, 1994; Tong et al., 1996; Li et al., 1998). Finally, a considerable body of evidence from ultrastructural (review in Geinisman, 2000; Muller et al., 2000), biochemical (Benson et al., 2000), and real-time imaging studies (Engert and Bonhoeffer, 1999; Maletic-Savatic et al., 1999; Jontes and Smith, 2000; Lendvai et al., 2000; Thompson, 2000; review in Segal, 2001) suggests that structural changes in existing and/or induction of new synaptic connections are associated with strong synaptic stimulation (Engert and Bonhoeffer, 1999; Maletic-Savatic et al., 1999; Toni et al., 1999) and learning behavior (Lendvai et al., 2000; Thompson, 2000).

VESICULAR NEUROTRANSMITTER RELEASE

Vesicle transport and vesicle-plasma membrane interaction, including vesicle docking, priming and fusion, are common process shared among all eukaryotic cells (review in Burger and Schaefer, 1998). Vesicular release of neurotransmitter is no exception. However, at sites of fast synaptic transmission these processes are tightly controlled to suit the need for rapid and regulated transmitter release (review in Bajjalieh, 1999; Lin and Scheller, 2000; Sudhof, 2000; Brunger, 2001; Morgan et al., 2001; Sun and Wu, 2001). The last step in the life-cycle of a transmitter vesicle, its fusion with the plasma membrane (PM) and the concurrent release of neurotransmitter into the synaptic cleft, is usually triggered by a rapid elevation in $[Ca^{2+}]_i$ from a resting

concentration of ~ 100 nM to several hundred μM (review in Delaney, 2000). These high levels of $[Ca^{2+}]_i$ are only being reached in microdomains around the channel mouth of N- and P/Q- type voltage gated calcium channels (VGCCs) which are an integral part of the presynaptic release site (also called the active zone). Opening of VGCCs is usually triggered rapidly - within < 200 μs (Sabatini and Regehr, 1999) - by APs invading the presynaptic terminal. The extremely short delay between the AP and vesicle release is facilitated by co-localization (within tens of nanometers) of VGCCs and vesicles docked at release sites (Roberts et al., 1990). This co-localization is achieved by binding of the α1B subunit of N-type calcium channels to the SNARE (SNAP-receptor; SNAP: soluble NSF-attachment factor; see below) proteins syntaxin and SNAP-25 through a synaptic protein interaction (synprint) site (review in Catterall, 1999).

Even though many of the proteins involved in synaptic vesicle trafficking and release have been identified (review in Brunger, 2001), the exact chronology of molecular interactions between synaptic Ca^{2+} entry and vesicular release has not yet been fully understood. The minimal protein machinery necessary for vesicle fusion is comprised of two target proteins located at the PM, syntaxin and SNAP-25, as well as the vesicle associated membrane protein VAMP (review in Burger and Schaefer, 1998; Brunger, 2001). These SNARE proteins can form thermodynamically stable complexes with coiled coils structures, reminiscent of the ones found within single viral fusion proteins, called SNAREpins. Formation of the SNAREpin is thought to provide energy for the membrane fusion between the vesicle and the PM (review in Burger and Schaefer, 1998), a step that does not require hydrolysis of ATP or GTP. In addition to this minimal release machinery there is a steadily growing number of proteins which are either directly involved in the release process - e.g. synapsin and synaptotagmin -, or in vesicle targeting and tethering - such as the sec6/8 complex and rab GTPases (review in Bajjalieh, 1999).

Before a vesicle can be released it requires "docking" at the active zone. In this irreversible step, SNARE proteins mediate tethering of vesicles to the PM at the release site (review in Bajjalieh, 1999; Lin and Scheller, 2000; Xia et al., 2001). At hippocampal synapses the size of the anatomically "docked" vesicle pool has been estimated using electron microscopy (EM) (Schikorski and Stevens, 1997; Schikorski and Stevens, 2001); interestingly, it closely matches the size of the so-called "readily

releasable pool" of vesicles (~ 10) as defined by electrophysiological approaches (Dobrunz and Stevens, 1997; Schikorski and Stevens, 2001). Once a vesicle is docked at its release sites it requires a "priming" step to make it release-ready. Although still poorly understood, it is known that priming involves modification of the SNARE protein complex by NSF (N-ethylmaleimide-sensitive fusion protein - the first release machinery protein identified), ATP-dependent synthesis of phosphoinositides, and consecutive activation of the proteins Munc13-1 and protein kinase C (PKC) by diaglycerol (DAG) (review in Burger and Schaefer, 1998; Bajjalieh, 1999; Brunger, 2001). Finally, the identity of the Ca^{2+} sensor in the release process seems to have been revealed by recent studies, showing that the vesicular protein synaptotagmin is essential for release (Desai et al., 2000; Littleton et al., 2001) and that a synaptotagmin mutation, altering its Ca^{2+} binding capacity, will influence the probability of transmitter release (Fernandez-Chacon et al., 2001). In addition, vesicle release can be modified in a Ca^{2+}-independent manner through voltage-dependent modifications of the SNARE complex (Mochida et al., 1998), further evidenced by a direct interaction of synaptotagmin and the voltage-gated sodium channels (Sampo et al., 2000).

Although transmitter release usually requires synaptic calcium influx triggered by APs, there is also AP-independent release. As first described by Fatt and Katz (Fatt and Katz, 1950) for the NMJ (see above) so called miniature synaptic activity, triggered by spontaneous release of transmitter quanta, is also apparent in the CNS. The nature as well as the possible function of this phenomenon is still unclear. However, recent findings suggest a role for miniature activity in the developmental establishment (Ali et al., 2000; Collin et al., 2001) and maintenance (McKinney et al., 1999) of synaptic connections. Furthermore, miniature activity may contribute to the continuance of enhanced synaptic efficacy after the induction of long-lasting synaptic plasticity (Kombian et al., 2000; Emptage et al., 2001). There are conflicting reports on the role that Ca^{2+} plays in this process which, taken together, indicate that Ca^{2+} acts indirectly through activation of second messenger systems, but does not directly trigger miniature release (see **DISCUSSION** in **CHAPTER III**). In **CHAPTER III**, I will present an experimental approach to evaluate the relationship between spontaneous miniature and AP-dependent vesicle release at single presynaptic terminals using real-time imaging of these events.

Common to all forms of vesicular transmitter release is that plasma membrane material has to be reclaimed to produce vesicles and help replenish the constantly cycling vesicular pool (Betz and Angleson, 1998; Murthy and Stevens, 1998; Sudhof, 2000). Most important in this process are the molecules clathrin and its adapter proteins which form a coat around the budding vesicle, and dynamin, which actively pinches off membrane material from the PM (review in Slepnev and De Camilli, 2000). Vesicles retrieved this way will shed their clathrin coat, be refilled with neurotransmitter, and transported back into the pool of releasable vesicles. During recycling, the vesicle does not necessarily fuse with the endosomal network, which can accelerate the process considerably (Murthy and Stevens, 1998; Lin and Scheller, 2000). At fast synapses, the steps involved in vesicle recycling require more time - in the order of minutes; (Stevens and Tsujimoto, 1995; Stevens and Wesseling, 1999b) - than the release - in the millisecond range (Stevens and Tsujimoto, 1995; Schneggenburger and Neher, 2000; Beutner et al., 2001) - and the refilling - approximately 10 sec (Stevens and Tsujimoto, 1995) - of the readily releasable vesicle pool. Hence, during times of ongoing synaptic stimulation the releasable vesicle pool can be depleted and the ability of the synapse to release transmitter will be governed by the time constraints of vesicle synthesis, transport, and filling (Stevens and Wesseling, 1999b). Modification of these rate-limiting steps associated with exocytosis and endocytosis thus represent additional forms of presynaptic plasticity.

DEVELOPMENT AND ORGANIZATION OF POSTSYNAPTIC SPINES

During the early stages of CNS development, the elaboration of dendritic arbors and of axonal projections is responsible for establishing functional neuronal connectivity. An important step in this process is the proper molecular assembly of pre- and postsynaptic compartments, and their spatio-temporal regulation (O'Brien et al., 1997; Ahmari et al., 2000; Friedman et al., 2000; Garner et al., 2000; review in Scannevin and Huganir, 2000; Sorra and Harris, 2000; Zhang and Benson, 2000). In order for intercellular contact formation to occur, mechanisms of signaling and target recognition must be established between the developing pre- and postsynaptic elements. Initial mutual recognition may be facilitated by the differential distribution of cell adhesion molecules (CAMs) between axons (e.g. BIG-1, TAG-1/axonin-1) and dendrites (e.g. telencephalin) (review in Zhang and Benson, 2000). In addition, other

cell adhesion molecules, such as integrins, neuroligins/neurexins, and cadherins (review in Benson et al., 2000) may act at various stages during synaptogenesis to promote structural synaptic interaction and to modify the local adhesive environment (Zhang and Benson, 2000). In particular, recent findings show that the expression of the postsynaptically localized transmembrane protein neuroligin can induce formation and structural organization - such as synaptic vesicle development - of presynaptic terminals *in vitro* (Scheiffele et al., 2000). This effect is mediated by binding of neuroligin to its presynaptic *pendant* β-neurexin. In their respective synaptic compartments the cytoplasmic tails of these adhesion molecules are linked via the PDZ (PSD-95, ZO1/2, Disklarge) domain-containing proteins PSD-95, postsynaptically, and CASK, presynaptically, to complex signaling machineries (Scannevin and Huganir, 2000). It is conceivable that the neuroligin-neurexin interaction can thereby activate effectors (such as CaMKII and Munc-18) to induce synaptic organization and maturation (Cantallops and Cline, 2000). Furthermore, interaction via adhesion molecules may promote local presynaptic clustering of signaling molecules like ephrin, and consecutively activate postsynaptically localized Eph receptors, a receptor tyrosine kinase (RTK). Importantly, during early synaptogenesis, ephrin B stimulation induces a direct interaction of EphB with the NMDA receptor and regulates the number of synapses formed *in vitro* (Dalva et al., 2000; review in Drescher, 2000). Hence, analogous to the induction of postsynaptic acetylcholine (ACh) receptor clustering by presynaptic release of agrin during development of the NMJ, Eph signaling may present the earliest form of instructive chemical communication at central synapses. Most interestingly, it has clearly been demonstrated that neither AP-mediated (Craig et al., 1994; Benson and Cohen, 1996) nor spontaneous (Verhage et al., 2000) release of neurotransmitter is required for synaptogenesis or synaptic targeting.

In order for any interaction between the developing pre- and postsynapse to occur, both elements have to be in relatively close proximity to each other. It is now widely believed that this process is facilitated by the active movement of filopodia, mobile protrusions extending and retracting from dendrites of developing neurons (review in Jontes and Smith, 2000; Parnass et al., 2000; Rao and Craig, 2000; Segal, 2001). Using time-lapse imaging of fluorescently labeled dendrites, it has been established that the lifetime of filopodia during early CNS development *in vitro* (Dailey and Smith, 1996; Ziv and Smith, 1996) and *in vivo* (Lendvai et al., 2000) can be short

(in the order of minutes), and that morphological changes can be rapid (several µm per minute) (Dailey and Smith, 1996; Ziv and Smith, 1996; Dunaevsky et al., 1999; Wong and Wong, 2001). Moreover, with progressing development, the number and motility of filopodia significantly decreases, while, in parallel, spines with mature characteristics emerge and render dendritic branches. This developmental chronology has prompted the formulation of a model in which filopodia serve as functional precursors of spines by establishing contact to presynaptic terminals (review in Jontes and Smith, 2000; Parnass et al., 2000; Rao and Craig, 2000; Wong and Wong, 2000; Segal, 2001). The initial proposal of this model (Ziv and Smith, 1996) has recently been substantially supported by real-time imaging evidence that the induction of functional presynapses can be initiated within 30 min. after an axodendritic contact had been made by a filopodium or spine (Friedman et al., 2000). Moreover, EM analysis shows that filopopdial structures can contact mature presynaptic terminals (Fiala et al., 1998).

Filopodial movement is mediated by a continuous assembly and disassembly of the actin-rich filopodial cytomatrix (Fischer et al., 1998; Dunaevsky et al., 1999; Halpain, 2000; Matus et al., 2000; Rao and Craig, 2000; review in Smart and Halpain, 2000). Importantly, this process can be regulated by activation of glutamate receptors (Fischer et al., 2000), and stimuli that lead to the expression of long-lasting synaptic plasticity can induce growth of new and/or modification of existing filopodia and/or spines in an NMDA receptor dependent fashion (Engert and Bonhoeffer, 1999; Maletic-Savatic et al., 1999; Toni et al., 1999). How the receptor stimulation is linked to actin based plasticity is not yet understood; however, it is known that the small GTPases Rho, Rac, and Cdc42 regulate actin-dependent dendritic growth and that NMDA dependent Ca^{2+} influx can activate these effectors by stimulating the guanine nucleotide exchange factor (GEF) (Nakayama and Luo, 2000; Cline, 2001; Redmond and Ghosh, 2001). Downstream targets of activated GTPases include the Rho-associated kinase (ROCK) and the kinases PAK1 and PAK2, which may modify cytoskeletal arrangements (Nakayama and Luo, 2000; Cline, 2001; Redmond and Ghosh, 2001).

As the pre- and postsynaptic contact can lead to a rapid formation of functional synaptic junctions (Friedman et al., 2000), evenly fast mechanisms for setting up the complex protein machineries (Garner et al., 2000; Scannevin and

Huganir, 2000; Brunger, 2001) in both synaptic compartments have to be established. Interestingly, for the presynaptic side, the existence of such a mechanism has been indicated by recent findings showing that multi-protein complexes (pre-formed active zones) are shuttled to developing synaptic terminals (Ahmari et al., 2000). Whether an analogous mechanism exists for the postsynaptic side remains to be shown. It is possible that developing filopodia carry a minimal signal transduction machinery at all times. This machinery may translate contact formation with a presynaptic partner (see above) into a signal for localizing additional components, necessary to form functional postsynaptic sites, into these structures. Hence, presynaptic maturation (Friedman et al., 2000) and axo-dendritic contact may be paralleled by a postsynaptic stabilization (possibly through cell adhesion molecules) and maturation from filopodium to spine.

Mature postsynaptic spines possess complex protein machineries comprised of glutamate receptors, cytoskeletal proteins (e.g. actin, tubulin, and accessory proteins), and signal transduction molecules, concentrated at the postsynaptic density (PSD) (Hata and Takai, 1999; Garner et al., 2000; Scannevin and Huganir, 2000). In the PSD, PSD-95 interacts with many proteins such as NMDA receptors, neuroligin, nitric oxide synthase (NOS), and citron through its PDZ, guanylate kinase (GK), and SH_3 domains. It has been proposed that PSD-95 facilitates NMDA receptor clustering and tethers the postsynaptic signal transduction machinery close to NMDA mediated Ca^{2+} entry (Garner et al., 2000; Scannevin and Huganir, 2000). Furthermore, through its binding to citron, a Rho effector, as well as to MAP1A and CRIPT, both microtubule associated proteins (review in Hata and Takai, 1999), PSD-95 may be important for the structural integrity of developing and mature spines. Hence, to assess the localization of PSD-95 in developing dendrites and its relationship to the dynamic movement of filopodia, in **Chapter IV** I will present a series of experiments using time-lapse confocal imaging to monitor both, filopodial structure and PSD-95 transport.

II. ANALYSIS OF MULTIQUANTAL TRANSMITTER RELEASE FROM SINGLE CORTICAL NEURON TERMINALS

ABSTRACT

Single synapse recording methods have indicated that the amplitude of postsynaptic responses of single CNS synapses can vary greatly between repeated stimuli. To determine whether this observation could be attributed to synaptic terminals releasing a variable number of transmitter quanta, we have assessed the prevalence of multiquantal transmitter release in primary cultures of cortical neurons using the action potential (AP) dependent presynaptic turnover of the styryl dye FM1-43 (Betz and Bewick, 1992; Betz and Bewick, 1993; Betz et al., 1996). It was assumed that if a high proportion of vesicles within a synaptic terminal were loaded with FM1-43, the amount of dye released per stimulus would be proportional to the number of quanta released and/or the probability of release at a terminal. To rule out differences in the amount of release (between synapses) due to release probability or incomplete loading of terminals, conditions were chosen to maximize both release probability and terminal loading. 3-D reconstruction of FM1-43 loaded synaptic terminals was employed to ensure that terminal fluorescence was accurately measured. Analysis of the relationship between the loading of terminals and release indicated that presumed larger terminals (> FM1-43 uptake) release a greater amount of dye per stimulus than smaller terminals, suggesting multiquantal release. The distribution of release amounts across terminals was significantly skewed towards higher values, with 13 - 17 % of synaptic terminals apparently releasing multiple quanta per AP. In conclusion, our data suggest that most synaptic terminals release a relatively constant amount of transmitter per stimulus, however a subset of terminals release amounts of FM1-43 that are greater than that expected from a unimodal release process.

INTRODUCTION

The action potential (AP) dependent uptake and release of the styryl dye FM1-43 has been used to evaluate the behavior of single CNS synaptic terminals (Ryan and Smith, 1995; Ryan et al., 1996; Murthy et al., 1997; Murthy and Stevens, 1998) and neuromuscular junction endplates (Betz and Bewick, 1992; Betz et al., 1992). These studies have exploited the ability of released synaptic vesicles to recycle (Heuser and Reese, 1973) and be loaded with dye. Rigorous control studies by the Betz laboratory have established that FM1-43 is localized to synaptic vesicles and that its turnover correlates well with more direct capacitance measurements of release (Henkel et al., 1996; Smith and Betz, 1996). Use of FM1-43 in CNS studies indicates that the rate of dye release from loaded terminals is a reliable indicator of synaptic strength (Ryan et al., 1996; Isaacson and Hille, 1997; Murthy et al., 1997). Furthermore, application of FM1-43 uptake and release to CNS neurons has been used to provide data for statistical analyses of transmitter release (Murthy et al., 1997; Ryan et al., 1997; Murthy and Stevens, 1998). These studies suggest a multimodal release process in CNS neurons in which individual quantal peaks can be identified in data from FM1-43 labeling of vesicles. It has been argued that these peaks reflect single vesicle release events. One assumption made in the study by Murthy et al. (Murthy et al., 1997; Murthy and Stevens, 1998) was that CNS terminals release at the most one vesicle per AP stimulus. Therefore, if terminals were restricted to releasing a single vesicle apparent differences in the amount of FM1-43 turnover between terminals would reflect release probability (Murthy et al., 1997; Murthy and Stevens, 1998). We have extended these studies and further tested these assumptions in primary cultures of cortical neurons by using conditions under which maximal loading of terminals was achieved, where release probability was high, and where analysis procedures were used to assure that terminal fluorescence was accurately measured. Our results indicate that multiquantal release occurs, yet is restricted to a small but potentially significant fraction of cultured cortical neuron synapses (< 20 %).

METHODS

Embryonic cortical neurons and glial cells (from day 18 rat fetuses) were grown 3-4 weeks *in vitro* on poly-D-lysine coated glass coverslips before use in imaging experiments. Coverslips were cut into two pieces, placed into a customized perfusion chamber (~500 µl vol.), and fixed by platinum weights to prevent drifting. Continuous perfusion was supplied by a Hanks balanced saline solution (HBSS) medium containing (in mM) 137 NaCl, 5.0 KCl, 0.34 $Na_2HPO_4(7H_2O)$, 10.0 Na^+-HEPES buffer, 1.0 $NaHCO_3$, and 22.0 glucose at pH 7.4 and ~ 315 mosm. $CaCl_2$ and $MgSO_4$ were altered as indicated. To stimulate activity dependent synaptic uptake (loading) and release (unloading) of FM1-43, constant current stimulation (30 mA) was delivered via two platinum electrodes fixed on opposite sides of the perfusion chamber (distance ~8 mm). This field stimulation reliably induced AP generation in single neurons (see Fig. 1). All experiments were conducted at room temperature (~ 23°C).

Terminal loading was achieved by application of 1200 stimuli at 10 Hz in the presence of 10 µM FM1-43; $CaCl_2$ and $MgSO_4$ were supplemented at 2.5 mM and 1.0 mM, respectively. We expected that this number of stimuli would result in complete loading of vesicle pools, as FM1-43 experiments (Liu and Tsien, 1995; Murthy et al., 1997) and ultrastructural analysis (Harris and Sultan, 1995) estimate that, on average, cortical synapses contain less than 500 synaptic vesicles. During AP evoked FM1-43 loading, synaptic activity was blocked using a cocktail of glutamate receptor blockers 6-cyano-7-nitroquinoxaline-2,3-dione (CNQX; 3 µM) and 2-amino-5-phosphono-valeric acid (D,L-APV; 60 µM). The time of FM1-43 exposure coinciding with AP trains was ~2 min. and continued for 60 s after the last AP to allow for completion of endocytosis (Ryan and Smith, 1995). After terminal loading, the preparation was washed for 15 min.. The washing medium was $CaCl_2$-free and contained 5 mM $MgSO_4$ to minimize synaptic FM1-43 release attributed to spontaneous action potentials and miniature synaptic activity. Terminal unloading was performed in a medium expected to result in maximal release probability (5 mM $CaCl_2$ and 1 mM $MgSO_4$). CNQX (3 µM) and APV (60 µM) were also supplemented to block recurrent synaptic stimulation.

Confocal imaging with a Bio-Rad MRC 600 system attached to a Zeiss upright (Axioskop) microscope with an Olympus 0.9 NA 60X water immersion objective was

used for all experiments. Laser intensity was attenuated to 1 % and the confocal pinhole was set to 3.5 (Bio-Rad units). To improve signal-to-noise properties, the slow scan mode (without averaging) was used. Corrections in image intensity were made for field inhomogeneity (signal attenuation on edges) associated with high NA objectives by dividing data sets by a control image (carboxyfluorescein solution).

For data acquisition a field of 128*128 μm (400*400 pixels) was scanned every 3 s during baseline and periods of AP trains (see Fig. 3). Imaging during the first 45 s (baseline) was used to calculate signal-to-noise properties at each synapse and was followed by a continuous 1 Hz field stimulation (21 s) to determine synaptic FM1-43 unloading responses. After this first train stimulus, a second baseline without stimulation (30 s) was established to allow reloading of the readily releasable pool of vesicles. Finally, a second 1 Hz train (21 s) consisting of either 21 paired (10 ms interpulse interval; n = 18 experiments) or unpaired stimuli (n = 4 experiments) was applied and presynaptic FM1-43 fluorescence intensity was monitored. This acquisition was followed by a 10 Hz stimulus train (120 s) to determine the total amount of FM1-43 fluorescence that was releasable by APs (Fig. 3 B). A (vertical) Z-series of 13 consecutive confocal images (spaced at 0.54 μm) over the area of interest was acquired for each experiment utilizing a computer controlled focus motor. Each terminal's fluorescence intensity in the focal plane was corrected based on its relative position within the confocal Z-section (Fig. 2). Additionally, terminals contaminated by signals from stained structures above or below their focal plane were eliminated from further analysis (e.g. Fig. 2 terminal #2 and #3).

Confocal images were exported as byte arrays by removal of data headers and analyzed using custom routines written with the IDL (Research Systems Inc., Boulder, CO) programming language. For each experiment, 300 putative synaptic terminals were analyzed and fluorescence changes over time were averaged over ~ 3.7 μm^2 at each site. Non-releasable FM1-43 fluorescence (defined as background fluorescence remaining after the 1200 pulse stimulus train) was subtracted at each terminal before further analyses were performed. FM1-43 release in response to AP-inducing field stimulation was averaged over the 21 s stimulus train (7 images), and an automated response criterion was used to select responsive from non-responsive putative terminals (Fig. 3 A). To be considered for further analysis, terminals had to meet the following criteria: 1) the decrease in FM1-43 fluorescence in response to two 1 Hz

trains of stimulation had to be greater than 2.5*the standard deviation (SD) of the baseline fluorescence (Fig. 2; Fig. 3 A) the baseline variation (SD) had to be less than 10 % of the terminal's total releasable fluorescence. For experiments in which the effect of changes in $[Ca^{2+}]_o$ on paired pulse modulation (PPM) were examined, the first selection criterion was modified (the decrease in FM1-43 fluorescence in response to the paired 1 Hz train stimulation alone had to be greater than 2.5*the SD of the baseline fluorescence). This more strict criterion was used to counteract effects of low $[Ca^{2+}]_o$ on the signal-to-noise properties of FM1-43 release values due to low release probability and to more accurately measure PPM by avoiding selection of terminals exhibiting high release during both stimulus trains.

To determine the degree of PPM at each terminal, the relative FM1-43 release (normalized to baseline period 2) during the second (paired) stimulus train was divided by the relative FM1-43 release (normalized to baseline period 1) during the first (unpaired) stimulus train (Fig. 3 A & B; Fig. 4 B). Analysis was restricted to terminals with PPM values between 0 and 10 (98 % of all sites). For control experiments, both stimulus trains consisted of unpaired stimuli (Fig. 4 A), and the FM1-43 release ratio was calculated accordingly (relative FM1-43 release during second/first stimulus train).

Whole cell current clamp experiments (Hamill et al., 1981) were conducted using an Axon Instruments Axopatch 200B amplifier and 7 Mohm electrodes pulled from 1.5 mm glass capillaries. The patch pipettes were filled with a solution containing (in mM): 0.05-0.3 mM fluo-3 K^+ salt, 122 K^+MeSO_4, 20 NaCl, 5 Mg-ATP, 0.3 GTP, and 10 HEPES (pH = 7.2); in some cases EDTA was substituted for fluo-3 as a Ca^{2+} buffer.

For statistical testing of normality, the Kolmogorov-Smirnov test was used. Non-parametric tests were applied for comparisons of medians (Mann-Whitney test). For correlation analysis, the non-parametric Spearman test was used over the Pearson test when it resulted in a better fit to a linear model. One-way analysis of variance (ANOVA) was used to confirm that data acquired in different experiments could be pooled.

RESULTS

Activity dependent turnover of the synaptic vesicle probe FM1-43 was used in primary cultures of cortical neurons to estimate the number of transmitter quanta released from a single terminal in response to AP stimulation. To ensure that FM1-43 terminal loading and release were accurately measured, several control experiments were performed. Using whole cell current clamp recordings it was established that electric field stimulation (1 ms; 30 mA) reliably resulted in single APs (n = 8 cells; data not shown). Paired field stimuli (10 ms interpulse interval; 5 mM Ca^{2+}, 1 mM Mg^{2+}) applied every 1 s for up to 50 s also reliably induced AP pairs (Fig. 1 A; n = 4 cells). Additionally, high frequency trains of APs (up to 600 APs at 10 Hz) were reliably delivered without failure of APs (Fig. 1 B; n = 4 cells). Thus, whole cell current clamp records suggest that the number of field stimuli applied are indicative of the number of APs produced. For studies in which field stimuli were employed, a stimulus intensity of ~ 50 % above threshold was used to ensure that most terminals were responsive. This threshold was established three ways, direct measurement of the relationship between FM1-43 release and field voltage, current clamp recordings, and the use of fluo-3 loaded cultures (data not shown) as described by others (Ryan and Smith, 1995).

The goal of our experiments was to quantitate the amount of FM1-43 released from terminals to determine if single or multiple vesicles were released per AP. Stained terminals could potentially be out of focus and were also subject to signal contamination from neighboring terminals or other stained structures. Therefore, we corrected each terminal's fluorescence intensity based on its relative position within the vertical (Z-) axis of the specimen (Fig. 2; see Methods) and excluded terminals contaminated by signals from stained structures above or below their focal plane (e.g. Fig. 2 terminal #2 and #3). To establish whether presumed terminals generated a significant FM1-43 unloading response during field stimulation, automated software procedures were used that selected responsive terminals based on their individual signal-to-noise properties (Fig. 3 A; see Methods). FM1-43 fluorescence that could not be released during a 10 Hz field stimulation train (1200 APs; Fig. 3 B) was subtracted at each site to ensure that fluorescence values obtained accurately represent a pool of releasable synaptic vesicles (Ryan and Smith, 1995; Murthy et al., 1997). Analysis of

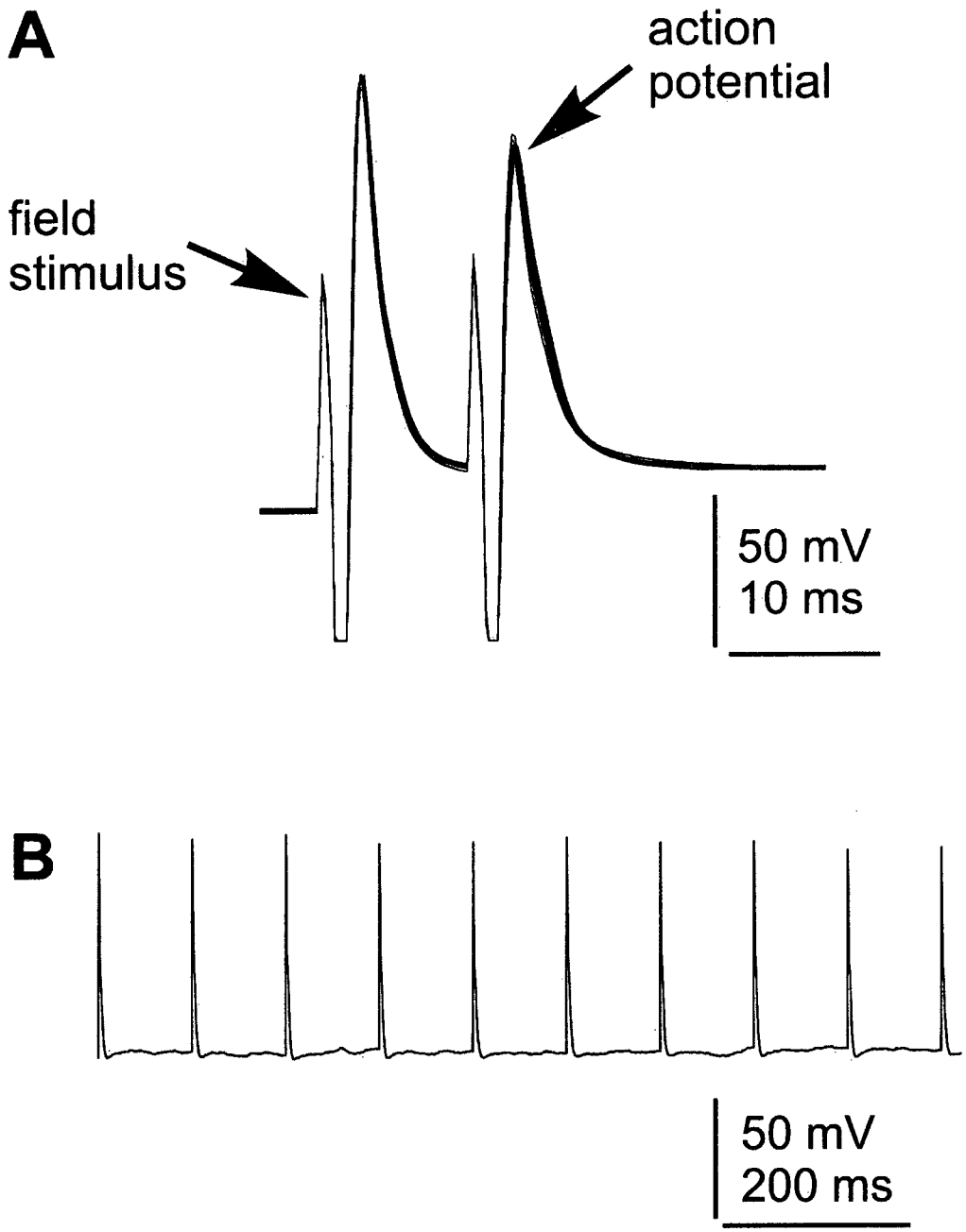

Fig. 1 Electric field stimulation results in reliable action potential generation

Recordings were made using whole cell current clamp under conditions used for FM1-43 loading and unloading (3 μM CNQX; 60 μM D,L-APV). **A)** Paired APs were induced by 1 ms field pulses applied at 10 ms interpulse interval in 5 mM $[Ca^{2+}]_o$ and 1 mM $[Mg^{2+}]_o$; 40 trials are superimposed. **B)** An example of a neuron following 10 Hz field stimulation with single APs in 2.5 mM $[Ca^{2+}]_o$ and 1 mM $[Mg^{2+}]_o$; the stimulus artifacts have been removed from the trace.

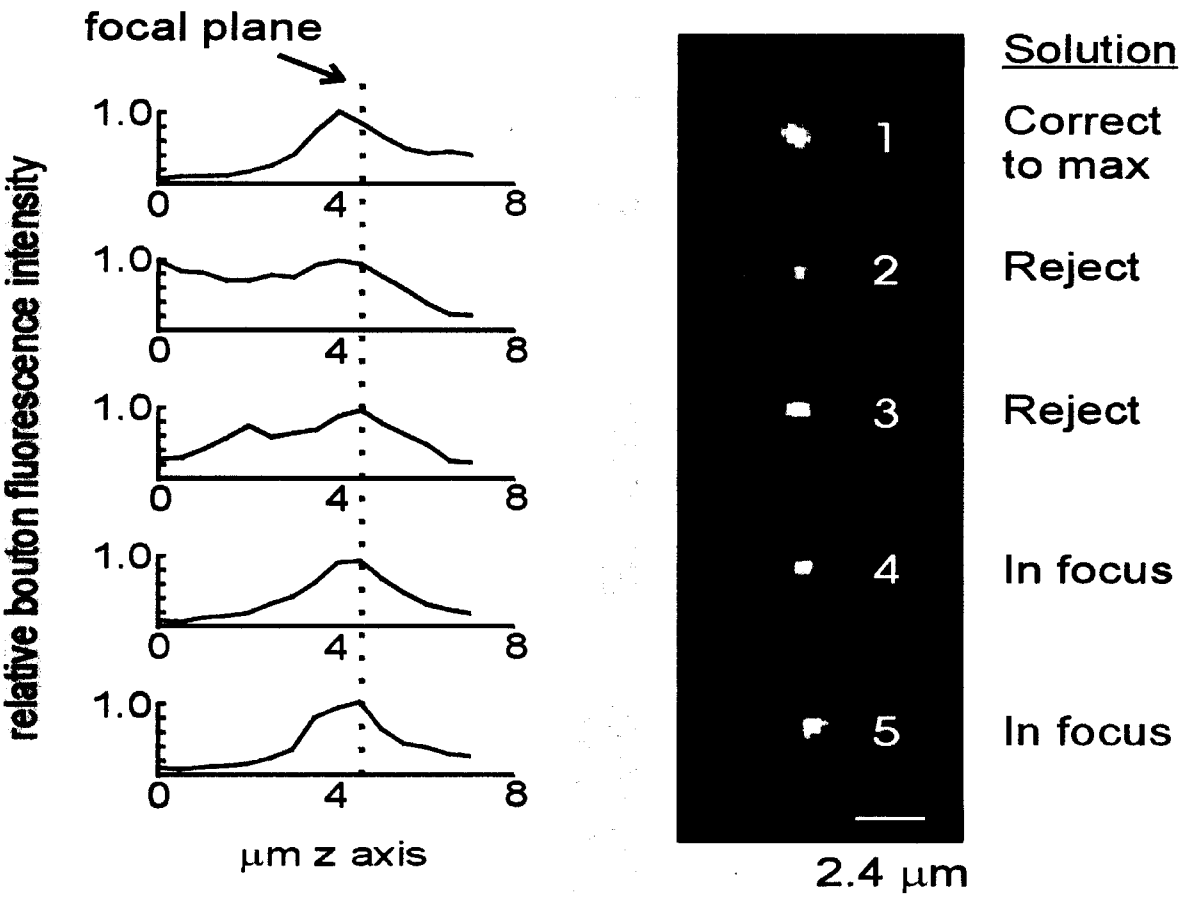

Fig. 2 Analysis of synaptic FM1-43 fluorescence data

Terminal loading corrected for the relative position of the terminal within the focal plane. Using a focus motor, serial optical sections were collected and the fluorescence Z-profile of each terminal was established offline. An automated procedure was employed to correct FM1-43 fluorescence of out-of-focus terminals based on their position within the Z-section. For example, the intensity of terminal #1 was multiplied by its maximal fluorescence (4 μm position) divided by that observed at the focal plane. Terminals that had complex Z-profiles such as 2 and 3 were not analyzed as a significant amount of signal may be contained in terminals above or below the terminal of interest. Based on the expected size of synaptic vesicle clusters and the apparent point spread function for the microscope, we estimated that presynaptic vesicle clusters would be within an apparent 1 - 2 μm Z-section (measurements defined at full-width 1/2 maximal intensity).

the relative release rates indicated that, on average, little depression occurred over the 21 stimuli applied at 1 Hz (Fig. 3 C).

We have assumed that the amount of FM1-43 release from a single terminal is proportional to release probability, the fraction of the vesicular pool loaded with FM1-43, and the number of quanta released with a single AP (see equations 1 and 2, Discussion). Since release probability ($P_{rel.}$) is dependent on $[Ca^{2+}]_o$ (Dodge and Rahamimoff, 1967; Katz and Miledi, 1968; Mintz et al., 1995), we have elevated $[Ca^{2+}]_o$ to 5 mM to maximize $P_{rel.}$ and thus ensure that potential differences in FM1-43 release reflect the number of quanta released and not $P_{rel.}$. To confirm a high release probability under these conditions, we used paired pulse stimulation (Stevens and Wang, 1995; Debanne et al., 1996; Castro-Alamancos and Connors, 1997; Dobrunz et al., 1997; Dobrunz and Stevens, 1997). In all experiments (n = 18) we have applied a second paired stimulus train (21 paired stimuli at 1 Hz; interpulse interval 10 ms) after the initial 1 Hz stimulus train and calculated the degree of paired pulse modulation (PPM) at each terminal (n = 1772) by dividing the relative FM1-43 fluorescence change (% change) observed during the second train by that observed during the first train (Fig. 3 B; Fig. 4 B). To allow sufficient time for reloading the readily releasable pool of synaptic vesicles (Stevens and Tsujimoto, 1995; Dobrunz et al., 1997; Dobrunz and Stevens, 1997; Stevens and Sullivan, 1998b), we established a second baseline period (30 s) between the two stimulus trains. As a control, we conducted experiments (n = 4) in which both first and second stimulus trains were comprised of only single stimuli. In these control experiments, the ratios of the FM1-43 fluorescence changes during stimulus train 2 vs. stimulus train 1 were distributed around a median of 0.96 (n = 448 terminals; Fig. 4 A). The slightly higher mean release ratio of 1.13 ± 0.83 was attributed to only 5 % of values (outside the median release ratio ± 2*SD); exclusion of these potentially spurious values resulted in a mean release ratio of 1.00 ± 0.52. This result demonstrated a constant rate of FM1-43 release at single terminals in response to identical consecutive stimulation protocols. This control is important as it establishes that the system is stable and exhibits little run-down or facilitation.

The values for paired pulse modulation (1 Hz paired/1 Hz single stimuli) at single synaptic terminals were distributed around a median of 1.36 (mean 1.77 ± 1.46; n = 1772; Fig. 4 B). A PPM ratio of 2.0 would be predicted if both the first and second stimulus were successful. Comparison of the release ratios obtained with the two

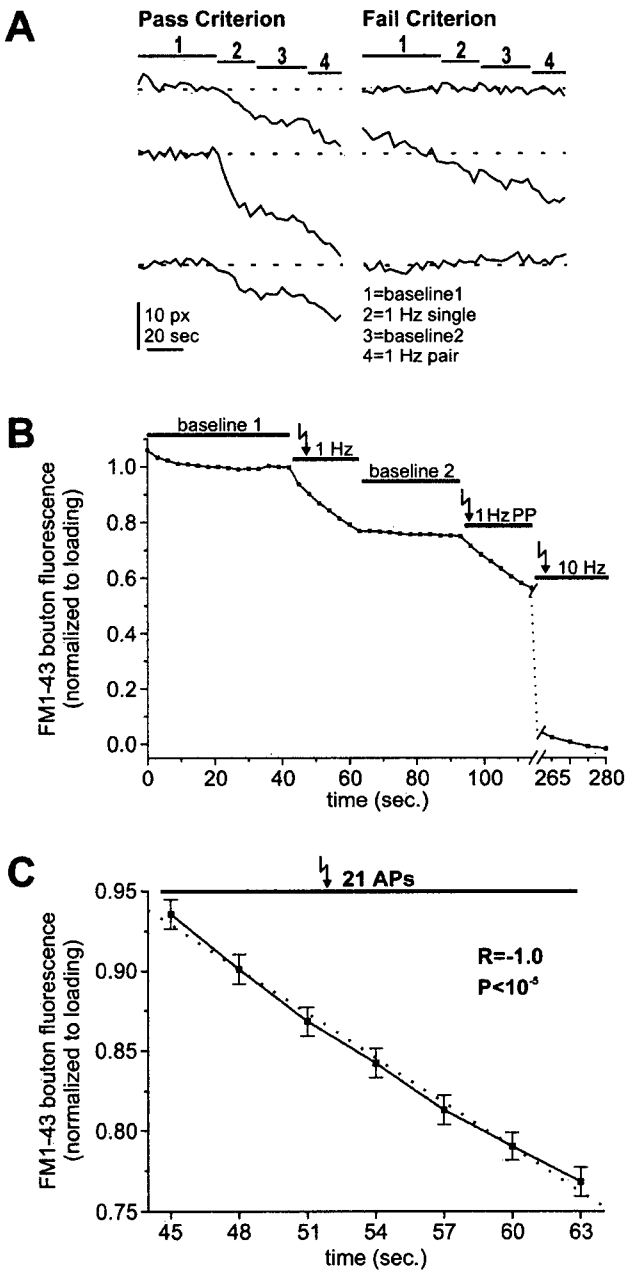

Fig. 3 Unloading of FM1-43 loaded terminals in response to action potential inducing field stimulation

Synaptic terminals were loaded with 1200 pulses delivered at 10 Hz in the presence of 60 µM APV and 3 µM CNQX (blockers of synaptic transmission) and 10 µM FM1-43. After extensively washing the specimen in a medium which decreases spontaneous release (5 mM Mg^{2+}, no added Ca^{2+}), sequential images of FM1-43 fluorescence were acquired during a baseline period and consecutive field stimulation. FM1-43 terminal fluorescence shown in B) and C) is normalized to terminal loading. **A)** A customized software procedure was used to select putative synaptic terminals for further analysis. To be selected, terminals had to pass the following criteria: 1) combined fluorescence change during the 2 stimulation periods had to be greater than 2.5*SD of fluorescence change during identical period of baseline; 2) SD of the baseline had to be < 10 % of the total releasable fluorescence. Left panel: examples of FM1-43 fluorescence traces versus time of terminals passing the criteria; right panel: terminals failing criteria. **B)** Average change of FM1-43 fluorescence during baseline periods and in response to field stimulation (n = 1292 terminals; 18 experiments). **C)** Linearity of FM1-43 unloading during 21 s of 1 Hz train stimulation (each point is mean ± SE; n = 1292 terminals). Dotted line represents linear fit to data ($r = -1.0$; $p < 10^{-5}$).

different stimulation paradigms indicated greater release with paired stimuli than with single stimuli (Mann-Whitney test: $p < 10^{-4}$). However, the majority of synapses (> 75 %) showed PPM values < 2, confirming that most synapses in these cultured preparations possess a high $P_{rel.}$ in 5 mM $[Ca^{2+}]_o$. Additional control experiments (n = 4; 1 mM $[Ca^{2+}]_o$) indicated that evoked FM1-43 could be elevated by 60 % (difference in median release rate; Mann-Whitney test: $p < 10^{-4}$) when increasing $[Ca^{2+}]_o$ from 1 to 5 mM (n = 51/691 terminals). Paralleling this increase in FM1-43 release rates, we find a significant decrease in PPM (25 % difference in median PPM; Mann-Whitney test: $p < 0.05$) when increasing $[Ca^{2+}]_o$ from 1 to 5 mM. These findings are in agreement with studies that show maximal $P_{rel.}$ and paired pulse depression in cortical and hippocampal synapses in 5 mM $[Ca^{2+}]_o$ (Castro-Alamancos and Connors, 1997). To further rule out that differences in FM1-43 release amounts between synaptic terminals were caused by differences in $P_{rel.}$, we restricted further analyses to terminals with a high initial $P_{rel.}$ (PPM ratio < 2; n = 1292 terminals).

To measure the AP-induced FM1-43 release from single terminals, we averaged the change in FM1-43 fluorescence over 7 images (recorded every 3 s) during 1 Hz stimulation (= 21 stimuli; Fig. 3 B & C). Data was pooled data from 18 separate experiments that were conducted under comparable conditions (constant confocal gain and pinhole setting, laser intensity, and FM1-43 concentration). To determine that these experiments were comparable, we conducted a one-way analysis of variance on both baseline variation and FM1-43 release data. This analysis demonstrated that for the 18 experiments analyzed, both the stimulated FM1-43 release and the baseline noise values were drawn from the same distributions and thus could be pooled (one-way ANOVA: $p < 0.05$). Similarly, one-way analysis of variance found that the FM1-43 release ratios obtained in 4 control experiments were also drawn from the same distribution and thus could be pooled ($p < 0.05$). In the analysis of the pooled data we found that the relative FM1-43 fluorescence decrease over the 21 s of stimulation was linear (linear regression: $r = -1.0$; $p < 10^{-5}$; average of n = 1292 terminals; Fig. 3 C), indicating that, on average, little depression of release occurred during this period. Within this population of synapses we found that the degree of FM1-43 unloading during the 21 APs train varied considerably (mean 5.80 ± 3.21 pixel value). Accordingly, we also found a high coefficient of variation (CV = SD/mean: 0.44) for FM1-43 unloading after subtraction of the baseline variance. Furthermore,

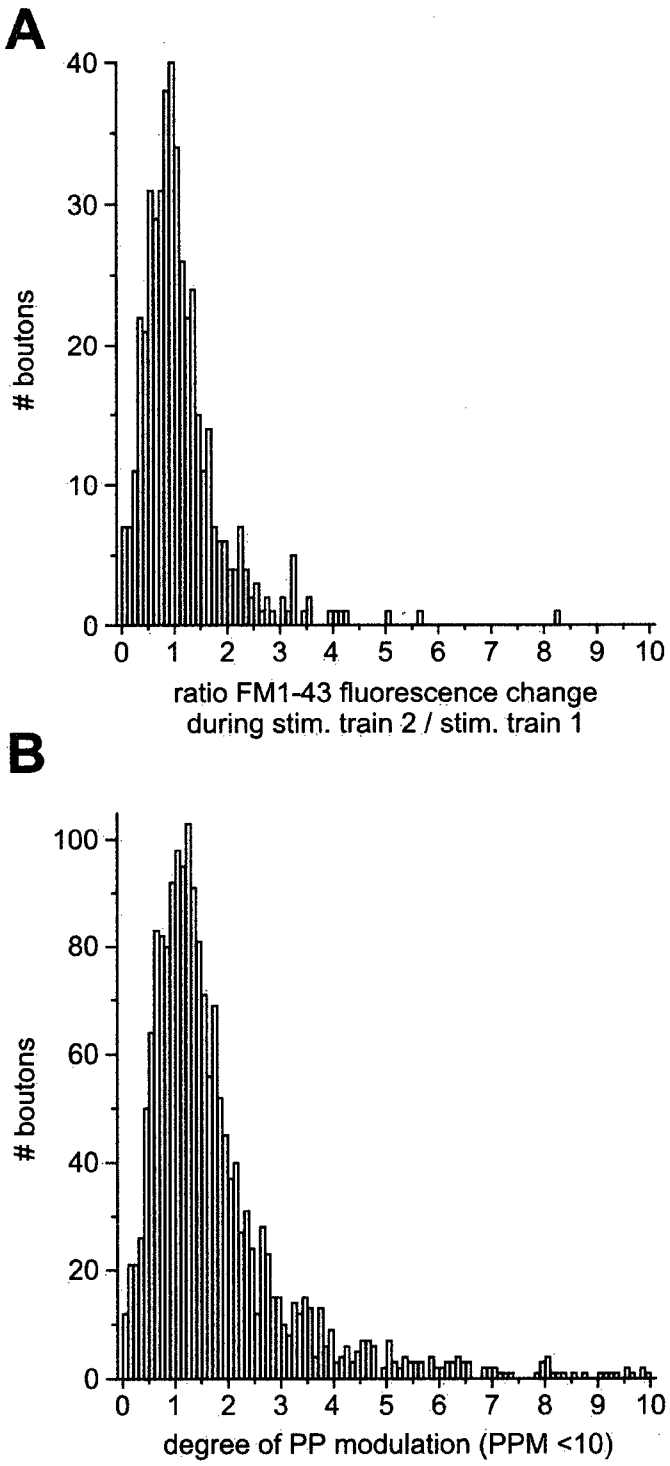

Fig. 4 Ratio of FM1-43 release rates from two consecutive stimulation trains

Distributions of FM1-43 release ratios at synaptic terminals during two consecutive trains of APs separated by 30 s (in 5 mM $[Ca^{2+}]_o$, 1 mM $[Mg^{2+}]_o$). The release ratio for each terminal was obtained by dividing the fractional FM1-43 release during stimulus train 2 by that during stimulus train 1. **A)** In 4 control experiments (n = 448 terminals) both stimulus trains were comprised of 21 single stimuli at 1 Hz. The release ratios are clustered around the median of 0.96. **B)** In 18 experiments (n = 1772 terminals) the first stimulus train was comprised of 21 single stimuli, the second train of 21 paired stimuli (interpulse interval: 10 ms). The distribution is positively skewed due to 25 % of the terminals showing apparent facilitation during stimulus train 2 (PPM values > 2). These terminals are excluded from further analysis. 75 % of all terminals (n = 1292) do not exhibit paired pulse facilitation in 5 mM $[Ca^{2+}]_o$ (PPM values < 2).

we found that the amount of FM1-43 loading into terminals after 1200 APs, a measure of the vesicular pool and thus synapse size (Henkel et al., 1996), exhibits a similar high degree of variability (mean 39.7 ± 18.4 pixel value; CV baseline variance-subtracted: 0.46). When comparing the amount of FM1-43 loading to the amount of FM1-43 fluorescence released per AP we observed a significant positive correlation ($r = 0.65$; $p < 10^{-5}$; $n = 1292$ terminals) between these two parameters (Fig. 5 A). However no significant correlation ($r = -0.03$; $p = 0.50$) was found between the amount of FM1-43 unloading during 21 APs and the degree of baseline variation measured over an identical time period (Fig. 5 B). Hence, factors such as FM1-43 bleaching or dye loss from non-vesicular pools contributed little to the observed positive correlation between synaptic FM1-43 loading and release.

As our data indicated that the amount of FM1-43 released per AP and the total FM1-43 loading of terminals was not constant (Fig. 5 A), we analyzed the distribution of FM1-43 release amounts across terminals. This distribution demonstrated a positive skew when data sets comprising most terminals (PPM < 10; skew = 2.17 pixel value; n = 1772 terminals) or only those terminals with high $P_{rel.}$ (PPM < 2; skew = 2.43 pixel value; n = 1292 terminals) were examined (Fig. 6 A & B). Hence, the positive skew towards higher FM1-43 release amounts was not attributed to terminals with low initial $P_{rel.}$ (480 terminals with PPM > 2). Furthermore, the degree of PPM (a measure of $P_{rel.}$) contributed little to the observed positive skew in FM1-43 release amounts at synaptic terminals with high $P_{rel.}$ (PPM < 2; n = 1292 terminals) as we find a poor correlation ($r = -0.25$) between the amount of FM1-43 release and the degree of PPM at single sites. In contrast, when considering the full range of PPM values (0 - 10; n = 1772 terminals) we find a better correlation ($r = -0.54$) between PPM and FM1-43 release amounts, mostly caused by terminals with low initial release amounts (Fig. 6 C).

As we observed that data sets with a broad range of PPM values (< 10) could contain terminals with low initial $P_{rel.}$ (high PPM values), we restricted further analysis to data sets in which terminals possessed PPM values of < 2 (Fig. 6 B). To examine how the distribution of the FM1-43 release amounts compared to the noise within this data set (due to bleaching, background dye loss, and instrument noise), we calculated the FM1-43 fluorescence variation at each terminal during a baseline period identical to the stimulus train duration (Fig. 6 B; baseline noise as gray histogram). The baseline noise data was not positively skewed (median: - 0.07 pixel value; mean: -

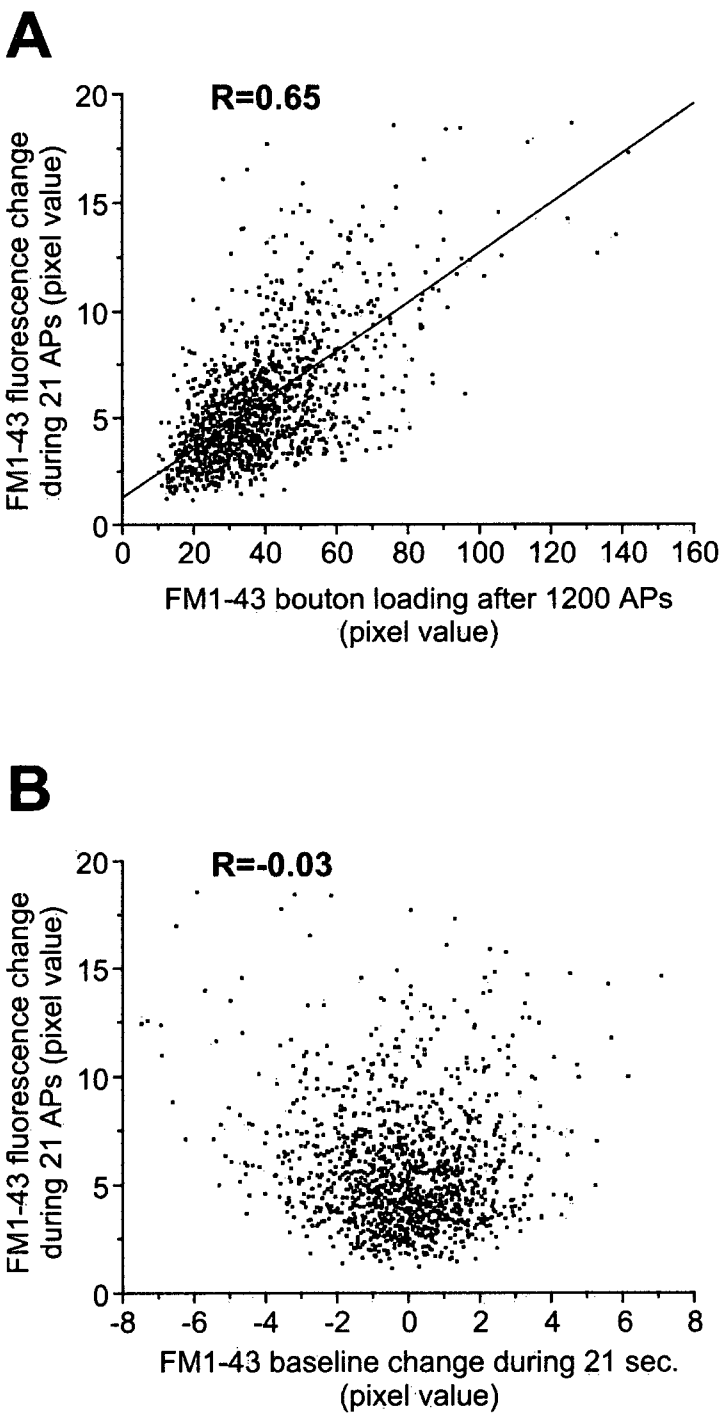

Fig. 5 Relationship between terminal loading and unloading under conditions of high release probability

Synaptic terminals were loaded using 1200 pulses of 10 Hz field stimulation, and then washed for 15 min. in a Ca^{2+}-free, 5 mM Mg^{2+} solution. For terminal unloading, the medium was changed to one containing 5 mM Ca^{2+}, 1 mM Mg^{2+}. Data represents 1292 synaptic terminals with high initial release probability (PPM < 2) that were pooled from 18 experiments and selected by an automated criterion. **A)** A significant linear correlation (r = 0.65) at single terminals between the amount of FM1-43 terminal loading and the amount of unloading in response to 21 field stimuli (1 Hz). **B)** No significant correlation (r = -0.03) between the amount of FM1-43 unloading in response to 21 field stimuli (1 Hz) and FM1-43 baseline variation during a 21 s period.

0.11 ± 1.93 pixel value; skew: - 0.13 pixel value) and hence could not account for the positive skew observed in the distribution of FM1-43 release amounts. Additionally, the negative skew in the baseline noise distribution was attributed to only 0.2 % (3/1292) of the values; exclusion of these values resulted in a normally distributed baseline noise population (Kolmogorov-Smirnov test versus a gaussian distribution: $p > 0.05$). Comparison between the distributions of evoked release amounts and baseline noise indicated that the variation in evoked release amounts between terminals was significantly greater than that expected from baseline variation alone (Kolmogorov-Smirnov test: $p < 10^{-5}$).

To estimate the fraction of terminals exhibiting multiquantal release, we used two different methods: determination of the number of release values that 1) cause the positive skew of the distribution; and 2) are outside the median release value + 2*SD of the baseline noise. Using the first approach, we found that the skew in the distribution of evoked FM1-43 release could be attributed to 17 % (n = 221/1292) of all terminals with the highest FM1-43 release amounts (Fig. 6 B), as exclusion of these terminals from the analysis resulted in a population that was not different from the baseline noise distribution (Kolmogorov-Smirnov test versus baseline noise: $p > 0.05$). Using the second approach, we found that 13 % (n = 167/1292) of the values were greater than the median release value + 2*SD of the baseline noise. Using a computer simulation that modeled the signal-to-noise properties of our system, we observed that the Kolmogorov-Smirnov test could reliably detect a skewed population (n = 1292 release values) attributed to even < 10 % of terminals exhibiting multiquantal release. Thus, during stimulation most of the terminals released FM1-43 amounts that could be described by a gaussian distribution while release amounts of the remaining sites (13 - 17 %, depending on the analysis) were outside a unimodal distribution and were apparently the result of multiquantal release.

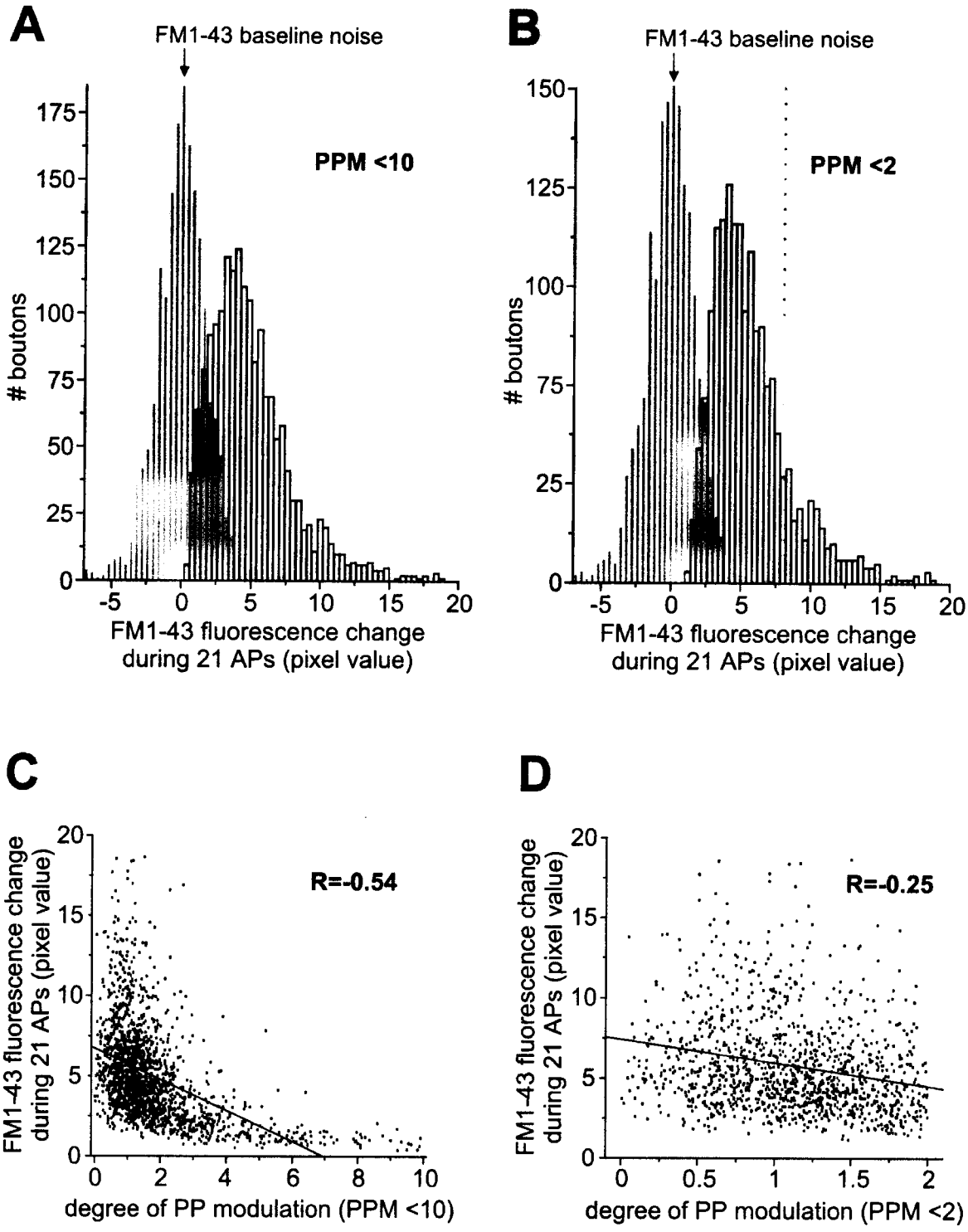

Fig. 6 Distribution of evoked FM1-43 release amounts at synapses under conditions of high release probability

Unloading of FM1-43 was evaluated at synapses of cultured cortical neurons under conditions of enhanced release probability (5 mM $[Ca^{2+}]_o$, 1 mM $[Mg^{2+}]_o$). **A)**

Distribution of FM1-43 release amounts for (n = 1772) terminals with wide range of paired pulse modulation values (PPM < 10). Superimposed (gray) is the distribution of baseline fluorescence change that was recorded over a period identical to the period used to calculate AP evoked release. **B)** The distribution of FM1-43 release values for (n = 1292) synapses with high initial release probability (PPM < 2) is positively skewed. As in A), the distribution of baseline noise (gray bars) is superimposed. The dashed line indicates the minimum release value of all the terminals contributing to the positive skew (i.e. 221 terminals to the right of the line; see Results). **C)** FM1-43 unloading of 1772 terminals as a function of their degree of PPM. After the initial 1 Hz train stimulation, synapses received a second stimulus train comprised of paired 1 Hz stimuli (see Fig. 3A & B). A significant correlation between PPM (fractional FM1-43 release during 2^{nd} train/1^{st} train) and the initial unloading is found when a large range of PPM values (PPM < 10) is considered (r = - 0.54). **D)** Correlation between FM1-43 release and PPM for terminals with high initial release probability (PPM < 2). The degree of PPM contributes little to the amount of release (r = - 0.25).

DISCUSSION

We have observed a significant positive correlation between loading of single terminals (with FM1-43) and the amount of FM1-43 they release in response to APs generated using field stimuli (Fig. 5 A). Betz and Bewick (Betz and Bewick, 1993) have previously reported similar results for neuromuscular synapses. These authors found that despite variability in the intensity of single FM1-43 spots, most sites appeared to release a relatively constant percentage of loaded FM1-43 per stimulus. Their conclusion was that larger release sites release proportionally more transmitter. Studies by Isaacson and Hille (Isaacson and Hille, 1997) and Ryan et al. (Ryan et al., 1997) indicated a similar relationship in central neurons by showing that while the size of synaptic terminals varies greatly the percentage of FM1-43 release from loaded terminals only varies little. These observations indicated that CNS synaptic terminals do not release a constant amount of transmitter per impulse. Ryan et al. (Ryan et al., 1997), using FM1-43 endocytosis in response to single APs, reported that multiquantal release may occur from hippocampal terminals. However, it is possible that the apparent differences in the number of quanta released may reflect differences in release probability between terminals (Hessler et al., 1993; Rosenmund et al., 1993; Murthy et al., 1997; Murthy and Stevens, 1998), or conceivably incomplete loading of vesicle pools. Murthy et al. (Murthy et al., 1997) using FM1-43 endocytosis reported that larger terminals, those with greater FM1-43 loading, had a higher release probability. An assumption made by Murthy et al. (Murthy et al., 1997; Murthy and Stevens, 1998) and (for some experiments) by Ryan et al. (Ryan et al., 1997) was that endocytosis and exocytosis were matched so that the degree of FM1-43 loading (endocytosis) would be a measure of release probability. We have extended these findings by directly measuring release of FM1-43 (and not endocytosis) using conditions in which two complicating variables, vesicle pool loading and release probability have been fixed at saturating levels. Additionally, to prevent synaptic depression we have used brief and low number stimulation protocols (21 APs at 1 Hz) that result in the release of only a small fraction (on average 15 %) of the dye-loaded vesicle pool. As vesicle repriming (availability of vesicles once released) has been estimated to have a $t_{½}$ of ~20-30 s (Ryan et al., 1993; Ryan et al., 1996), we did not expect significant dilution by unlabeled vesicles during our dye unloading measurements. Using this

experimental approach, we confirm the findings of Korn et al. (Korn et al., 1993), Trussell et al. (Trussell et al., 1993), Tong and Jahr (Tong and Jahr, 1994), Vincent and Marty (Vincent and Marty, 1996), Ryan et al. (Ryan et al., 1997), and Auger et al. (Auger et al., 1998) which indicate that multiquantal transmitter release can occur at single synaptic terminals, albeit at a relatively small proportion of terminals (< 20 %). Presumably' multiquantal release could account for a portion of the apparent variability in the amplitude of synaptic responses that are recorded from single terminals (Liu and Tsien, 1995; Murphy et al., 1995; Forti et al., 1997).

Our observation that, under conditions of high release probability, presumed larger terminals (greater FM1-43 loading) release more FM1-43 per impulse than smaller terminals suggests multiquantal release. As larger terminals possess greater release site areas and more docked vesicles (Schikorski and Stevens, 1997) they provide a conceivable anatomical basis for multivesicular release. Fitting the amount of FM1-43 released versus terminal loading to a model where terminal volume was proportional to release site area failed to describe our data. This model would predict a curve with a slope proportional to terminal radius^{-1} (terminal area/terminal volume; $\pi r^2/4/3\pi r^3 = 0.75r^{-1}$). The data was better described by a simple linear relationship between terminal loading and the amount of release. However, analysis of the correlation indicates that a relatively large fraction of the observed variance in release amounts (42 % ; $r^2 = 0.42$; Fig. 5 A) could be accounted for by a linear relationship with terminal loading.

As synaptic terminals possess a variety of parameters that control the rate of evoked vesicular release (excitability, probability of release, amount of release, stimulation induced facilitation or depression), we used different controls to confirm that differences in the rate of FM1-43 unloading between terminals would reflect differences in the amount of vesicular release and not other parameters of synaptic variability. First, we have chosen stimulus parameters that result in a linear rate of FM1-43 release during a train of APs (Fig. 3 C). This apparent linear rate of release was confirmed by the analysis of consecutive images of FM1-43 loaded terminals as in Isaacson and Hille (Isaacson and Hille, 1997). Second, we used conditions expected to result in maximal release probability at all terminals and excluded terminals from the analysis that showed the potential of further increase of release probability (Fig. 4; Fig. 6). Additionally, factors such as AP propagation failure were unlikely to account

for the variability in release amounts between terminals (Allen and Stevens, 1994; Mackenzie et al., 1996).

Consistent with the idea of multiquantal release, analysis of the distribution of release amounts demonstrated a significant skew towards higher release amounts, which was in excess of the system noise. Making the assumption that the peak with the smallest amplitude reflects the fluorescence value of a single vesicle, we would expect that most terminals, on average, release one vesicle and that a subpopulation of terminals (< 20 %) release two or more vesicles per stimulus.

Equation 1: $F_{rel.} = P_{rel.} * n * F_{ves.} * (Ves._{FM1\text{-}43}/Ves._{total})$

Equation 2: $Frel. \sim n * Fves.$

Equation 1 (above) describes the proposed relationship between the amount of FM1-43 release ($F_{rel.}$) and release probability ($P_{rel.}$), the fluorescence of a single vesicle ($F_{ves.}$), a constant, the proportion of FM1-43 loaded vesicles ($Ves._{FM1\text{-}43}/Ves._{total}$), and the number of vesicles released per AP (n). If we assume that $P_{rel.}$ approaches 1.0 (confirmed by the lack of paired pulse facilitation), and that a high proportion of the vesicle pool is loaded by the saturating loading conditions ($Ves._{FM1\text{-}43}/Ves._{total} \sim 1$), then we can simplify equation 1 to equation 2. Equation 2 shows that under the assumptions we have made, the amount of FM1-43 release (measured at single terminals) is expected to be proportional to the number of quanta released (n) and the fluorescence of a single vesicle ($F_{ves.}$, a constant).

The apparent linear relationship between release amount and the terminal size would suggest a process in which terminals can regulate the number of quanta released based on their size. However, this is not a strict relationship as additional synaptic parameters (other than terminal size) could contribute to the skew in FM1-43 unloading of terminals. Structural analyses of forebrain excitatory synapses suggest that a significant proportion (10 - 20 %) contain multiple release sites (Edwards, 1995). From our data it is not possible to determine whether terminals that release a larger amount of FM1-43 per impulse contain multiple release sites. Furthermore, in using mass cultures of neurons we assume that all neurons regardless of phenotype (i.e. glutamatergic or GABAergic) load a similar amount of FM1-43 into their terminals. This is most likely the case since the dye is loaded passively (Betz et al., 1996) into vesicles which posses similar sizes in different phenotypes of CNS synaptic terminals

(Hamori et al., 1990). Nevertheless, regardless of the above caveats, our data obtained by analysis of FM1-43 loading and unloading suggests that CNS terminals can release multiple quanta, adding caution to interpretation of experiments that apply quantal analysis to CNS synapses.

III. CORRELATION OF MINIATURE SYNAPTIC ACTIVITY AND EVOKED RELEASE PROBABILITY IN CORTICAL NEURONS

ABSTRACT

Spontaneous miniature synaptic activity is caused by action potential (AP) - independent release of transmitter vesicles and is regulated at the level of single synapses. In cultured cortical neurons we have utilized this spontaneous vesicle turnover to load the styryl dye FM1-43 into synapses with high rates of miniature synaptic activity. Automated selection procedures restricted analysis to synapses with sufficient levels of miniature activity mediated FM1-43 uptake. Following FM1-43 loading, vesicular FM1-43 release in response to AP-stimulation was recorded at single synapses as a measure of release probability. We find that synapses with high rates of miniature activity possess significantly enhanced evoked release rates compared to a control population. As the difference in release rates between the two populations is $[Ca^{2+}]_o$-dependent, it is most likely due to a difference in release probability. Within the sub-population of synapses with high miniature activity, we find that the probabilities for miniature and AP-evoked release are correlated at single synaptic sites. Furthermore, the degree of miniature synaptic activity is correlated with the vesicle pool size. These findings suggest that both evoked and miniature vesicular release are regulated in parallel and that the frequency of miniature synaptic activity can be used as an indicator for evoked release efficacy.

INTRODUCTION

Spontaneous miniature synaptic activity exists throughout the vertebrate nervous system. Miniature activity is attributed to spontaneous AP-independent presynaptic release of one (Frerking et al., 1997) or more (Vautrin and Barker, 1995; Wall and Usowicz, 1998) transmitter quanta. Findings from our laboratory utilizing postsynaptic imaging of miniature activity indicate that the probability for miniature release is highly variant between synapses even on the same dendrite (Murphy et al., 1994; Wang et al., 1999). This variability among synapses indicates that miniature release can be regulated on the level of individual synapses. It has been shown that $[Ca^{2+}]_i$ can regulate miniature release in the central nervous system (CNS) (Minota et al., 1991; Doze et al., 1995; Scanziani et al., 1995; Capogna et al., 1996a; Poisbeau et al., 1996; Capogna et al., 1997; Schoppa and Westbrook, 1997; Bao et al., 1998; Li et al., 1998) and peripheral nervous system (PNS) (Matthews and Wickelgren, 1977; Marcus et al., 1992; Katz et al., 1995). Furthermore, downstream of Ca^{2+} influx second messenger systems such as protein kinase C (PKC) (Ghirardi et al., 1992; Parfitt and Madison, 1993; Capogna et al., 1995; Carroll et al., 1998; Stevens and Sullivan, 1998b) and cAMP-dependent protein kinase A (PKA) (Chavez-Noriega and Stevens, 1994; Chen and Regehr, 1997; Kondo and Marty, 1997) have been implicated in the regulation of miniature activity. Both PKA (Ghirardi et al., 1992; Hell et al., 1995; Tong et al., 1996) and PKC (Ramakers et al., 1997; Majewski and Iannazzo, 1998) have also been shown to regulate action potential (AP)-dependent transmitter release.

Miniature release, unlike (AP-) evoked transmitter release (Haage et al., 1998), can be blocked by antagonists of low-threshold voltage gated calcium channels (VGCCs) (Parfitt and Madison, 1993; Momiyama and Takahashi, 1994; Scanziani et al., 1995; Bao et al., 1998). Although the pathway of calcium entry may differ between AP-evoked and spontaneous release, there is good evidence that miniature and evoked release can be regulated in parallel at presynaptic terminals of the mammalian nervous system. First, synaptic vesicles available for AP-evoked and AP-independent release are drawn from the same readily releasable pool (Rosenmund and Stevens, 1996). Second, both forms of release are controlled by core parts of a common release machinery (Capogna et al., 1996b; Mochida et al., 1997; Hua et al., 1998). And third, changes in evoked release following the induction of short-term (Kamiya

and Zucker, 1994; Cummings et al., 1996; Zucker, 1996; review in Fisher et al., 1997) and of long-term (Minota et al., 1991; Malgaroli and Tsien, 1992; Arancio et al., 1995; but see Cormier and Kelly, 1996; Tong et al., 1996) synaptic plasticity are paralleled by changes in miniature frequency.

These findings led us to address whether synapses that display high rates of miniature synaptic activity would also possess elevated evoked release properties. Using the styryl dye FM1-43 (Betz and Bewick, 1992; Betz and Bewick, 1993) that allows monitoring of vesicular turnover at single synaptic terminals (Ryan et al., 1993; Murthy et al., 1997; Ryan et al., 1997), we have developed a protocol to selectively load the dye into terminals with high miniature synaptic activity, as previously reported in abstract form (Prange and Murphy, 1997; Prange and Murphy, 1998). We find that at synapses with high levels of miniature activity AP-evoked release is elevated.

MATERIAL & METHODS

Cortical neurons and glia were dissociated from 18 day old Wistar rat fetuses and cultured for 16-25 days on poly-D-lysine coated 12 mm glass coverslips prior to experiments (Mackenzie et al., 1996). For the experiments, coverslips were cut into two pieces, placed into a customized perfusion chamber (~ 500 µl vol.), and fixed by platinum weights to prevent movement. Continuous perfusion was supplied by a Hanks balanced salt solution (HBSS) medium containing (in mM) 137 NaCl, 2.5 $CaCl_2$, 1.0 $MgSO_4$ 5.0 KCl, 0.34 $Na_2HPO_4(7H_2O)$, 10.0 Na^+-HEPES buffer, 1.0 $NaHCO_3$, and 22.0 glucose at pH 7.4 and ~315 mosm. $CaCl_2$ and $MgSO_4$ concentrations were altered as indicated in the Results and Figure legends. Additionally, the glutamate receptor antagonists D-amino-5-phosphono-valeric acid (D,L-APV, 60 µM) and 6-cyano-7-nitroquinoxaline-2,3-dione (CNQX, 3 µM) were added to prevent spontaneous action potentials (APs) and recurrent excitation during field stimulation. Constant current stimulation (30 mA; 1 ms pulse duration) was delivered via two platinum electrodes fixed on opposite sides of the perfusion chamber (distance ~8 mm).

In control experiments, presynaptic terminals were loaded by applying a 1200 pulse field stimulus train at 10 Hz in the presence of 10 µM FM1-43 (see Fig. 7). FM1-43 exposure continued for 60 s after the stimulus train to allow for complete vesicle endocytosis (Ryan and Smith, 1995). In experiments where FM1-43 uptake was achieved by miniature activity, the specimens were continuously exposed to 10 µM FM1-43 for 10-20 min (see Fig. 7). To promote miniature synaptic activity during the exposure, the medium was supplemented with 5 mM $[Ca^{2+}]$, 0.6 µM Tetrodotoxin (TTX), and lacked $[Mg^{2+}]$. To ensure that each treatment group received the same amount of AP- and high $[Ca^{2+}]_o$-stimulation, prior to FM1-43 loading, the miniature-loading trials were exposed to 1200 field stimuli in 2.5 mM $[Ca^{2+}]_o$ and 1 mM $[Mg^{2+}]_o$. Accordingly, prior to AP-dependent loading, control trials were exposed to 5 mM $[Ca^{2+}]_o$ and 0.6 µM TTX for 10-20 min (followed by a 5 min washout of TTX in 2.5 mM $[Ca^{2+}]_o$ and 1 mM $[Mg^{2+}]_o$). With these pre-loading treatments, both groups were exposed to the same solutions and stimuli before FM1-43 loading and unloading was performed (Fig. 7). This was designed to minimize differences in the protocols between miniature-loading and AP-loading (control) experiments.

For (reloading) experiments in which multiple loading and unloading trials were performed over the same area of interest (see Fig. 13 A), FM1-43 terminal loading by field stimulation was achieved using 4 trains of 300 stimuli (10 Hz) spaced by 5 second intervals. This protocol was expected to result in complete loading of vesicle pools. Therefore, the total amount of FM1-43 terminal fluorescence would be a measure of terminal size (Henkel et al., 1996), and the amount of evoked FM1-43 release a measure of release probability (see Appendix, Equation 3). FM1-43 terminal loading by miniature activity was achieved by 10 min of continued dye exposure with 0.6 μM TTX and 5 mM $[Ca^{2+}]_o$ present. Based on the estimated average vesicle pool sizes for cultured CNS terminals (~200 vesicles) (Liu and Tsien, 1995; Murthy et al., 1997; Ryan et al., 1997), this protocol was expected to result in sub-maximal loading of vesicle pools. Hence, the amount of FM1-43 fluorescence at a synaptic terminal would be a measure of its miniature activity (probability) during the loading time (see Appendix, Equation 4). For all experiments, preparations were washed for 15-25 min after dye loading in the above medium supplemented with 5 mM Mg^{2+} but no added Ca^{2+} to minimize synaptic FM1-43 release attributed to spontaneous action potentials and miniature synaptic activity. FM1-43 terminal unloading was achieved using field stimulation protocols consisting of a 2 Hz stimulus train during which FM1-43 unloading was recorded, followed by a 10 Hz stimulus train to determine the total amount of releasable FM1-43 fluorescence (see Fig. 7). All experiments were conducted at room temperature (~ 23°C).

Confocal imaging was performed on a Bio-Rad MRC 600 (Bio-Rad Microscience Ltd., Herts, UK) system attached to a Zeiss (Carl Zeiss, Oberkochen, FRG) upright microscope (Axioskop) using an Olympus 0.9 NA 60x water immersion objective (Olympus Optical Co., Ltd., Tokyo, JP). Laser intensity was attenuated to 1 % for imaging experiments. The confocal pinhole was set to 4.5 (Bio-Rad units) for reloading experiments, and to 3.0 for all other experiments. To improve signal-to-noise properties, the confocal slow scan mode (without averaging) was used. For data acquisition, a field of 128 x 128 μm (400 x 400 pixels) was scanned every 5 s during baseline and periods of field stimulation (see Fig. 7). Image collection during the baseline period was used to calculate the signal-to-noise ratio at each synapse and was followed by 15 s of 2 Hz field stimulation to determine the fractional FM1-43 unloading (see Fig. 8 and 11; see Appendix, Equations 1 and 2). For experiments in which

absolute (rather then fractional) FM1-43 fluorescence changes were evaluated (see Figs. 10, 13 - 15), corrections were made for uneven illumination (lower signal at edges of field) by dividing all fluorescence by a control image of a carboxyfluorescein solution. Additionally, in these experiments a (vertical) Z-series of 13 consecutive confocal images (spaced at 0.54 μm) over the area of interest was acquired after each loading trial utilizing a computer controlled focus motor. Each terminal's fluorescence intensity in the focal plane was corrected based on its relative position within the confocal Z-series (Prange and Murphy, 1999). Furthermore, terminals contaminated by signals from stained structures above or below their focal plane were eliminated from further analysis (Prange and Murphy, 1999).

Confocal images were exported as byte data and analyzed using customized routines written in IDL (Research Systems Inc., Boulder, CO). For each experiment, 100-400 putative synaptic terminals were analyzed and fluorescence changes over time were averaged over ~2.6 μm^2 at each site. Putative terminals were randomly selected based on averaged images acquired during the non-stimulated baseline period. For experiments that determined the number of responsive terminals within the visual field (see Fig. 9 C & D), the selection of responsive terminals was maximized by using a difference image that depicted the loci of FM1-43 release during field stimulation.

Non-releasable fluorescence (i.e. fluorescence remaining after the 1200 pulse field stimulus train) was subtracted at each terminal before further analysis was performed. FM1-43 changes were averaged over 15 s of a 2 Hz stimulus train (3 images) and during an identical time interval of non-stimulated baseline (see Fig. 7). For (reloading) experiments employing multiple loading and unloading trials (see Figs. 13 - 15) and experiments comparing absolute amounts of FM1-43 uptake (see Fig. 9 D; Fig. 10), raw FM1-43 fluorescence (ΔF) changes were analyzed (see Appendix Equation 3). For all other experiments, FM1-43 fluorescence changes were normalized to the total amount of releasable FM1-43 fluorescence ($\Delta F/F$) (see Appendix Equation 1). An automated response criterion was used to select responsive from non-responsive putative terminals (see Fig. 8). To be considered for further analysis, terminals had to meet the following criteria: 1) there must be a net decrease in FM1-43 fluorescence in response to a 2 Hz and a 10 Hz train of field stimuli; and 2) the standard deviation (SD) of the baseline had to be < 10 % of the terminals total releasable fluorescence. The

criteria were modified for reloading experiments as follows: 1) the terminals total releasable fluorescence after loading by miniature activity had to be > 5 x SD of the baseline fluorescence; 2) the decrease in FM1-43 fluorescence during 40 stimuli at 2 Hz had to > 2.0 x SD of the baseline fluorescence. Additionally, in these experiments analysis was restricted to terminals at which the amount of FM1-43 uptake during 1200 AP stimulation exceeded the amount of FM1-43 uptake during 10 min incubation time in a miniature activity promoting medium (80 % of all sites selected). This was done to ensure that FM1-43 loading using 1200 APs resulted in a fluorescence measurement representative of the entire vesicle pool.

Whole cell patch clamping (Hamill et al., 1981) was conducted using an Axon Instruments Axopatch 200B amplifier (Axon Instruments, Foster City, CA) and 7 MΩ electrodes pulled from 1.5 mm glass capillaries. The patch pipettes were filled with a solution containing (in mM): 122 K^+MeSO_4, 20 NaCl, 5 Mg^{2+}-ATP, 0.3 GTP, and 10 HEPES, 200-300 μM Fluo-3 K^+ salt, (pH = 7.2). Voltage-clamp recordings had APV (60 μM) present in the extracellular medium to isolate the AMPA-mediated current of the postsynaptic EPSCs.

For statistical testing of normality, the Kolmogorov-Smirnov test was used. For comparison of the means of normally distributed distributions, the unpaired and paired t-test was used as indicated. The medians of non-Gaussian distributions were compared using the non-parametric Mann-Whitney test. For correlation analysis, the non-parametric Spearman test was used over the Pearson-test when it resulted in a better fit to a linear model.

RESULTS

FM1-43 loading into synapses using APs and high rates of miniature synaptic activity

Using field electrical stimulation and confocal microscopy, we have been able to image loading and release of the styryl dye FM1-43 from presynaptic terminals of cultured cortical neurons. For FM1-43 uptake into vesicle pools of synaptic terminals (terminal loading), two different protocols were used. The first protocol consisted of a large number of AP-inducing field stimuli (1200 pulses at 10 Hz) in the presence of FM1-43 with continued dye exposure for 60 s after stimulation to allow complete endocytosis (Ryan and Smith, 1995) (Fig. 7). This protocol is expected to result in loading of all synaptic sites within the electrical field independent of their degree of miniature activity which occurs at much lower rates (Murphy et al., 1995; Stevens and Sullivan, 1998b; Wang et al., 1999). Previously, we had confirmed that each field stimulus reliably elicits a single action potential (AP) when recurrent excitation was blocked by a combination of glutamate receptor antagonists APV and CNQX (Prange and Murphy, 1999).

The second protocol for FM1-43 terminal loading used conditions that facilitated spontaneous miniature synaptic activity by elevating $[Ca^{2+}]_o$ to 5 mM (no added $[Mg^{2+}]_o$) and suppressed AP-dependent activity using 0.6 µM TTX (Fig. 7). Findings from our laboratory indicate that most synapses within a neuron have low rates of miniature activity ($\leq$ 0.01 Hz), but a sub-population of synapses exhibits high rates (0.1 Hz and more) (Wang et al., 1999). Based on these rates we chose FM1-43 exposure times of 10 - 20 min (in 5 mM $[Ca^{2+}]_o$ 0.6 µM TTX) to preferentially load the dye into synapses with high levels of miniature activity. Using these conditions, we were able to utilize miniature synaptic activity to load FM1-43 into a vesicle pool that was releasable by APs (Fig. 8 B & D). We confirmed that miniature synaptic activity was enhanced under these conditions by using whole-cell patch clamp recordings (n = 5 neurons). These experiments demonstrated that the frequency of miniature activity was significantly increased (on average 9.0 ± 5.4 fold; $p < 0.05$, paired t-test) when $[Ca^{2+}]_o$ was elevated from 0 to 5 mM and $[Mg^{2+}]_o$ was decreased in parallel from 5 to 0

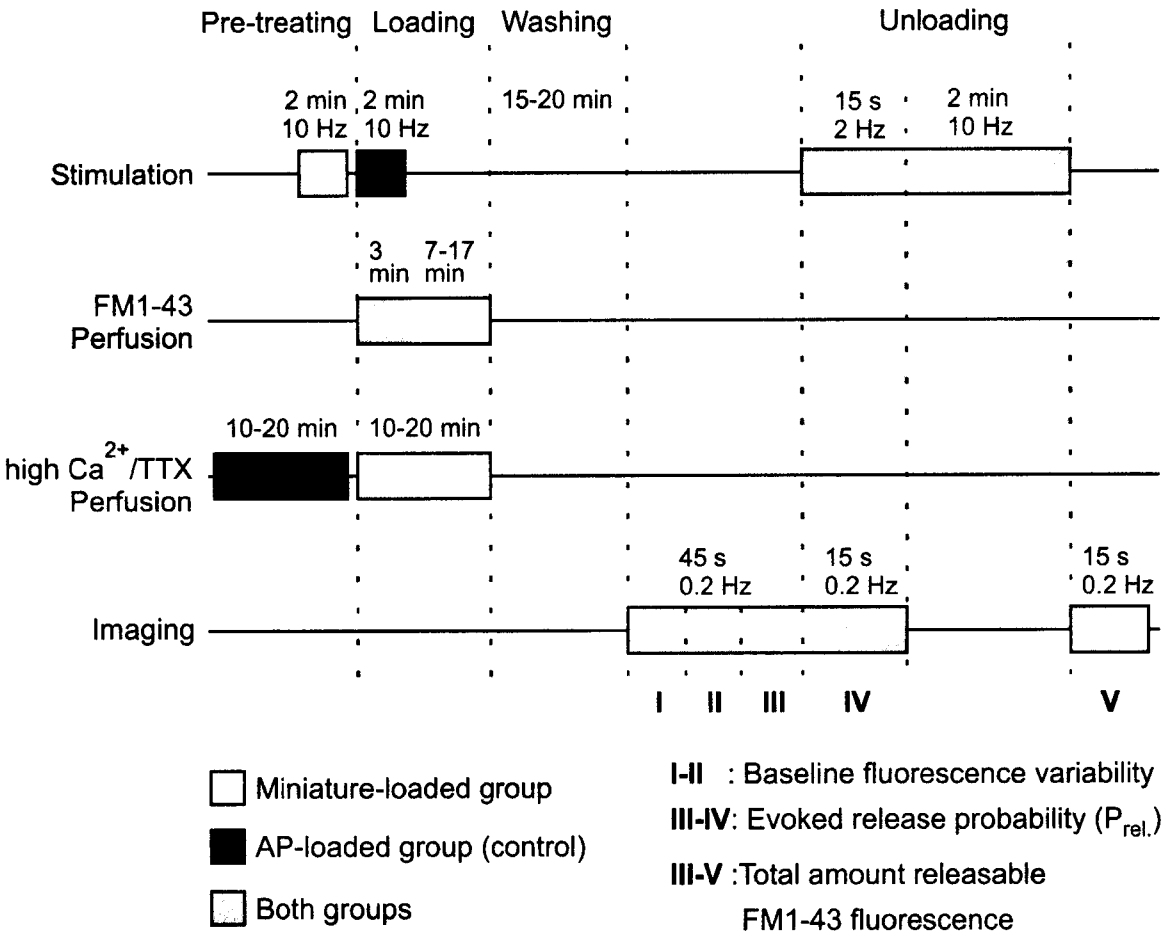

Fig. 7 FM1-43 uptake into synaptic terminals using miniature synaptic activity and AP-inducing field stimulation

FM1-43 was loaded into a subpopulation of synapses with high miniature activity (white symbols) by using miniature activity promoting conditions (5 mM $[Ca^{2+}]_o$ / 0.6 µM TTX) during 10-20 min FM1-43 exposure. A control group of synapses (black symbols) was loaded with FM1-43 using AP-inducing field stimulation (10 Hz) during 2 min dye exposure. Both groups received respective pre-treatments prior to dye loading to minimize differences between the individual loading protocols. After loading, for both groups (grey symbols) identical protocols for excess dye washout (15-20 min), field stimulation (2 Hz and 10 Hz) and imaging (every 5 s) were used. Synaptic FM1-43 fluorescence was recorded during a non-stimulated baseline period, a period of AP-inducing field stimulation, and after complete unloading of vesicle pools using 10 Hz field stimulation for 2 min. To account for the different loading protocols of both groups, evoked FM1-43 fluorescence changes were normalized to the total

amount of releasable fluorescence at each synapse (see Appendix, Equation 2). Changes in FM1-43 baseline fluorescence (I-II) and the total amount of releasable fluorescence (III-IV) were used to determine the signal-to-noise properties of each terminal. For both groups, the rate of FM1-43 fluorescence decrease during 2 Hz field stimulation was used as a measure of evoked release probability ($P_{rel.}$) at individual synapses. During periods of stimulation glutamate receptor antagonists CNQX (3 μM) and APV (60 μM) were present to block recurrent excitation.

mM (Fig. 9 A & B). In additional (n = 14) experiments, we compared the extent of synaptic FM1-43 loading during 13 min dye exposure under conditions expected to elevate miniature synaptic activity (5 mM $[Ca^{2+}]_o$, 0.6 µM TTX, no added $[Mg^{2+}]_o$) and suppress it (5 mM $[Mg^{2+}]_o$, no added $[Ca^{2+}]_o$), respectively. An automated procedure was used to quantitatively select FM1-43 stained terminals from non-specific background staining (see Methods). We found a significant difference in the number of terminals that loaded FM1-43 into their vesicle pools by miniature synaptic activity when comparing sister cultures exposed to high vs. low $[Ca^{2+}]_o$ during FM1-43 presence. Of all putative sites tested 7.0 % (n = 49 of 700) loaded in 5 mM $[Ca^{2+}]_o$ / 0.6 µM TTX, but only in 1.4 % (n = 10 of 700) loaded in the Ca^{2+}-free 5 mM $[Mg^{2+}]_o$ solution ($p < 0.05$, unpaired t-test) (Fig. 9 C). However, the average amount of FM1-43 uptake into terminals was not different under the different loading conditions (high $[Ca^{2+}]_o$-loading: 23.4 ± 10.5 pixel value; low $[Ca^{2+}]_o$-loading: 27.3 ± 15.8 pixel value; $p > 0.10$, unpaired t-test) (Fig. 9 D). Taken together, these findings indicated that, while miniature activity persists at relatively high levels at a very small number of synapses in an apparently $[Ca^{2+}]_o$-independent fashion, the elevation of $[Ca^{2+}]_o$ greatly facilitates the total number of synapses that reach these high levels of miniature activity.

Next, in (n = 17) experiments we compared the amounts of synaptic FM1-43 uptake between terminals loaded by miniature synaptic activity during 10 min vs. terminals loaded by 1200 AP-inducing field stimuli (controls). To accurately measure synaptic FM1-43 in both groups, identical imaging settings were used and out-of-focus correction for the FM1-43 fluorescence of each terminal was employed (see Methods). We found that synaptic FM1-43 uptake during 1200 field stimuli (8 experiments; n = 822 terminals) exceeded the FM1-43 uptake during 10 min of miniature activity (9 experiments; n = 335 terminals) significantly by on average 40 % ($p < 0.0001$, Mann-Whitney test) (Fig. 10). These results indicated that miniature activity during 10 min results in detectable, yet sub-maximal FM1-43 uptake into vesicle pools of a sub-population of synaptic terminals.

After FM1-43 loading and excess dye washout (Fig. 7; and see Methods), we could show that FM1-43 fluorescence was associated with the loading of synaptic vesicle pools by eliciting dye unloading upon AP-inducing field stimulation (Fig. 8). Due to the amphiphilic nature of FM1-43 (Betz et al., 1996) background staining can

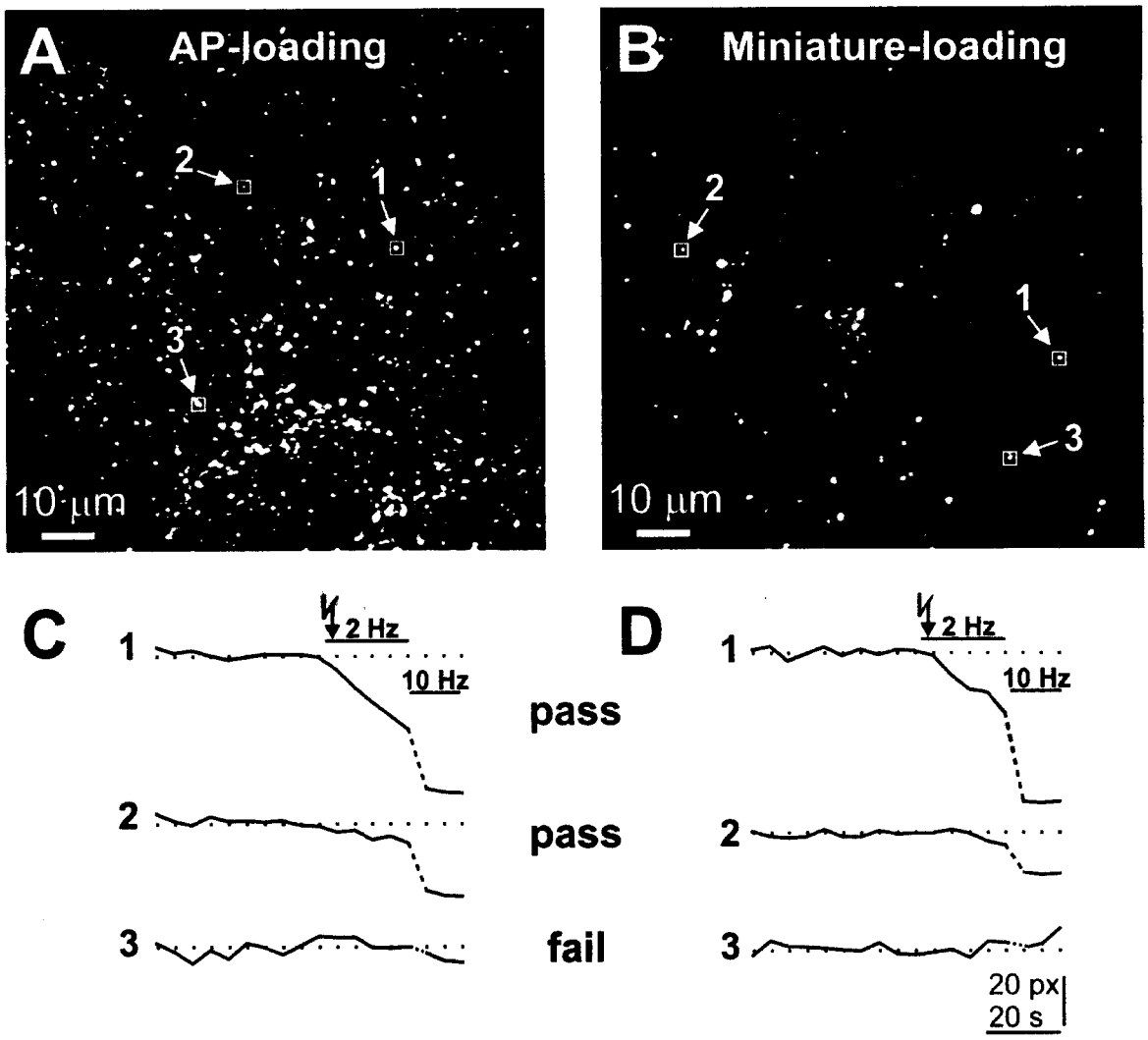

Fig. 8 Automated procedure to select responsive from non-responsive putative synaptic sites

A) & B) Confocal image showing punctate FM1-43 staining pattern in cultured cortical neurons after (A) delivery of 1200 field stimuli with dye present (controls) or (B) incubation in miniature synaptic activity promoting medium for 15 min with dye present. For both FM1-43 loading protocols excessive background dye was washed out for 15-20 min. Under conditions that promote miniature synaptic activity only a sub-population (~20 %) of all terminals load a significant amount (see Methods) of FM1-43 into a pool releasable by APs. Boxes #1 - #3 refer to putative synaptic terminals that were subjected to an automated criterion selecting responsive from non-responsive putative terminals (see C, D). **C) & D)** Plot of FM1-43 fluorescence versus time at

putative synaptic terminals highlighted in A and B, respectively. Confocal images were taken every 5 s during 45 s of baseline and 15 s of 2 Hz field stimulation. Residual FM1-43 fluorescence remaining after a 1200-pulse stimulus train (10 Hz) was subtracted at each site to determine the total amount of releasable dye. To be selected for further analysis, putative synapses have to pass the following automated criteria (see Methods): 1) total amount of releasable dye has to be > 0; 2) variation (SD) of baseline fluorescence has to be < 10 % of total amount of releasable fluorescence. Putative synaptic terminals #1 and #2 pass, and #3 fail the criterion. Lightning bolt depicts onset of AP-inducing field stimulation.

often be detected, even after extensive periods of dye washout. Hence, we developed an automated procedure to identify synaptic terminals based on their individual signal-to-noise ratio and their FM1-43 unloading response upon field stimulation (Fig. 8). This automated procedure selected putative terminals (i.e. punctate FM1-43 spots of < 2.6 μm^2) for further analysis only if they showed a net reduction in fluorescence during field stimulation and if their baseline variance was low relative to the amount of release (Fig. 8 B & D; and see Methods). Using this procedure, we were able to sort responding from non-responding putative terminals. Furthermore, it allowed us to select a group of terminals with "high miniature activity" based on their degree of FM1-43 loading. We are aware that the binary distinction created by the criterion does not necessarily reflect a biological threshold. However, it made it possible to analyze the data with a minimized impact of observer bias. For (control) experiments in which FM1-43 loading was achieved by field stimulation, we found that 62 % (n = 2439 of 3920) of small punctate FM1-43 staining structures exhibited significant unloading in response to a 10 Hz stimulus train, and therefore were likely to be synaptic terminals. In contrast, for experiments that utilized miniature synaptic activity (and not APs) to load FM1-43, only 14 % of putative synaptic terminals (n = 1617 of 11050) were selected by the automated criteria. These results indicate that only a sub-population of 23 % (= 14 % ÷ 62 %) of synaptic terminals exhibit sufficient miniature activity during 10 - 20 min to load a significant amount of FM1-43 into their vesicle pools that is releasable by APs (compare Fig. 8 A and B). Although this procedure did not give us a quantitative measure of vesicle turnover caused by spontaneous miniature release, it provided us with a method to select a sub-population of CNS terminals based on their degree of miniature synaptic activity.

Comparing release rates between synapses with high miniature activity and a control population

After establishing conditions under which we could reliably load FM1-43 into synaptic terminals with miniature activity, our aim was to compare the release probability ($P_{rel.}$) at sites loaded by miniature activity vs. (control) sites loaded by AP stimulation. To estimate the $P_{rel.}$ at synapses of both groups (see Appendix Equation 1 and 2), the initial rate of FM1-43 fluorescence release during 15 s of a low frequency

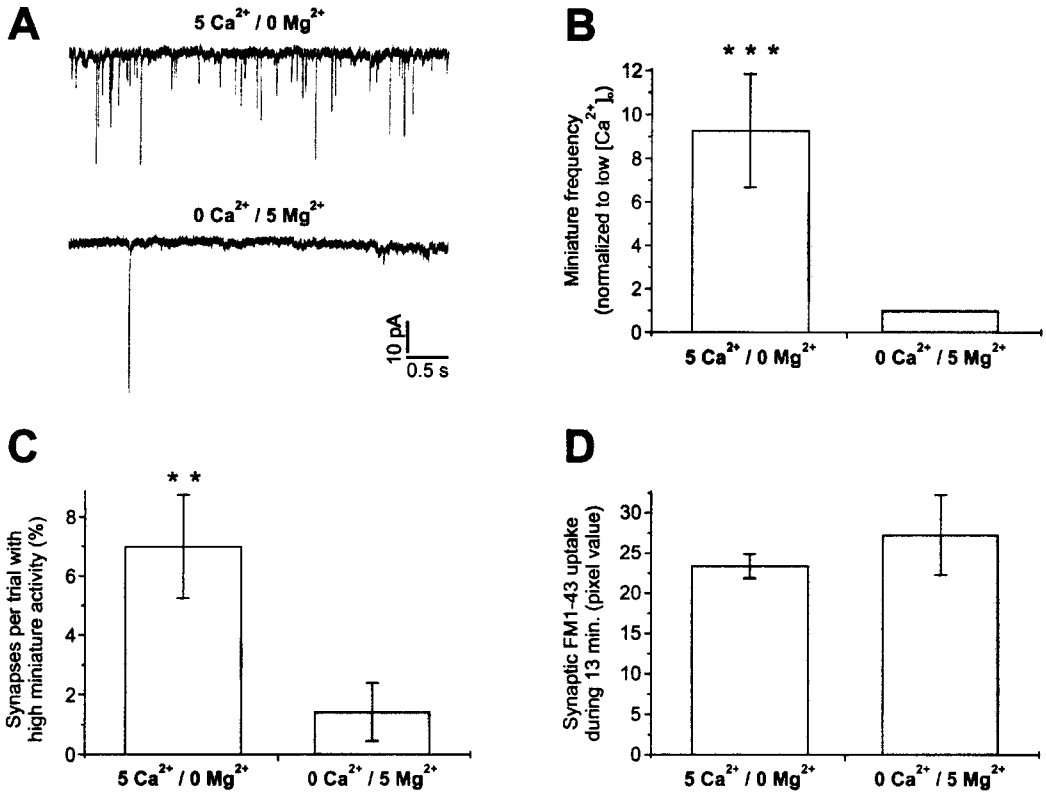

Fig. 9 Elevated miniature synaptic activity in the presence of high $[Ca^{2+}]_o$

A) Whole-cell voltage-clamp recordings were performed to measure the effect of $[Ca^{2+}]_o$ on the rate of miniature synaptic activity. Examples of voltage-clamp records from one cell. The cell was perfused with the indicated extracellular divalent ion concentrations (in mM); 0.6 μM TTX was added to block spontaneous APs. **B)** Plot of the ratio of miniature activity (events/sec) in high vs. low $[Ca^{2+}]_o$ from (n = 5) cells. Miniature activity is significantly elevated in all cells during multiple trials of $[Ca^{2+}]_o$ wash-in (***$p < 0.0001$). Error bar depicts SEM ratio across cells. **C)** Percentage of synapses loaded with FM1-43 by miniature synaptic activity as a function of $[Ca^{2+}]_o$. Synapses of sister cultures were perfused with either a high or low $[Ca^{2+}]_o$ containing medium during 13 min of dye exposure (n = 14 experiments). An automated criterion was applied to select terminals that showed significant FM1-43 uptake during the different treatment periods. The average percentage of terminals that load FM1-43 into their releasable vesicle pools by miniature activity significantly increases (by 4.9 x; **$p < 0.05$) when elevating $[Ca^{2+}]_o$ from 0 to 5 mM. **D)** The average amount of miniature activity-mediated FM1-43 uptake does not differ between the groups. Ion concentrations in mM. Error bars depict SEM.

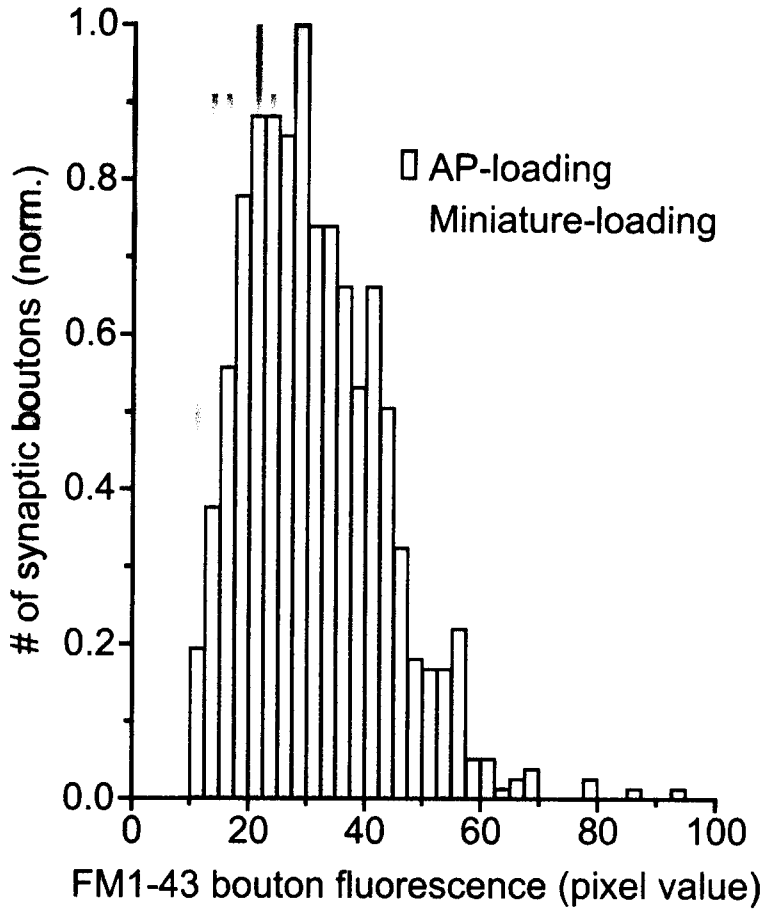

Fig. 10 Sub-maximal FM1-43 loading of vesicle pools during 10 min of miniature synaptic activity

The amount of synaptic FM1-43 loading was compared between two groups of synapses subjected to different loading conditions. In the first group, (gray bars; n = 335 terminals) FM1-43 uptake was achieved by 10 min of dye exposure in a miniature activity-promoting medium (5 mM Ca^{2+} / 0.6 µM TTX). In the second (control) group (white bars; n = 822 terminals) FM1-43 uptake was stimulated by 1200 AP-inducing field stimuli. Responsive terminals were selected by an automated criterion (see Fig. 8). Distributions of the FM1-43 uptake amounts in the two groups indicate that AP-stimulation results on average in 40 % more synaptic FM1-43 uptake than miniature activity during 10 min. For comparison, each histogram is scaled to its maximal bin value (bin size = 2.5 pixel value).

(2 Hz) stimulus train (in 2.5 mM $[Ca^{2+}]_o$, 1.0 mM $[Mg^{2+}]_o$) was determined (Fig. 11 A & B). Over this time period, we observed a linear decrease in FM1-43 fluorescence in both groups (linear regression; $r = -1.0$; $p < 0.0001$), indicating that little depression occurred (Fig. 11 B). To determine whether differences in FM1-43 release rates between terminals were attributed to non-specific dye loss, we analyzed FM1-43 fluorescence changes during a baseline period identical in length (15 s) to that one used for calculation of AP-evoked FM1-43 release (see Fig. 7, and Methods). We found unspecific FM1-43 fluorescence decrease during a 15 s baseline period to be relatively small (0.16 % for miniature loaded synapses; 0.55 % for AP-loaded controls) compared to the decrease observed during 15 s of 2 Hz field stimulation (12.1 % for miniature loaded synapses; 9.8 % for AP-loaded controls). Moreover, as our analysis showed no positive correlation between FM1-43 baseline changes and evoked release (correlation coefficient $r = -0.18$ for miniature-loaded synapses; $r = -0.18$ for AP-loaded synapses), evoked release rates were not corrected for baseline variation.

Absolute amounts of FM1-43 release from vesicle pools depend on the degree of vesicle pool loading (see Appendix, Equation 2). As vesicle pool loading was expected to differ between the different loading protocols (Fig. 10), we normalized stimulus-evoked FM1-43 fluorescence changes (ΔF) to baseline fluorescence (F) for each terminal (Fig. 11 A & B) (see Appendix, Equation 2). Using the initial normalized rate of release ($\Delta F/F$ during 15 s of 2 Hz field stimulation), we were able to pool data from a large number of experiments ($n = 22$ miniature-loaded; $n = 19$ AP-loaded) in each group. Comparison of the AP-evoked release rates between miniature-loaded and AP-loaded synapses showed that ($n = 842$) synapses with high levels of miniature activity released significantly more FM1-43 per stimulus than ($n = 1014$) control sites loaded by APs (24 % difference; $p < 0.0001$) (Fig. 11 C).

Calcium dependency of enhanced release at synapses with high miniature synaptic activity

As our data suggested that synapses with high miniature synaptic activity release more FM1-43 per stimulus than control synapses, we further characterized this relationship under conditions expected to change release probability. Therefore, $[Ca^{2+}]_o$ was altered to 1.0 and 5.0 mM to either reduce or increase release probability

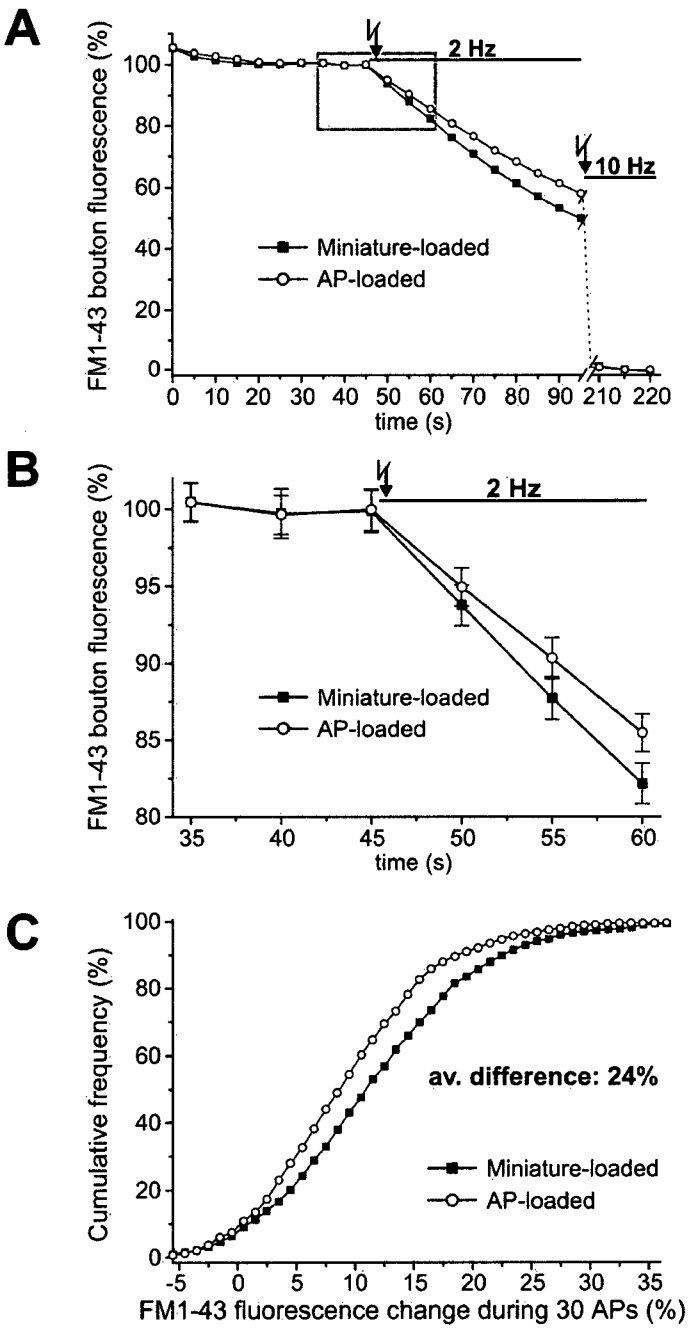

Fig. 11 Synapses with high miniature synaptic activity show significantly enhanced AP-dependent vesicular release

A) AP-evoked FM1-43 release was monitored at two groups of synaptic terminals loaded by distinct protocols. Average FM1-43 terminal fluorescence versus time for (n = 842) synapses loaded under miniature activity promoting conditions (Mini-loaded) and (n = 1014) control synapses loaded by APs (AP-loaded). Terminals were unloaded by a 2 and 10 Hz AP-producing stimulus protocol in 2.5 mM $[Ca^{2+}]_o$ (see Fig. 7). Background fluorescence remaining after a 10 Hz AP train (1200 stimuli) was subtracted from each terminal and terminal fluorescence was normalized to FM1-43 loading (average baseline fluorescence between 35-45 s). Lightning bolt depicts onset of AP-inducing electrical field stimulation. **B)** Magnification of FM1-43 fluorescence traces in boxed region from (A). AP-evoked FM1-43 release at each synapse during 30 APs was calculated by averaging data points from 50-60 s and subtracting this value from the FM1-43 loading (= 100 %). Bars depict SEM. **C)** Cumulative frequency plot shows that evoked FM1-43 release is shifted towards higher release values at miniature-loaded sites as compared to AP-loaded controls.

($P_{rel.}$), respectively. In these experiments (as for the experiments in 2.5 $[Ca^{2+}]_o$) FM1-43 baseline fluorescence variation did not contribute significantly to the rates of FM1-43 release during stimulation. As expected, we found that decreasing $[Ca^{2+}]_o$ from 2.5 to 1.0 mM (n = 8 experiments) reduced the average AP-dependent FM1-43 release significantly in both miniature-loaded (by 25 % ; $p < 0.005$; n = 335) and AP-loaded (by 34 % ; $p < 0.001$; n = 822) synapses (Fig. 12 A & B). Conversely, increasing $[Ca^{2+}]_o$ from 2.5 to 5.0 mM (n = 12 experiments) significantly enhanced AP-dependent release in miniature-loaded (by 24 % ; $p < 0.001$; n = 440) and AP-loaded (by 43 % ; $p < 0.001$; n = 603) terminals (Fig. 12 C & D). These results suggest that $P_{rel.}$ could be altered in a $[Ca^{2+}]_o$-dependent fashion.

We then analyzed how $[Ca^{2+}]_o$ affected the difference in unloading rates between synapse populations loaded by miniature activity vs. (AP-loaded) controls. When decreasing $[Ca^{2+}]_o$ to 1 mM during stimulation, we observed a significant difference in the mean release rate (mean difference: 39 % ; $p < 0.0001$, unpaired t-test) between the two groups (Fig. 12 A & B). This mean difference (39 %) exceeded the one obtained when comparing unloading between the groups in 2.5 mM $[Ca^{2+}]_o$ (24 % ; see Fig. 11). Conversely, elevating $[Ca^{2+}]_o$ to 5 mM during stimulation reduced the difference in mean release rates between groups to a non-significant level (mean difference: 7 % ; $p > 0.05$, unpaired t-test) (Fig. 12 C & D). While the AP-dependent unloading rates of controls increased by on average 85 % when elevating $[Ca^{2+}]_o$ from 1 to 5 mM, the unloading rates of miniature-loaded sites increased at the same time by only 45 %. This data suggests that synapses with high levels of miniature activity possess on average a high initial $P_{rel.}$ (compared to controls) that restricts further increases by elevation of $[Ca^{2+}]_o$.

The probability for miniature and AP-dependent release is correlated at single synapses

To more directly determine the relationship between miniature and evoked release probability, we designed experiments to directly measure both parameters at the same synapse (see Methods; Fig. 13 A). Therefore, synapses were first loaded using a field stimulation protocol (four 10 Hz trains of 300 APs) that was expected to saturate vesicle pools with FM1-43 (Ryan and Smith, 1995) and then unloaded by field

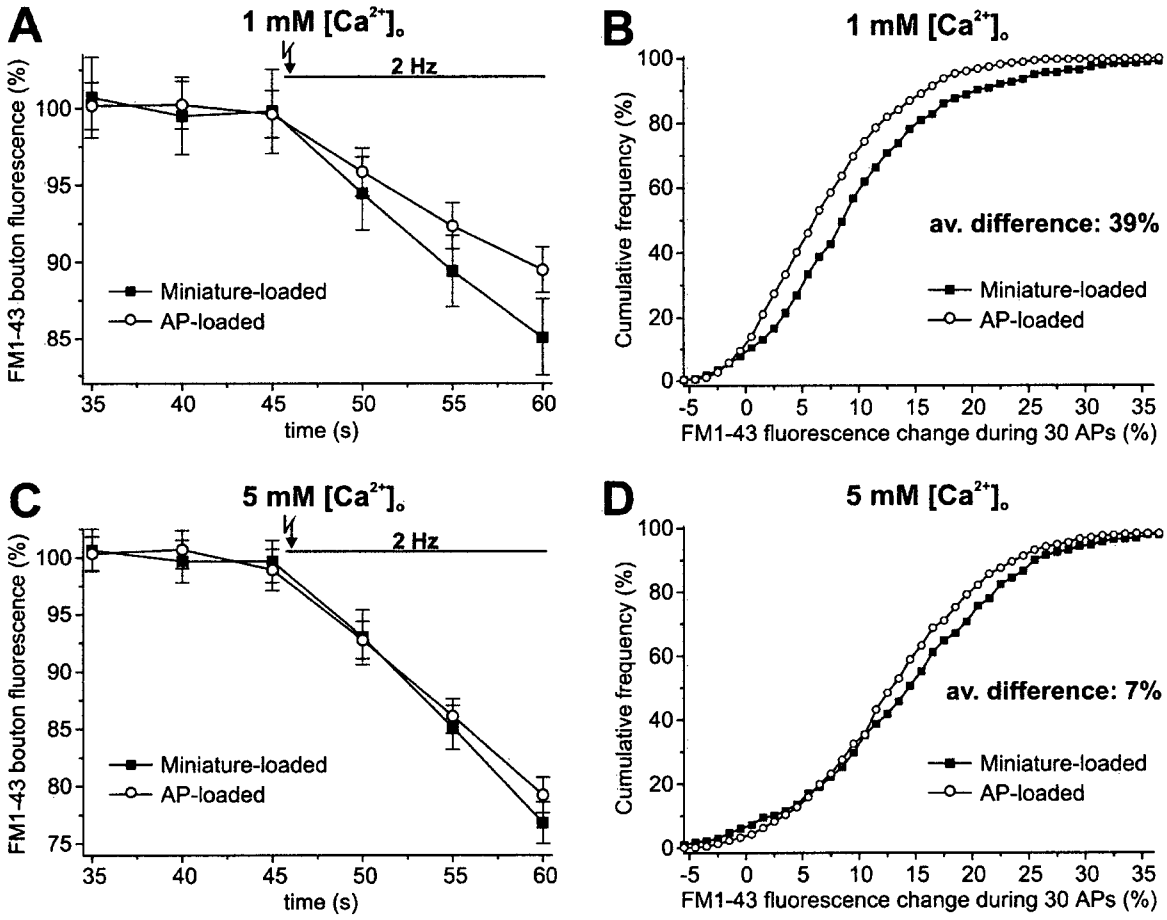

Fig. 12 The difference in release rates between synapses with high miniature activity and controls is dependent on $[Ca^{2+}]_o$

FM1-43 loading was performed for two groups of synaptic terminals using specific loading protocols as described above (see Fig. 7). For AP-evoked FM1-43 unloading, $[Ca^{2+}]_o$ levels were changed to alter release probability as indicated. **A) & B)** Conditions of reduced release probability (1.0 mM $[Ca^{2+}]_o$). Average trace (A) and cumulative frequency plot (B) of FM1-43 release during the first 15 s of AP-producing field stimulation. The difference in the average release rate between sites loaded by high miniature activity (Miniature-loaded) and (AP-loaded) controls is 39.1 % ; it is larger than the difference in 2.5 $[Ca^{2+}]_o$ (compare to Fig. 11). **C) & D)** Conditions of high release probability (5.0 mM $[Ca^{2+}]_o$). Averaged trace (C) and cumulative frequency plot (D) of FM1-43 release during the first 15 s of stimulation. The average FM1-43 release rate is not significantly different between the groups (7 % ; $p > 0.05$; unpaired t-test). Lightning bolt depicts onset of AP-inducing field stimulation. Bars depict SEM.

stimulation (Fig. 13 A Trial 1). Consecutively, the same synapse population was exposed to FM1-43 under miniature activity promoting conditions (Fig. 13 A Trial 2). An automated procedure selected synapses for analysis that showed both significant AP-dependent and -independent FM1-43 turnover (see Methods). This approach allowed us to independently measure AP-dependent $P_{rel.}$ (i.e. the amount of FM1-43 release in response to field stimulation) and miniature $P_{rel.}$ (i.e. the amount of FM1-43 uptake by miniature activity = P_{mini}) at the same synapse (see Appendix, Equations 3 and 4).

Using this protocol, we were able to identify presynaptic terminals that loaded FM1-43 into their vesicle pools with both AP-stimulation and miniature activity (n = 143 terminals; 7 experiments). Analysis of the stimulus evoked dye release at these sites demonstrated a significant positive correlation ($r = 0.59$; $p < 0.0001$) between AP-dependent release probability ($P_{rel.}$; FM1-43 released during 15 s of 2 Hz stimulation) and miniature frequency (P_{mini}; FM1-43 uptake during 10 min exposure in high $[Ca^{2+}]_o$ / TTX) at single terminals (Fig. 13 B). A similarly positive correlation between $P_{rel.}$ and P_{mini} ($r = 0.58$; $p < 0.0001$) was found when normalizing the FM1-43 release amounts to the median value in each trial before pooling the data (data not shown), indicating that the relationship was not caused by differences in absolute release amounts between experiments. These findings suggested that AP-evoked release and AP-independent miniature release are co-regulated at synaptic terminals.

Miniature activity and AP-dependent release probability are functions of vesicle pool size

As outlined above (and see Methods), we used a field stimulus protocol that was expected to result in complete loading of synaptic vesicle pools (Ryan and Smith, 1995) (Fig. 13 A) to provide us with a measure of vesicle pool size, and thus synapse size (Henkel et al., 1996). Using this approach, we estimated the size of the (n = 143) presynaptic terminals that were consecutively re-loaded in a miniature activity-promoting medium (see above section, Fig. 13 A). Comparison between this measure of synapse size (the total amount of releasable fluorescence) and the measure of miniature frequency (the amount of FM1-43 uptake by miniature activity = P_{mini}) indicated that both parameters were significantly correlated ($r = 0.64$; $p < 0.0001$) at single synaptic sites (Fig. 14). This suggested that the size of the synaptic terminal is

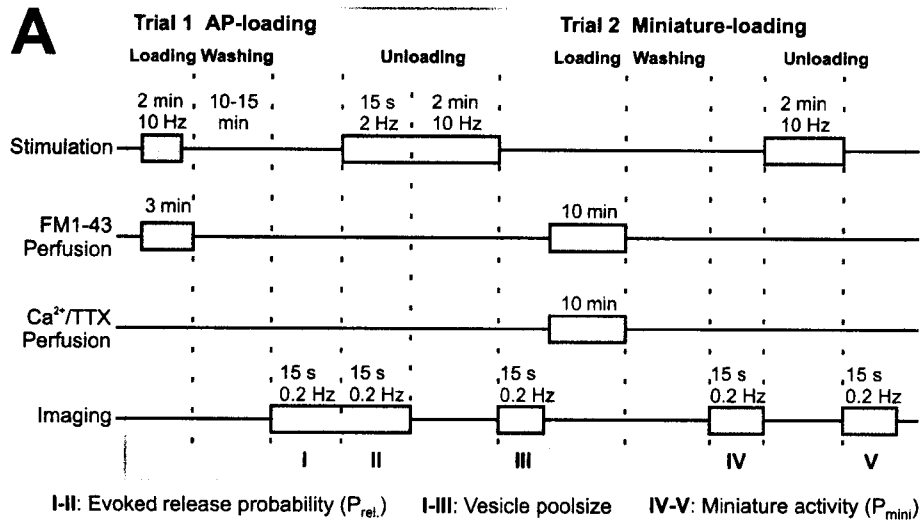

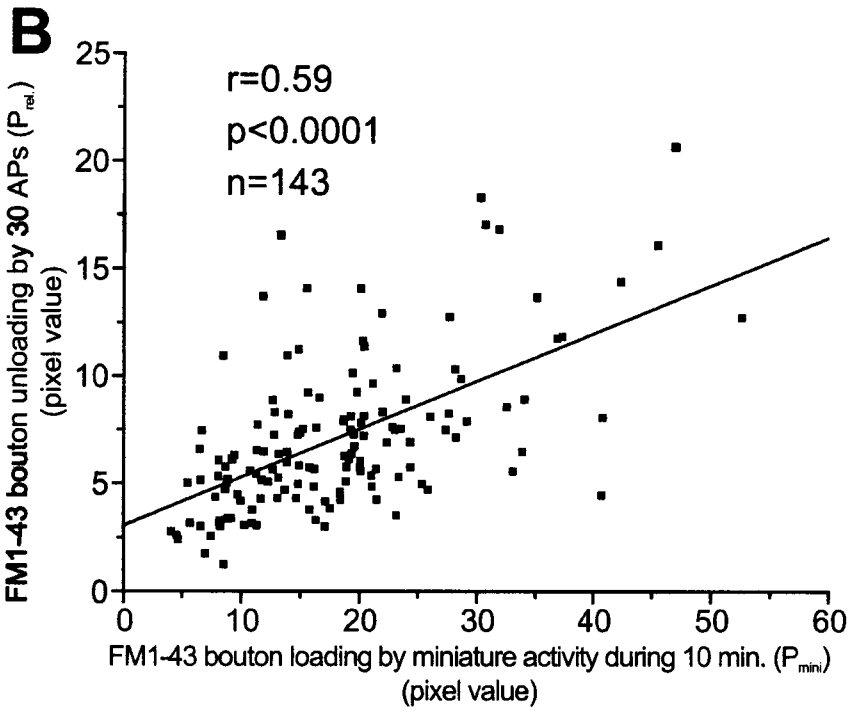

Fig. 13 Measures of AP-evoked release probability and miniature release probability are positively correlated at single synaptic terminals

A) Synaptic terminals were loaded with FM1-43 using a large number of AP-inducing field stimuli (4 x 300) to saturate vesicle pools (Trial 1 "AP-loading"). After washing, the change in FM1-43 fluorescence during 30 APs was recorded as a measure of evoked release probability ($P_{rel.}$). After this measurement, the same synapse population was re-loaded with FM1-43 under miniature activity promoting conditions (5 mM Ca^{2+} / 0.6 µM TTX) for 10 min (Trial 2 "Miniature-loading"). The amount FM1-43 fluorescence uptake during that time was a measure of the synapses probability of miniature activity (P_{mini}). An automated criterion was applied to select responsive from non-responsive sites in both trials (see Methods). **B)** A significant positive correlation between P_{mini} and P_{evoked} ($r = 0.59$; $p < 0.0001$) was observed at ($n = 143$) synaptic terminals (7 experiments).

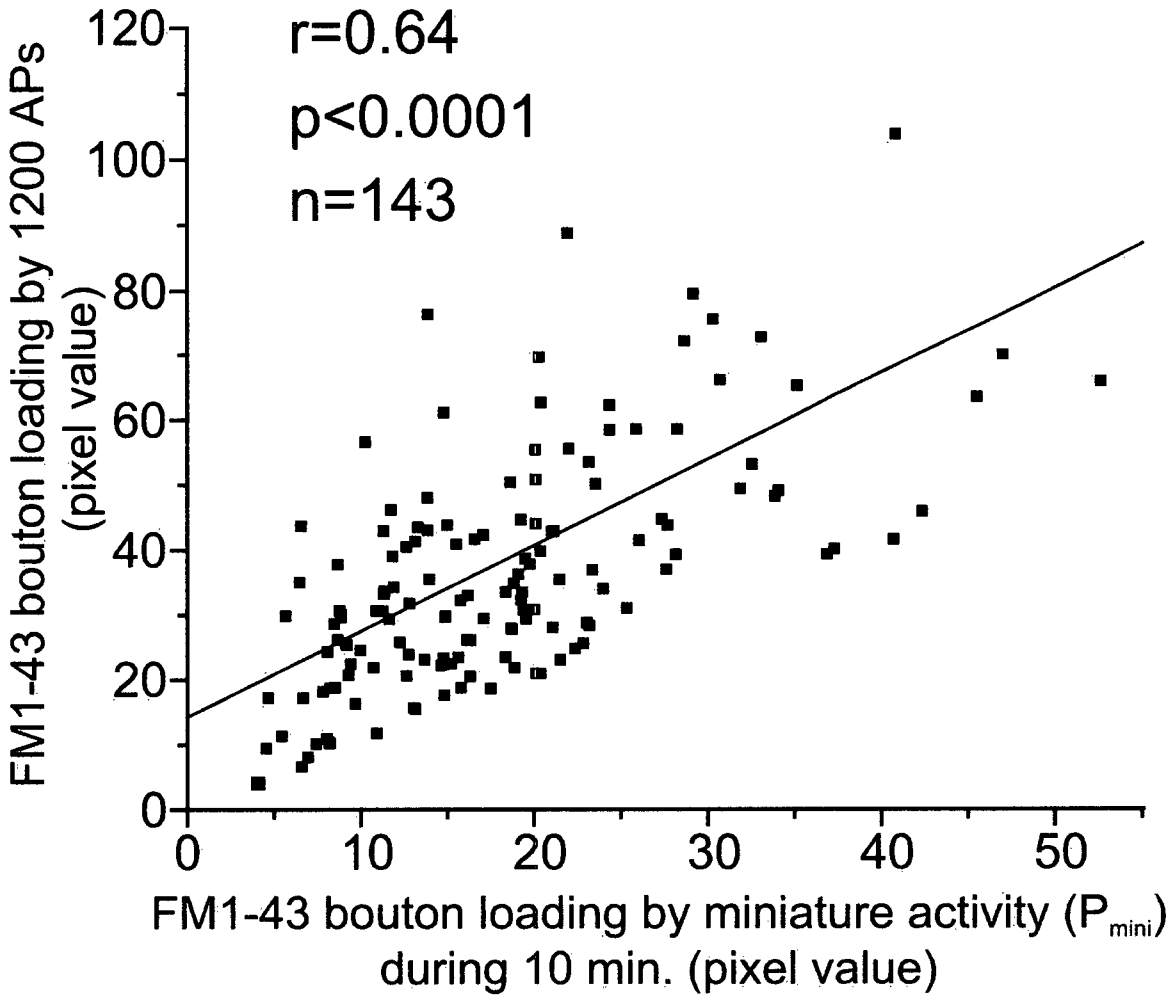

Fig. 14 The probability for miniature activity is positively correlated with a measure of terminal size

Data from the same experiments shown in Fig. 13. A significant positive correlation ($r = 0.64$; $p < 0.0001$) is found between the amount of FM1-43 uptake during 10 min incubation in a miniature activity promoting medium (P_{mini}) and the amount of FM1-43 loading by 1200 APs, a measure of terminal size.

related to the extent of spontaneous release and, hence, that larger synapses on average possess higher levels miniature synaptic activity. A similar correlation was found between synapse (vesicle pool) size and AP-dependent release probability at single synaptic terminals ($r = 0.57$; $p < 0.0001$; data not shown), confirming previously reported findings (Rosenmund and Stevens, 1996; Murthy et al., 1997).

As the vesicle pool size of a synapse is inversely proportional to its fractional release rate (see Appendix, Equation 2) we compared vesicle pool sizes between terminals with high rates of miniature synaptic activity and a control population. This comparison is important since the reported difference in fractional release rates (see Figs. 11 and 12) could potentially be caused by a systematic difference in the average pool size of the groups (see Appendix, Equation 2). Therefore, from the experiments shown in Figs. 13 and 14 a control population of synapses was selected solely based on its FM1-43 unloading response to AP-inducing field stimulation (Fig. 13 A Trial 1). The synaptic vesicle pool size of this group was compared to the pool size of synapses that, in addition to fulfilling the response criterion for controls, also exhibited significant FM1-43 uptake with miniature activity in the re-loading trial (Fig. 13 A Trial 2). This experiment differs from those presented in Figs. 11 and 12 in that synapses with high miniature activity and control synapses were selected from the same culture (synapse population) and were loaded using identical protocols. After normalizing the AP-mediated FM1-43 fluorescence release to the amount of loading (see Appendix, Equation 2), we found that sites with high miniature activity release 20 % more FM1-43 during 30 pulses of 2 Hz AP-stimulation than the control group ($p < 0.0001$, unpaired t-test). This value is comparable to that reported comparing sister cultures loaded with different protocols (24 %, see Fig. 11 C). This finding confirms that the proportionality between release probability and vesicle pool size (see Appendix Equation 2) differs between the groups of synapses with high miniature activity and controls. Furthermore, comparison of the average vesicle pool size between these two groups demonstrated that vesicle pools were significantly larger at synapses with high miniature activity (difference in size: 29 % ; $p < 0.0001$, Mann-Whitney test) (Fig. 15 A). This indicates that the difference in the fractional release rates between synapses with high miniature activity and control synapses cannot be accounted for by a relative larger size of control synapses. In fact, the relatively larger average size of miniature-loaded terminals (compared to controls) suggests that the difference in $P_{rel.}$

between the groups (calculated based on fractional release rates; see Appendix, Equation 2) is likely an underestimate, since fractional release in inversely proportional to pool size. Accordingly, we compared the absolute amounts of evoked FM1-43 release during AP-stimulation between the two groups. Absolute FM1-43 release is a measure for $P_{rel.}$ that is not influenced by the synapse's vesicle pool size (see Appendix, Equation 3). This comparison showed that terminals with high rates of miniature activity release on average 59 % more FM1-43 fluorescence per stimulus than the control group recruited from same population of synapses (Fig. 15 B).

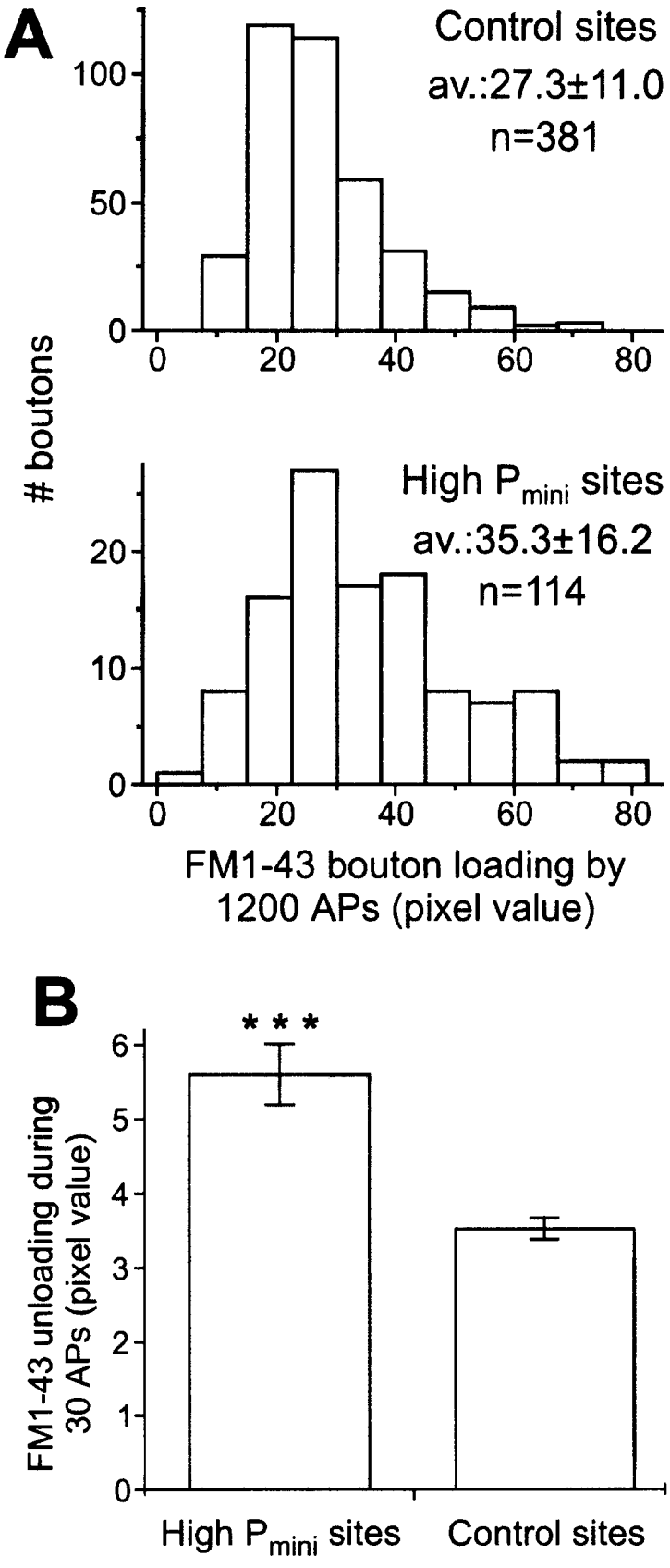

Fig. 15 Terminals with high levels of miniature synaptic activity possess larger vesicle pools and release more vesicles per stimulus train

Synapse (vesicle pool) size and release probability ($P_{rel.}$) were compared between two groups of terminals recruited from an identical population using the re-loading protocol described above (see Fig. 13 A). Both groups had to show FM1-43 uptake and release during AP-stimulation and were sorted based on their ability to re-load FM1-43 under miniature synaptic activity promoting conditions. To pass the automated selection procedure in each respective trial, the terminals' baseline variation had to be < 10 % of its total releasable fluorescence (see Fig. 8). **A)** Histograms of terminal sizes measured by FM1-43 terminal loading with 1200 APs (bin size = 7.5

pixel values). Upper panel: terminal sizes of control sites (n = 381) that were selected based on their response to field stimulation. Lower panel: terminal sizes of synapses (n = 114) that, in addition to matching the criterion for the control group, showed significant FM1-43 uptake under miniature activity promoting conditions (high P_{mini} sites). Significant difference (29 % , $p < 0.0001$, Mann-Whitney test) in the average terminal size between the two groups. **B)** The average amount of FM1-43 release in response to 30 APs was compared between the two groups in shown in A. Note that this measure of $P_{rel.}$ is independent of terminal size (see Appendix, Equation 3). Evoked FM1-43 release is increased by 59 % ($p < 0.0001$, Mann-Whitney test) at terminals with high miniature synaptic activity (high P_{mini} sites) compared to controls.

DISCUSSION

We have used confocal imaging of the vesicular turnover marker FM1-43 to study evoked transmitter release at synapses with high rates of miniature synaptic activity. Using this experimental approach to directly measure transmitter release rather than its postsynaptic effect, we were able compare the AP-dependent release efficacies among single synaptic sites. The use of FM1-43 as a vesicle-turnover marker has two important advantages for our study: it allowed us 1) to selectively stain synapses with high miniature activity; and 2) to compare the release rates between individual synapses under conditions that are not affected by postsynaptic responsiveness. Our results indicate that synapses with high rates of miniature activity possess on average enhanced AP-evoked release probabilities when compared to controls. Furthermore, by directly measuring both the probability of miniature synaptic activity and AP-evoked release at the same synapse, we find that the two parameters are significantly correlated. These findings suggest a co-regulation of miniature synaptic activity and AP-evoked release probability at presynaptic terminals. Therefore, miniature rates may indicate the readiness of the vesicle release machinery to discharge a transmitter quantum in the presence of an appropriate stimulus that is common for both forms of release.

Miniature synaptic activity has been well described in the CNS and PNS. However, it remains to be shown whether miniature synaptic activity serves a specific function in synaptic transmission or is just a stochastic process. As miniature synaptic activity is modifiable (Malgaroli and Tsien, 1992; Chavis et al., 1998), it argues for the first point. Furthermore, recent findings indicate that at some synapse types miniature activity is involved in the developmental formation (Gottmann et al., 1994; O'Brien et al., 1997) as well as in the structural maintenance of synaptic connections (McKinney et al., 1999). As rates of miniature synaptic activity are up-regulated following the induction of short-term (Kamiya and Zucker, 1994; Cummings et al., 1996; review in Zucker, 1996; Fisher et al., 1997) and long-term (Minota et al., 1991; Malgaroli and Tsien, 1992; Arancio et al., 1995; but see Cormier and Kelly, 1996; Tong et al., 1996; Chen and Regehr, 1997) synaptic enhancement, a possible role for miniature release could be the selective maintenance of such synaptic connections that have received context relevant priming in an activity- (AP-) dependent fashion.

There are additional findings indicating that miniature and evoked release probability are co-regulated at synaptic terminals. For example, inhibition of synaptotagmin in cholinergic synapses (Mochida et al., 1997), activation of muscarinic receptors on GABAergic neurons (Baba et al., 1998), BDNF treatment of hippocampal cells (Li et al., 1998), and activation of cannabinoid receptors on Purkinje cells (Levenes et al., 1998) all induce parallel modulation of miniature and evoked release rates. Our results support findings of an activity-dependent co-regulation of both miniature and evoked transmitter release by showing 1) that synapses with high miniature activity possess on average significantly enhanced AP-dependent release rates (Figs. 11, 12 and 15 C); and 2) that there exists a correlation between miniature and evoked release probability at single synapses (Fig. 13 B).

Miniature release can be regulated in a $[Ca^{2+}]_i$-independent manner by agents that directly affect the presynaptic release machinery, e.g. alpha-latrotoxin (Ceccarelli et al., 1988; Capogna et al., 1996b) or ruthenium red (Trudeau et al., 1996). However, under physiological conditions, a strong $[Ca^{2+}]_i$-dependence of miniature synaptic activity is well documented (Matthews and Wickelgren, 1977; Marcus et al., 1992; Doze et al., 1995; Katz et al., 1995; Scanziani et al., 1995; Capogna et al., 1996a; Poisbeau et al., 1996; Capogna et al., 1997; Schoppa and Westbrook, 1997; Bao et al., 1998; Li et al., 1998). Using somatic recordings, we confirmed these findings by showing significantly enhanced rates of miniature activity after the elevation of $[Ca^{2+}]_o$ from 0 to 5 mM (see Results). Accordingly, we found that $[Ca^{2+}]_o$ elevation from 0 to 5 mM lead to a significant increase in the number of terminals that were labeled by FM1-43 with miniature synaptic activity. These results are consistent with findings by Chavis et al. (Chavis et al., 1998) and Ma et al. (Ma et al., 1999) suggesting that activation of the cAMP-dependent protein kinase PKA, a downstream target of Ca^{2+}, induces vesicular cycling at previously inactive uptake sites. A small number of synapses (~1 %), however, showed continued high rates of FM1-43 uptake by miniature activity under nominally $[Ca^{2+}]_o$-free conditions comparable to those rates achieved in high $[Ca^{2+}]_o$. This surprising finding indicates that a sub-population of synapses can sustain high rates of miniature activity even in low $[Ca^{2+}]_o$. The inability to resolve a difference in the amount of FM1-43 uptake between the two groups loaded in high vs. low $[Ca^{2+}]_o$ may be attributed to the use of

an automated criterion which selects synapses only if they show a sufficient signal-to-noise ratio (see Methods).

In contrast to AP-dependent release (Haage et al., 1998), Ca^{2+} seems to mediate its effects on miniature release by entry through low-threshold rather than high-threshold VGCCs (Parfitt and Madison, 1993; Momiyama and Takahashi, 1994; Scanziani et al., 1995; Bao et al., 1998), indicating the existence of differential control mechanisms over both forms of transmitter release. Moreover, Ca^{2+} does not seem to act directly on the release machinery to mediate miniature release, but rather indirectly through activation of second messenger systems such as PKC (Malenka et al., 1986; Parfitt and Madison, 1993; Capogna et al., 1995; Carroll et al., 1998; Stevens and Sullivan, 1998b) and PKA (Chavez-Noriega and Stevens, 1994; Capogna et al., 1995; Carroll et al., 1998; Chavis et al., 1998). Kondo and Marty (Kondo and Marty, 1997) and Chen and Regehr (Chen and Regehr, 1997) show that PKA activation alone is sufficient to stimulate miniature synaptic release even in the absence of $[Ca^{2+}]_o$. There are additional findings indicating the existence of molecular pathways that differentially affect miniature and evoked release, including the activation of nor-adrenaline (Kondo and Marty, 1998) and adenosine (Dittman and Regehr, 1996) receptors and the differential regulation of release machinery proteins (Deitcher et al., 1998; Hua et al., 1998). If differential mechanisms exist to independently regulate miniature and evoked transmitter release, how could a co-regulation of both forms of release be achieved? A plausible explanation would be an activity-dependent switch from separate to parallel regulation of miniature and evoked release. Such a switch could conceivably be triggered by a strong stimulus (e.g. pulse train) activating common intracellular second-messengers, e.g. PKA (Byrne and Kandel, 1996; Tong et al., 1996; Chavis et al., 1998; Lonart and Sudhof, 1998; Villacres et al., 1998) or PKC (Leahy et al., 1993; Ramakers et al., 1997; Majewski and Iannazzo, 1998). The hypothesis of an activity-dependent switch from separate to parallel regulation of evoked and miniature release is supported by findings showing that after parallel up-regulation of miniature and evoked release rates, miniature synaptic release also becomes sensitive to agents that block high-threshold VGCCs (Scanziani et al., 1995).

It has been suggested that a potential mechanism for controlling synaptic activity is the regulation of synaptic structure (Calverley and Jones, 1990; Bailey and Kandel, 1993; Lisman and Harris, 1993; Edwards, 1995; Harris and Sultan, 1995; Buchs

and Muller, 1996; Rusakov et al., 1997, Mackenzie, 1999 #780). Our results indicate that the degree of miniature synaptic activity is positively correlated with the size of the vesicle pool (Fig. 14), and thus the size of the synaptic terminal (Henkel et al., 1996). Correspondingly, we find that synapses with high levels of miniature activity are on average larger than synapses drawn from a control population (Fig. 15 A). These results confirm findings that show a similar relationship between synapse size and AP-dependent release efficacy (Murthy et al., 1997; Prange and Murphy, 1999). Furthermore, they suggest a model in which the frequency of miniature release can be controlled by the number of readily releasable and/or docked vesicles, both parameters which significantly correlate with terminal size (Dobrunz et al., 1997; Dobrunz and Stevens, 1997; Schikorski and Stevens, 1997). Hence, modifications of synaptic structure could build the anatomical basis for controlling evoked and miniature release rates.

APPENDIX

We have used the following equations to describe the relationship between stimulus-evoked FM1-43 release and release probability in our experiments:

Equation 1: $F_{rel.} = P_{rel.} \times (Ves._{FM1\text{-}43}/Ves._{total}) \times F_{ves.}$

Equation 1 describes the proposed relationship between the amount of FM1-43 released per stimulus ($F_{rel.}$), the proportion of FM1-43 loaded vesicles ($Ves._{FM1\text{-}43}$) to the total size of the vesicle pool ($Ves._{total}$), and the fluorescence of a single vesicle ($F_{ves.}$), a constant. The number of FM1-43 loaded vesicles ($Ves._{FM1\text{-}43}$) was expected to differ depending on the protocol used for FM1-43 loading (AP-loading vs. miniature-loading). Therefore, to compare the FM1-43 release rates between AP- and miniature-loaded groups the amount of FM1-43 release per stimulus ($F_{rel.}$) was normalized to the total amount of FM1-43 loaded vesicles ($Ves._{FM1\text{-}43}$) at each synapse:

Equation 2: $F_{rel.}(norm.) = (P_{rel.}/Ves._{total}) \times F_{ves.}$

Equation 2 was derived from Equation 1 by dividing by $Ves._{FM1\text{-}43}$ and shows that the normalized (fractional) rate of stimulus evoked fluorescence ($F_{rel.}(norm.) = F_{rel.}/Ves._{FM1\text{-}43}$) is directly proportional to the release probability ($P_{rel.}$) and inversely proportional to the total size of the vesicle pool ($Ves._{total}$).

Equation 3: $Frel. = Prel. \times Fves.$

Equation 3 shows the relationship between the amount of FM1-43 released per stimulus ($F_{rel.}$) and the release probability ($P_{rel.}$) for experiments in which a large number of stimuli (4 x 300) were used to saturate synaptic vesicle pools with FM1-43 (Ryan and Smith, 1995). In this case, the number FM1-43 loaded vesicles ($Ves._{FM1\text{-}43}$) would approach the total size of the vesicle pool ($Ves._{total}$) and, hence, amount of fluorescence released per stimulus ($F_{rel.}$) would be directly proportional to the release probability ($P_{rel.}$). This equation was derived from Equation 1 setting ($Ves._{FM1\text{-}43}$ / $Ves._{total}$) = 1.

Equation 4: $Fuptake = Prel. \times Fves.$

Equation 4 describes the relationship between the amount of FM1-43 uptake (F_{uptake}) and release probability ($P_{rel.}$) (see Equation 1 in (Murthy et al., 1997)). The Equation is essentially derived from Equation 3 by replacing $F_{rel.}$ by F_{uptake}. This can be done under the following conditions: 1) Vesicle exocytosis and endocytosis are matched, i.e. for each vesicle released one vesicle will be retrieved. This is most likely the case for $[Ca^{2+}]_o$ used in our experiments (Smith and Betz, 1996; Gad et al., 1998; Rouze and Schwartz, 1998). 2) FM1-43 loaded vesicles intermingle with the rest of the pool and are not preferably released. This has been indicated by Ryan and Smith (Ryan and Smith, 1995). 3) F_{uptake} is not maximal, so it is not limited by the pool size. This is most likely the case in experiments utilizing miniature activity for FM1-43 uptake, as even the highest miniature rates (~0.1 Hz; Wang et al., 1999) are not expected to turnover the entire vesicle pool during 10 min. Hence, in experiments analyzing absolute amounts of FM1-43 fluorescence uptake in a miniature-promoting medium, we have used F_{uptake} as a measure of miniature activity and thus miniature $P_{rel.}$, termed P_{mini}

IV. PSD-95 CLUSTERING IS ASSOCIATED WITH STABLE FILOPODIA DURING EARLY DEVELOPMENT OF CORTICAL NEURONS

ABSTRACT

The stability of filopodia and spines and the localization of the postsynaptic density (PSD) protein PSD-95 were studied during early development of cultured cortical neurons using time-lapse confocal microscopy. Neurons were transfected with recombinant green fluorescent protein (GFP)-conjugated forms of either wild type (WT) PSD-95 or a mutant (MUT) PSD-95 that fails to form synaptic clusters (Craven et al., 1999). In WT PSD-95/GFP expressing neurons, we find that filopodia and spines with PSD-95/GFP clusters are significantly more stable (i.e. do not turn over) than those lacking clusters during 1 h of imaging. When comparing younger (average: 8 days *in vitro*) to older (average: 14 days *in vitro*) neurons we find a significant increase in stable filopodia and spines in both WT and MUT PSD-95/GFP expressing cells. These results suggest that although PSD-95 is associated with stable filopodia and spines, it alone is not sufficient to induce stabilization. In neurons of the younger age group we observe that ~ 10 % of PSD-95 clusters undergo rapid modular translocation into and/or out of filopodia and spines. We conclude that the trafficking of prefabricated PSD-95 clusters into filopodia is a developmentally regulated process that is associated with the stabilization of these structures.

INTRODUCTION

The postsynaptic density (PSD) protein PSD-95 is a founding member of the growing superfamily of PDZ (PSD-95, Disklarge, ZO1/ZO2) domain containing proteins (Craven and Bredt, 1998; Fanning and Anderson, 1999; Garner et al., 2000). The shared structural feature of these proteins, the PDZ domain, is made up of a repetitive sequence motif of ~90 amino acids that binds almost exclusively to C-terminal consensus sequences of target proteins. Some PDZ-proteins (e.g. SAP90/PSD-95, CASK/LIN-2) contain additional protein-protein interaction sites like src-homology 3 (SH3) and/or guanylate kinase (GK) domains, whereas other PDZ proteins (e.g. GRIP/ABP, PICK-1) lack these. Common to most PDZ-proteins is their function in the structural and functional organization of signaling complexes at pre- and postsynaptic elements through protein-protein interactions (Garner et al., 2000; Scannevin and Huganir, 2000).

PSD-95 is an integral protein of the postsynaptic density (PSD) at excitatory synapses. Binding partners of PSD-95 include the NMDA (via PDZ1&2) and Kainate (via SH3) receptors and the cell adhesion molecule Neuroligin (via PDZ3). Furthermore, binding to the proteins CRIPT (via PDZ3) and GKAP (via GK) that can tether PSD-95 and its binding partners to the intracellular tubulin and actin lattice, respectively (Scannevin and Huganir, 2000). PSD-95 exhibits a clustered distribution which is dependent on palmitoylation of two cysteine residues in the 3 and 5 N-terminal positions of the protein (Craven et al., 1999). Studies in neuronal cell cultures have shown that during early postnatal development (between 1 and 3 weeks in vitro) PSD-95 clustering shifts from a mostly non-synaptic to a mostly synaptic pattern (Rao et al., 1998). It has been suggested that this shift is associated with formation, and possibly consolidation of early synaptic contacts (Rao et al., 1998; Garner et al., 2000). During the same developmental period dendritic morphology is characterized by long, finger-like and highly motile protrusions, so-called filopodia (Harris, 1999; Jontes and Smith, 2000). As a number of imaging studies have shown, filopodial motility significantly decreases during the first three weeks *in vitro* (Dailey and Smith, 1996; Ziv and Smith, 1996; Dunaevsky et al., 1999) and *in vivo* (Lendvai et al., 2000) paralleling the progress in synaptic localization of PSD-95 (Jontes and Smith, 2000). It

has been suggested that this process of stabilization underlies the conversion of filopodia into more mature spines (Jontes and Smith, 2000; Parnass et al., 2000).

Currently it is still unknown what the consequences of localizing PSD-95 into filopodia are, and whether this localization is functionally related to the morphological stabilization of these structures. Here we use simultaneous time-lapse imaging of green fluorescent protein-labeled PSD-95 and of filopodial motility to test the hypothesis that PSD-95 clustering in filopodia is associated with stabilization of these processes.

METHODS

Cell culture and particle mediated gene transfer

Embryonic cortical neurons and glia were dissociated from 18 day old Wistar rat fetuses and cultured on poly-D-lysine coated 12 mm glass coverslips at a density of ~ 1.5 million cells/ml (Mackenzie et al., 1996). Cells were kept for 6-18 days in vitro (DIV) before use in experiments. Constructs encoding the following proteins were used: i) wild type (WT) full length PSD-95; ii) full length mutant (MUT) PSD-95/GFP in which the cysteine residues in the 3 and 5 N-terminal positions were changed to serine residues (cys3,5ser) (Craven et al., 1999). PSD-95 constructs were generated by PCR and subcloned into the HindIII and EcoRI of GW1 (British Biotechnology) (Topinka and Bredt, 1998); GFP was subcloned in-frame at the C terminus of PSD-95 at the EcoRI site. For particle mediated biolistic gene transfer cDNA constructs were ligated onto 0.6 μm gold microcarriers at a ratio of 1 μg DNA / 1 mg gold. Biolistic gene transfer was performed on cell cultures at 3-6 (average: 3.5 ± 0.2) DIV using a Bio-Rad Helios gene gun (Bio-Rad Microscience Ltd, Herts, UK) with helium pressure adjusted to140-160 psi and cultured for at least 3 more days after transfection. For experiments cells were sorted into two in vitro age groups. The first group consisted of cells at an average age of 7.9 ± 0.3 DIV (range: 6 - 10 DIV, n = 26 cells); the second group of cells cultured for 14.2 ± 0.4 DIV on average (range: 12 - 18 DIV; n = 15 cells). For simplicity in the paper we refer to the young and old cultures by their average age in vitro (8 and 14 DIV respectively).

Imaging and Electrophysiology

Coverslips were placed into a customized perfusion chamber (~ 500 μl vol.) and fixed by platinum weights to prevent movement. The cultures were continuously perfused (~ 1.5 ml/min) with a Hanks balanced salt solution (HBSS) containing (in mM) 137 NaCl, 10.0 Na^+-HEPES, 22.0 glucose, 5.0 KCl, 0.34 $Na_2HPO_4(7H2O)$, 1.0 $NaHCO_3$, 2.5 $CaCl_2$, 1.0 $MgSO_4$ at pH 7.4 and ~ 305 mosm. The solution was heated to 32 °C using a flow-through heater (Warner Instrument Corporation, Hamden, CT). Whole cell patch clamp on GFP fluorescence positive cells was conducted using an Axon Instruments

Axopatch 200B amplifier (Axon Instruments, Foster City, CA) and 7-10 MΩ electrodes pulled from 1.5 mm glass capillaries. The patch pipette solution contained (in mM): 122 K^+gluconate, 20 NaCl, 5 Mg^{2+}-ATP, 0.3 GTP, and 10 HEPES, 100 μM EGTA, and 500 μM sulforhodamine 101 (Molecular Probes, Eugene, OR) (pH = 7.2). The solution was allowed to perfuse into cells during whole cell recording for 3 - 5 min. during which spontaneous postsynaptic currents were recorded. After that period, the electrode was carefully removed from the cell soma allowing the membrane to re-seal. The dye was allowed to equilibrate in the cell for at least 10 min. before imaging experiments were performed.

Confocal time-lapse microscopy was performed on a Bio-Rad MRC 600 system attached to an Olympus BX50WI upright microscope (Olympus, Tokyo, JP) using an Olympus 0.9 NA 60x water immersion objective. The confocal pinhole was set to 3 - 4 (Bio-Rad units) and two-channel imaging was performed in slow scan mode (without averaging). For data acquisition, every 5 - 8 minutes a (vertical) Z-series was taken over an area of 96 x 128μm (384 x 512 pixels) containing the full thickness of the dendrite of interest. The spacing of successive Z-images was 1 μm. This provided sufficient optical overlap between consecutive sections as the optical depth of field was determined to be 2 μm at pinhole setting 3 (Bio-Rad units) using a fluorescent point source of light. The number of Z-images acquired ranged from 3 - 7 but was always constant within one experiment. To correct for potential vertical movement of the specimen between time points, all Z-series in one experiment were started from a marker point chosen within the first optical plane.

Immunohistochemistry

For quantifying co-localization of PSD-95 clusters with presynaptic markers, cell cultures expressing WT PSD-95/GFP were fixed in paraformaldehyde (PFA) at either 8 or 14 DIV. Cell cultures were immunolabeled using a mouse (IgG) monoclonal antibody (AB) against synaptophysin (Boehringer Mannheim GmbH, Germany) at 28 μg/ml (1:50), and an IgG polyclonal donkey-derived Texas Red-conjugated secondary AB (Jackson ImmunoResearch Laboratories, Inc., West Grove, PA) at 200ng/ml (1:50). Coverslips with immunostained cells were embedded in anti-fade (Molecular Probes, Eugene, OR) agent, and confocal dual-channel imaging was performed using a 100X Zeiss Fluar oil-immersion lens (Carl Zeiss, Oberkochen, Germany).

Analysis

For analysis of PSD-95 localization and filopodial stability, only cells were used that did not show any morphological signs of cellular degeneration or impending death (i.e. cell swelling and/or collective loss of filopodia) before, during, or after imaging. For each time point fluorescence data collected in a Z-series at was projected into one layer using the maximum intensity method. Two channel confocal images were separated offline into their respective channels (sulforhodamine-and GFP-signal) and coded. This procedure allowed analysis of filopodial-spine stability to be performed on the sulforhodamine signal (red channel) without knowledge of which construct (WT PSD-95, MUT PSD-95) the cells were transfected with. To be included for analysis, a filopodium-spine had to fulfill the following criteria: (i) being > 1 μm and < 10 μm in length, (ii) not contacting another process, (iii) not being extensively branched (< 3 branches), and (iv) being sufficiently filled with dye so that it is clearly visible throughout the entire period of imaging (~ 1 h). Processes that fit these criteria were not further subcategorized into either filopodia or spines, since unambiguous distinction by solely morphological criteria cannot be always made. The stability of each filopodium was judged by evaluating its status over 1 h of imaging. A filopodium-spine was defined as stable if it was present (visible) during the whole course of image acquisition. An unstable filopodium-spine either appeared new and/or disappeared during the time course of imaging. After this analysis, for each cell the Z-projection of the corresponding GFP-signal (green channel) was superimposed on the sulforhodamine (red channel) signal.

For WT PSD-95/GFP expressing cells, PSD-95 clustering was based on the data collected on the green channel. In spines and dendritic shafts the characteristics of each cluster were assessed throughout the period of imaging. In cases where clustering could not be unambiguously attributed to a specific accumulation of PSD-95/GFP rather than a volumetric effect of the dendritic process, the fluorescence intensity of a potential PSD-95/GFP cluster was divided by the fluorescence signal of an area adjacent to the cluster. This ratio was then compared to the fluorescence ratio between the same areas (obtained using the same co-ordinates) on the sulforhodamine (red) channel, which represents a volumetric marker. If the ratio obtained on the green channel was at least > 2X the ratio on the red channel the PSD/95-GFP clustering was concluded to be specific.

For analysis of co-localization between the Texas Red-conjugated antibody (AB)-labeled presynaptic marker synaptophysin (red channel) and PSD-95/GFP clusters (green channel) Z-series from both channels were superimposed. Synaptophysin and PSD-95/GFP clusters were considered co-localized and indicative of a putative synapse if they were present within the same focal plane and were overlapping by at least 0.4 μm (2 pixel rows).

For statistical analysis the non-parametric Mann-Whitney U test was used. Data are expressed as the mean ± the standard error of the mean (SEM).

RESULTS

We have used transfection of green florescent protein (GFP)-tagged postsynaptic density (PSD) protein PSD-95 constructs to examine the dynamics of filopodia and spines during development of primary cortical neurons. Biolistic particle mediated transfer of DNA constructs was performed at 3 - 6 (average: 3.5 ± 0.2; n = 41 cells) days after plating cell cultures. At this time, the total amount of endogenous PSD-95 and the degree of synaptic PSD-95 clustering is low (Rao et al., 1998). Hence, in transfected cells, GFP-tagged PSD-95 could exert its effect during the earliest stages of synaptic development. Transfection efficiency was generally low (< 1.0 %) using the biolistic gene transfer method. However, single transfected neurons could easily be identified by their strong GFP fluorescence (Fig. 16). Using polyclonal antibodies to PSD-95, we confirmed previous findings (El-Husseini et al., 2000a) demonstrating that PSD-95 was overexpressed by 5 - 10 fold in cells transfected with PSD-95/GFP constructs, when compared to untransfected neighboring cells (data not shown).

To assess the potential role of PSD-95 clustering in synapse development, maturation, and motility, we also transfected a mutant non-clustering form of PSD-95 into sister cultures of cortical neurons. In this mutant, cysteine residues in the 3 and 5 N-terminal positions were mutated to serine residues (cys3,5ser) preventing palmitoylation at these sites and abolishing correct synaptic targeting and clustering of the protein at PSDs. As previously shown (Craven et al., 1999), we find that the cys3,5ser mutant (MUT) PSD-95 is expressed diffusely throughout the neuronal soma and processes compared to the punctate PSD-95 distribution pattern in cells transfected with the construct for the GFP-tagged wild type (WT) form of PSD-95 (Fig. 16). Immunostaining indicated that the cys3,5ser mutant protein was overexpressed to a similar extent as the wild type PSD-95 (data not shown).

To simultaneously assess the localization of PSD-95 and the stability of filopodial processes, we have used patch-clamp techniques to inject a second fluorescence marker (sulforhodamine) with different spectral properties into neurons expressing PSD-95/GFP. This allowed us to reliably resolve filopodia and spines including ones that do not express the PSD-95/GFP protein (see Fig. 16, upper panel).

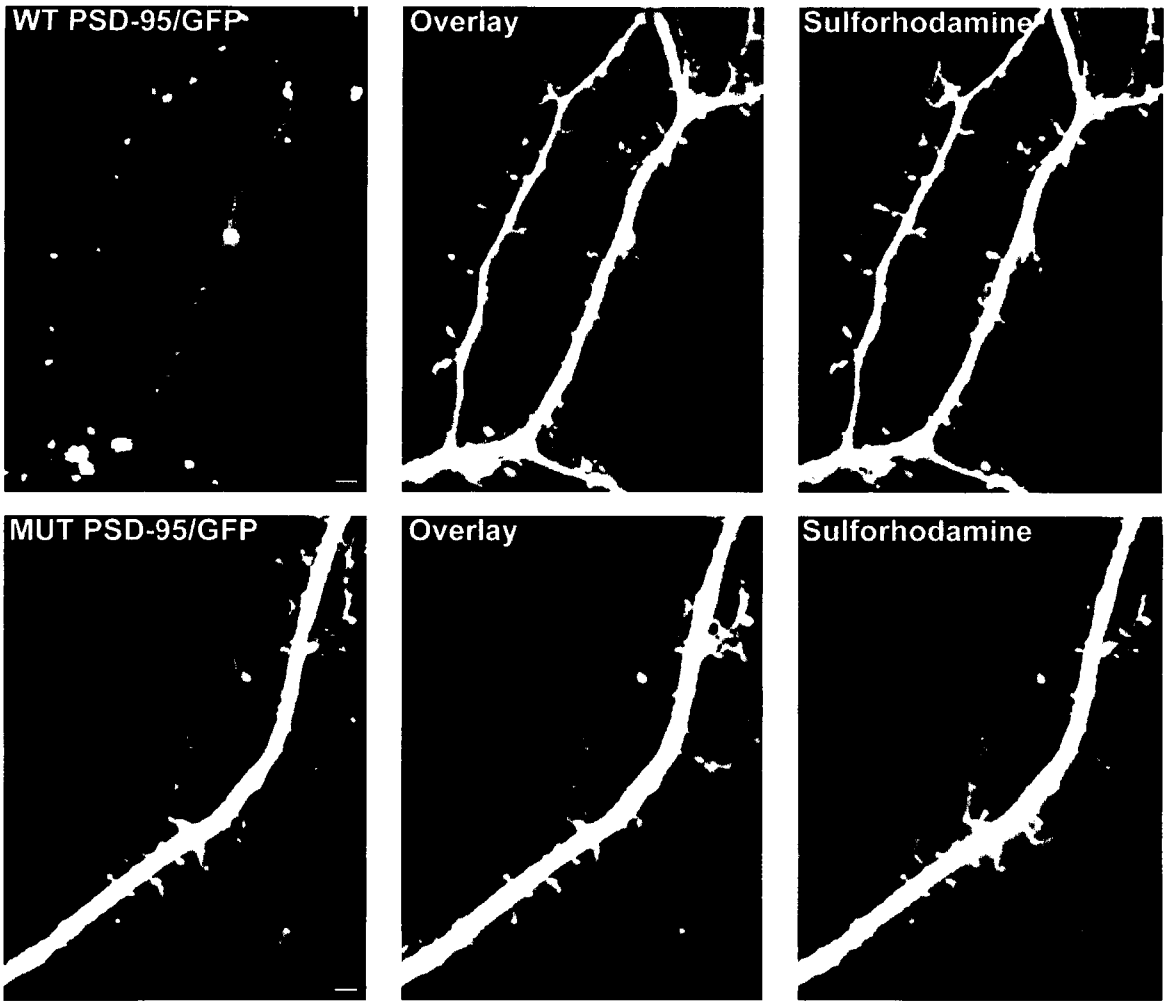

Fig. 16 Two channel confocal imaging to independently analyze PSD-95/GFP distribution and dendritic morphology

Cultured cortical neurons were transfected with green fluorescent protein (GFP)-tagged wild type (WT, upper panel row) or cys3,5ser mutant (MUT, lower panel row) forms of PSD-95. Prior to imaging, cells were co-labeled with sulforhodamine. Dual-channel confocal imaging was performed allowing the separation of the GFP (left panels) and sulforhodamine (right panels) signal. The middle panels show pseudo-colored composite images of the left and the right panels in their respective row; areas of GFP (green) and sulforhodamine (red) co-localization appear in yellow. Localization of PSD-95/GFP in dendritic shafts and spines is clustered in cells expressing WT PSD-95/GFP (upper row) and dispersed in cells expressing MUT PSD-95/GFP form (lower row). Cells were cultured for 13 days (upper panel) and 8 days (lower panel); bar = 5 μm.

At this early developmental stage it was often not possible to further sub-categorize processes into either filopodia or spines based solely on morphological features. Hence, we have used the term filopodia-spines to describe all dendritic protrusions of length > 1 μm and < 10 μm (see also Methods). Using two channel confocal microscopy double-labeled cells were imaged every 5 - 9 min over a time period of 60 - 65 min (Fig. 17). To insure that all filopodia-spines were captured within a particular dendritic segment, we collected serial Z-sections of 1 μm thickness over labeled dendrites, and produced a maximal intensity projection of each region. After imaging, two-color (PSD-95/GFP and sulforhodamine) fluorescence images were separated into their respective channels, time-lapse series were encoded, and analysis of filopodia-spine movement was performed using only the sulforhodamine (red) channel. This procedure ensured that analysis of filopodia-spine movement was done in an unbiased way without prior knowledge of PSD-95 disposition for particular spines or the type of construct introduced into a particular cell (WT or MUT PSD-95/GFP). Additionally, as the sulforhodamine signal approximates cytoplasmic volume, it was used to determine if apparent PSD-95/GFP clusters could be accounted for by regional differences in cytoplasmic volume or were due to specific clustering of protein. To examine the dynamics of PSD-95 clustering and its potential role during early synaptic development, we compared PSD-95 translocation and filopodium-spine motility at two different *in vitro* ages. Cells from the first group (labeled: 8 DIV) were studied at an average age of 7.9 ± 0.3 days *in vitro* (DIV) (range: 6 - 10 DIV; n = 26 cells), a period that is expected to correspond to the early onset phase of synaptogenesis (Lee and Sheng, 2000). The second group (labeled 14 DIV) consisted of cells at, on average, 14.3 ± 0.5 DIV (range 12 - 18 DIV; n = 15 cells), a developmental stage characterized by ongoing synapse formation (Ziv and Smith, 1996), stabilization of newly formed spines (Lee and Sheng, 2000), and enrichment of synaptic proteins within these structures (Rao et al., 1998).

First we compared the density of filopodia-spines between age groups. To do this we normalized the number of protrusions to the length of dendrite imaged for each cell. In neurons overexpressing WT PSD-95/GFP we found a significant increase (by 37 % ; $p < 0.05$) in the total number of filopodia-spines between cells at 8 DIV (125 ± 14 filopodia-spines per mm dendrite; 13 cells; n = 303 filopodia-spines) and at 14 DIV (171 ± 17 per mm dendrite; 10 cells; n = 440 filopodia-spines; $p < 0.05$) (Fig. 18).

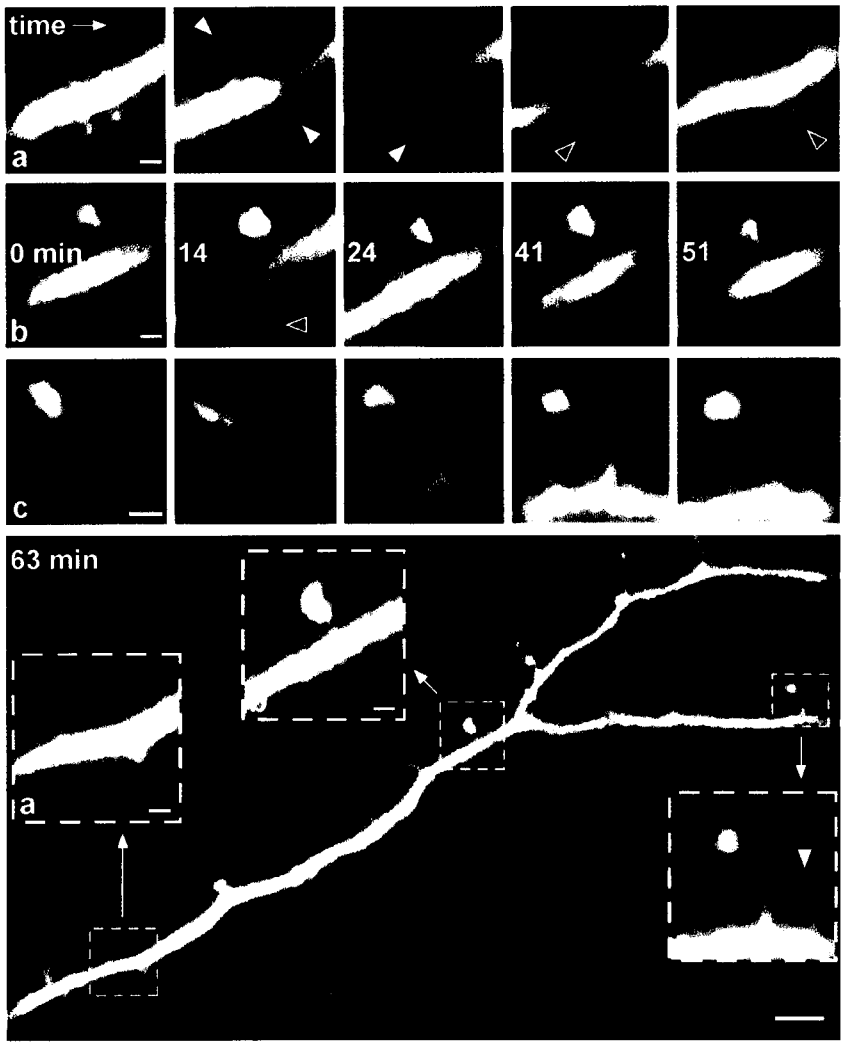

Fig. 17 Confocal time-lapse analysis of filopodia-spine stability and PSD-95 clustering

Time-lapse series of a neuron (10 days *in vitro*) expressing WT PSD-95/GFP (green) and filled with sulforhodamine (red). Spots of PSD-95/GFP clustering appear yellow. The lower panel shows an overview of the dendrite (bar = 5 µm). Three areas are magnified (see dashed outlines labeled a, b, and c). Time series in upper rows advances in columns from left to right for the three areas of interest; the second row shows time stamps in min. For simplicity, not every time point is shown. Newly forming (white arrowheads) and disappearing (black arrowheads) filopodia-spines are marked. Note that PSD-95/GFP containing structures are stable over time (i.e. they do not turn over), but can exhibit structural changes. Bar = 1 µm (magnified areas); bar = 5 µm (lower panel overview).

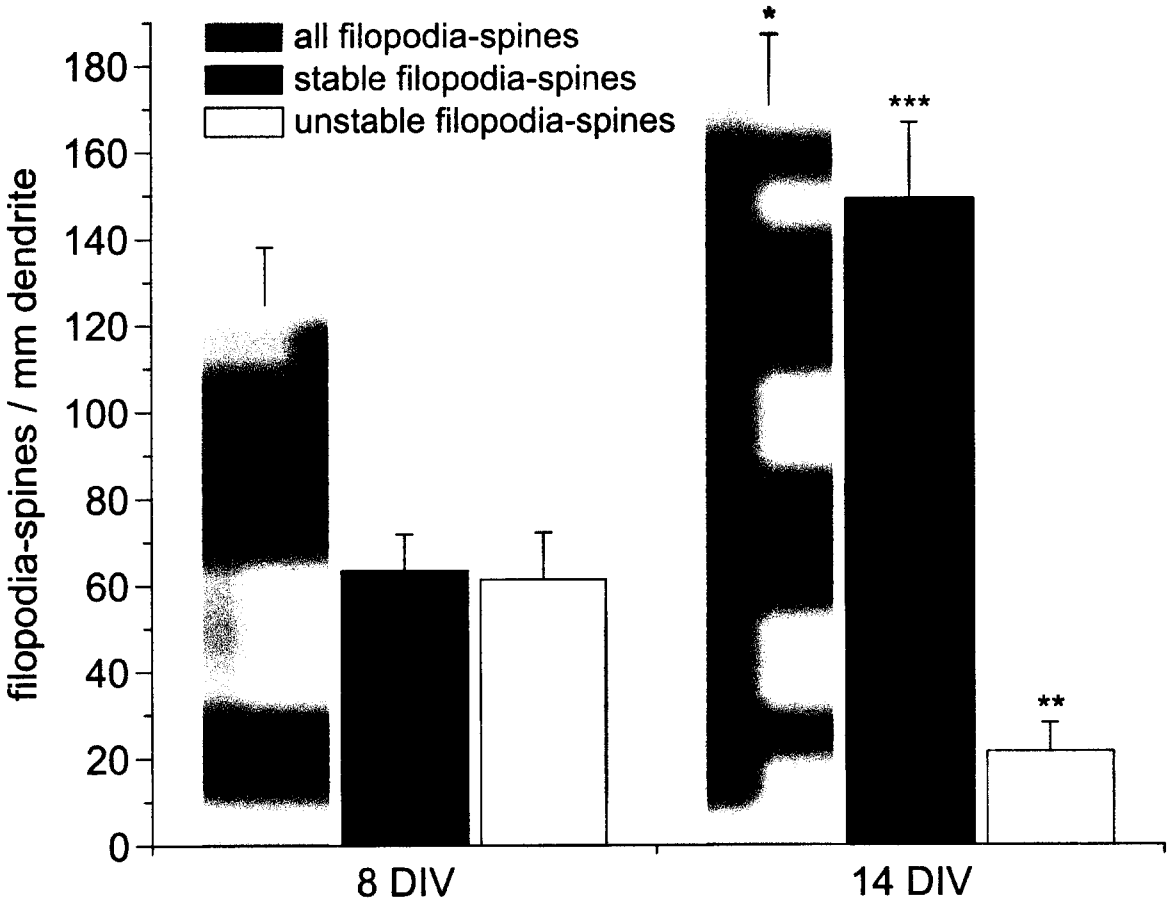

Fig. 18 Increase in number and stability of filopodia-spines during early neuronal development

Cortical neurons expressing WT PSD-95/GFP were kept for 6 - 10 (average 7.9 ± 0.3) days *in vitro* (DIV) (n = 13; 303 filopodia-spines) or for 12 - 18 (average 14.3 ± 0.5) DIV (n = 10; 440 filopodia-spines) before experiments. Cells were filled with sulforhodamine, and time-lapse confocal imaging was performed. The total number of filopodia-spines increases (by 37 %; *$p < 0.05$) between the two age groups; large increase and in the number of stable filopodia-spines (by 235 %; ***$p < 0.001$). A concomitant decrease (by 65 %; **$p < 0.01$) in the number of unstable filopodia-spines. All numbers are normalized to dendritic length.

Within this increasing population of filopodia-spines we found a disproportionally large increase (by 235 %) in filopodia-spines that were stable during 1 h of time-lapse imaging (from 63 ± 8 to 149 ± 18 per mm dendrite; $p < 0.001$), and a concomitant reduction (by 65 %) of unstable filopodia-spines (from 61 ± 11 to 22 ± 7 per mm dendrite; $p < 0.01$) between 8 and 14 DIV (Fig. 18). The same trend was found for cells transfected with the MUT PSD-95/GFP (see also below); the total number of filopodia-spines per mm increased from 156 ± 14 (8 DIV; 13 cells; n = 365 filopodia-spines) to 190 ± 26 (14 DIV; 5 cells; n = 165 filopodia-spines). There was no significant difference in the total number of filopodia-spines between WT and MUT PSD-95/GFP expressing cells in either age group (8 DIV $p > 0.2$; 14 DIV $p > 0.6$).

To reduce bias associated with selecting particular segments of dendrite for imaging, we further normalized the number of stable and unstable filopodia-spines to the total number of filopodia-spines per cell. This allowed us to compare the fraction of stable and unstable filopodia-spines between different ages and between different constructs used for transfection (Fig. 19). In both the WT and the MUT PSD-95/GFP transfected groups, the proportion of unstable filopodia-spines decreased significantly (WT $p < 0.001$; MUT $p < 0.005$) between 8 DIV (WT: 48 ± 6 %; MUT: 39 ± 6 %) and 14 DIV (WT: 13 ± 4 %; MUT: 14 ± 5 %) (Fig. 19), but was not significantly different between the WT and MUT group (8 DIV $p>0.2$; 14 DIV $p>0.5$) (Fig. 19).

To evaluate the relationship between PSD-95 clustering and filopodia-spine dynamics in neurons overexpressing the WT PSD-95/GFP construct, we separately analyzed data from the PSD-95/GFP (green) channel. First, we found a significant increase in the overall density of PSD-95 clusters in dendrites (from 86 ± 9 to 117 ± 19 per mm dendrite; $p < 0.05$) when comparing between stages of earlier (8 DIV) and later (14 DIV) *in vitro* development. This was due to a significant increase of filopodia-spines possessing PSD-95 clusters (from 17 ± 4 to 60 ± 12 per mm dendrite; $p < 0.001$) (Fig. 20). However, the density of PSD-95 clusters in dendritic shafts did not change significantly over the same period (from 69 ± 8 to 57 ± 9 per mm dendrite; $p > 0.4$) (Fig. 20).

We next examined which sub-population of filopodia-spines contributed most to the overall increase in filopodium-spines stability. We found a significant increase in the fraction of stable filopodia-spines with PSD-95 clusters (by 281 % ; $p < 0.01$) but

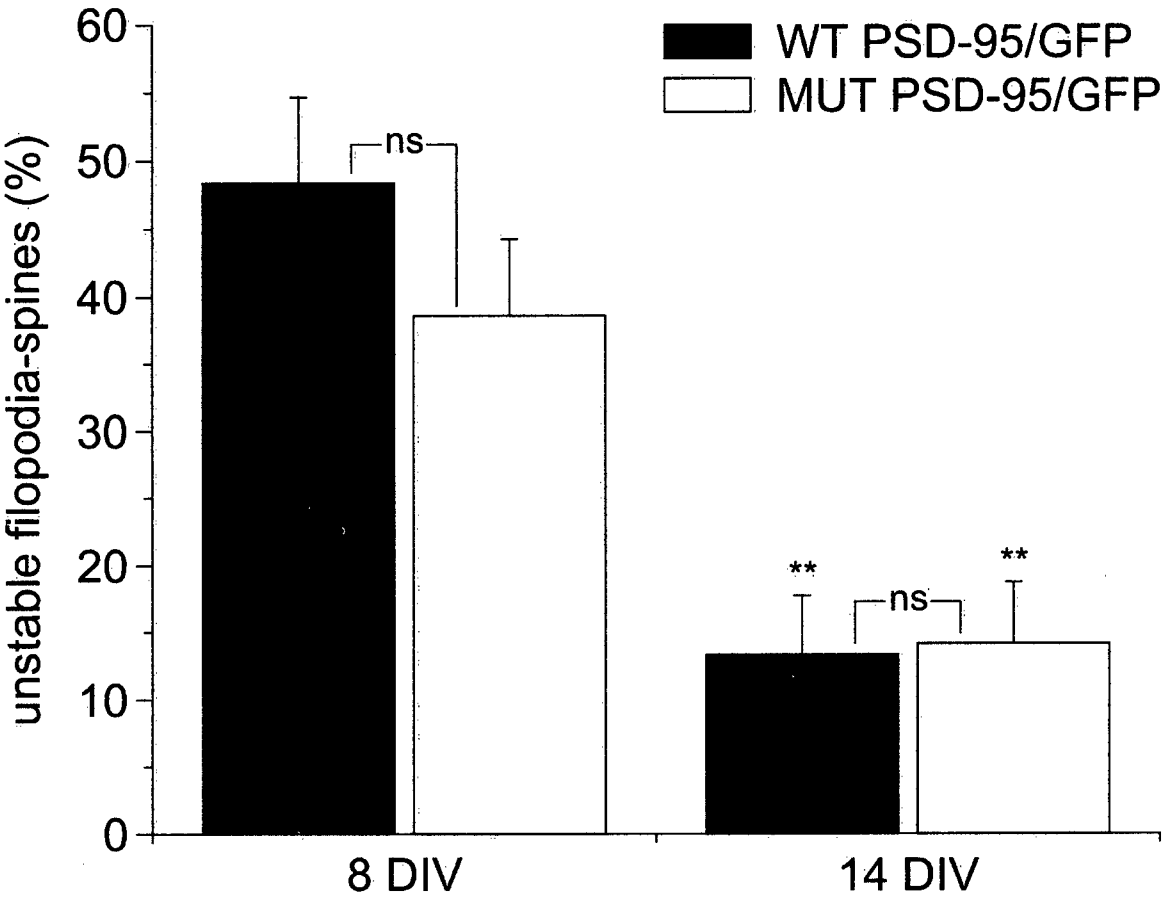

Fig. 19 Decrease in unstable filopodia-spines during early development is similar for *wild type* and *mutant* PSD-95/GFP expressing neurons

Cortical neurons were overexpressing either wild type (WT) PSD-95/GFP (n = 23 cells; 743 filopodia-spines) or the targeting deficient mutant (MUT) PSD-95/GFP (n = 18 cells; 530 filopodia-spines). Cells were cultured for, on average, either 8 or 14 days and filopodia-spine dynamics were imaged using confocal time-lapse microscopy. A significant decreases of unstable filopodia-spines in WT PSD-95/GFP expressing cells (***$p < 0.001$) between 8 and 14 days *in vitro* (DIV). A similar decrease (**$p < 0.005$) is found for MUT PSD-95/GFP expressing cells. No significant difference found between WT and MUT expressing cells in either age group. Numbers are normalized to the total number of filopodia-spines per cell.

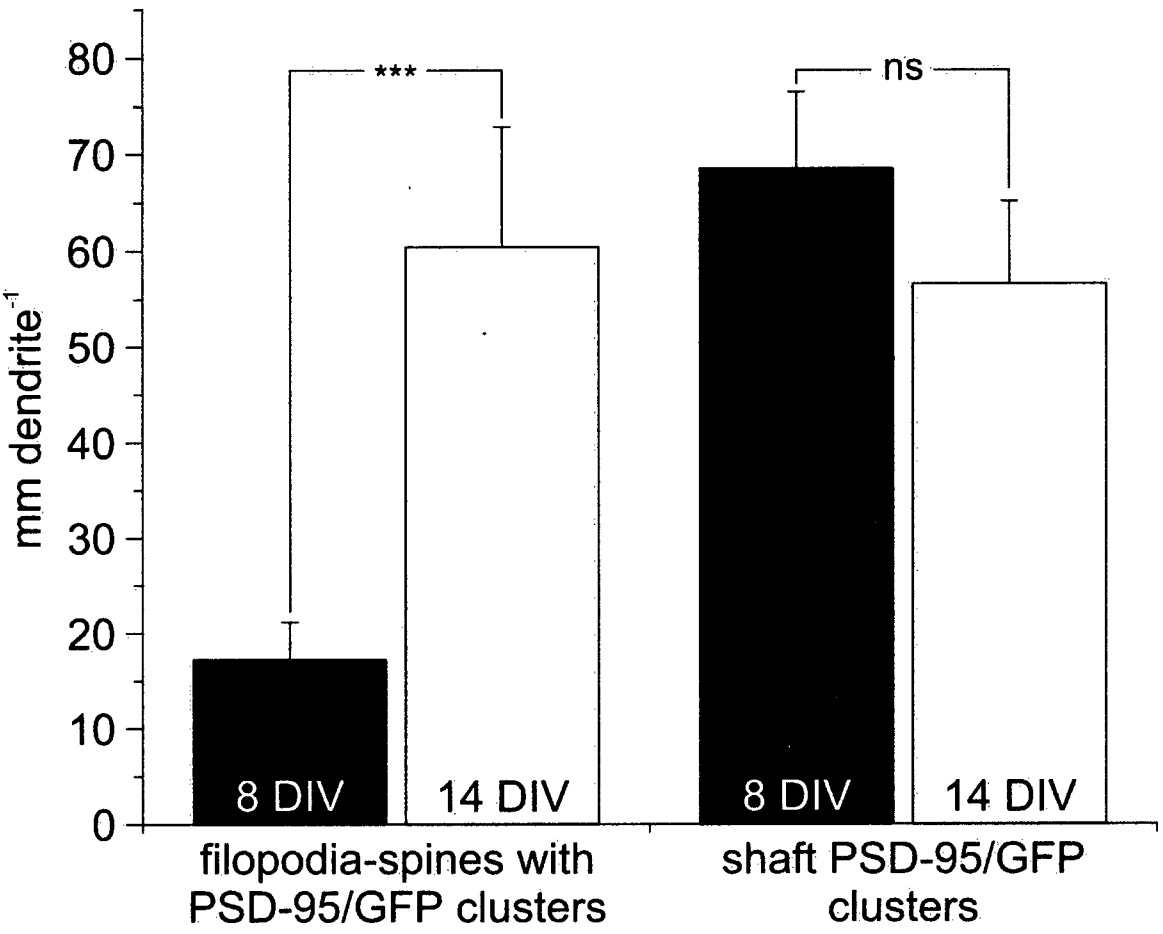

Fig. 20 Increase in the number of filopodia-spines with PSD-95 clusters, but not of PSD-95 shaft clusters during early neuronal development

In WT PSD-95/GFP overexpressing neurons, the number of PSD-95/GFP cluster bearing filopodia-spines and of PSD-95 shaft clusters was evaluated. Cells were kept for, on average, either 8 or 14 days *in vitro* (DIV). Comparing cells of the younger (n = 13 cells) to the older (n = 10 cells) age group, a significant increase in the density of filopodia-spines with PSD-95/GFP clusters is found (by 350 %; ***$p < 0.001$). No significant (ns) change in the number of PSD-95 shaft clusters (21 % decrease; $p > 0.4$). All numbers are normalized to dendrite length.

not in the fraction of stable filopodia-spines without PSD-95 clusters ($p > 0.1$) between 8 and 14 DIV (Fig. 21). In summary, these results indicate that an increase in PSD-95 cluster containing filopodia-spines could largely account for the overall increase in stable filopodia-spines between 8 and 14 DIV (see above) (Fig. 21).

We next analyzed the individual stability of all filopodia-spines with PSD-95/GFP clusters in WT PSD-95/GFP expressing cells (n = 23). Most compellingly we found that out of 190 filopodia-spines that possessed PSD-95/GFP clusters only 3 (1.6 %) were unstable during the ~ 1 h period of imaging. This high level of stability differed significantly from that of filopodia-spine without PSD-95 clusters in both age groups. At 8 DIV, 54 ± 6 % of all filopodia-spines without PSD-95/GFP clusters were unstable, whereas only 9 ± 8 % with PSD-95/GFP clusters were ($p < 0.001$) (Fig. 22). At 14 DIV only 1 ± 1 % of all filopodia-spines with PSD-95/GFP versus 20 ± 6 % without PSD-95/GFP clusters were unstable ($p < 0.005$) (Fig. 22).

As our data indicate that filopodium-spine structures with associated PSD-95 clusters are highly stable, we next determined the stability of the PSD-95 clusters themselves. Of all PSD-95 clusters found in dendritic shafts (n = 317) and in filopodia-spines (n = 190) we did not find a single case demonstrating the breakdown (disappearance) and/or the appearance of a PSD-95 cluster within 1 h of time-lapse imaging, indicating a slow turnover rate for PSD-95 clusters. However, uni- or bi-directional lateral movements of PSD-95 clusters within dendritic shafts, filopodia, and spines could be observed (see Fig. 23 for examples). Of all shaft PSD-95 clusters 14 ± 4 % exhibited lateral movement at 8 DIV over a 1 h period. This proportion decreased significantly to 2 ± 1 % at 14 DIV ($p < 0.05$). The range of movement of PSD-95 shaft clusters was usually relatively small (1 - 3 µm), but could in single cases be up to 5 µm within 20 min of imaging. Additionally, small 1 - 2 µm movements of PSD-95/GFP clusters could be observed in 20 ± 9 % (8 DIV) and 17 ± 7 % (14 DIV) of all filopodia-spines with PSD-95 clusters. Moreover, in a few occasions (< 5 % of all clusters) we were able to observe "splitting" of a PSD-95 cluster (see Fig. 23) or "merging" of two or more PSD-95 clusters into one.

Although PSD-95 clusters in filopodium-spine structures were mostly stable, we did occasionally observe filopodia-spines or small precursors to these structures in which a PSD-95/GFP cluster was transiently located (Fig. 23). Interestingly we found 9

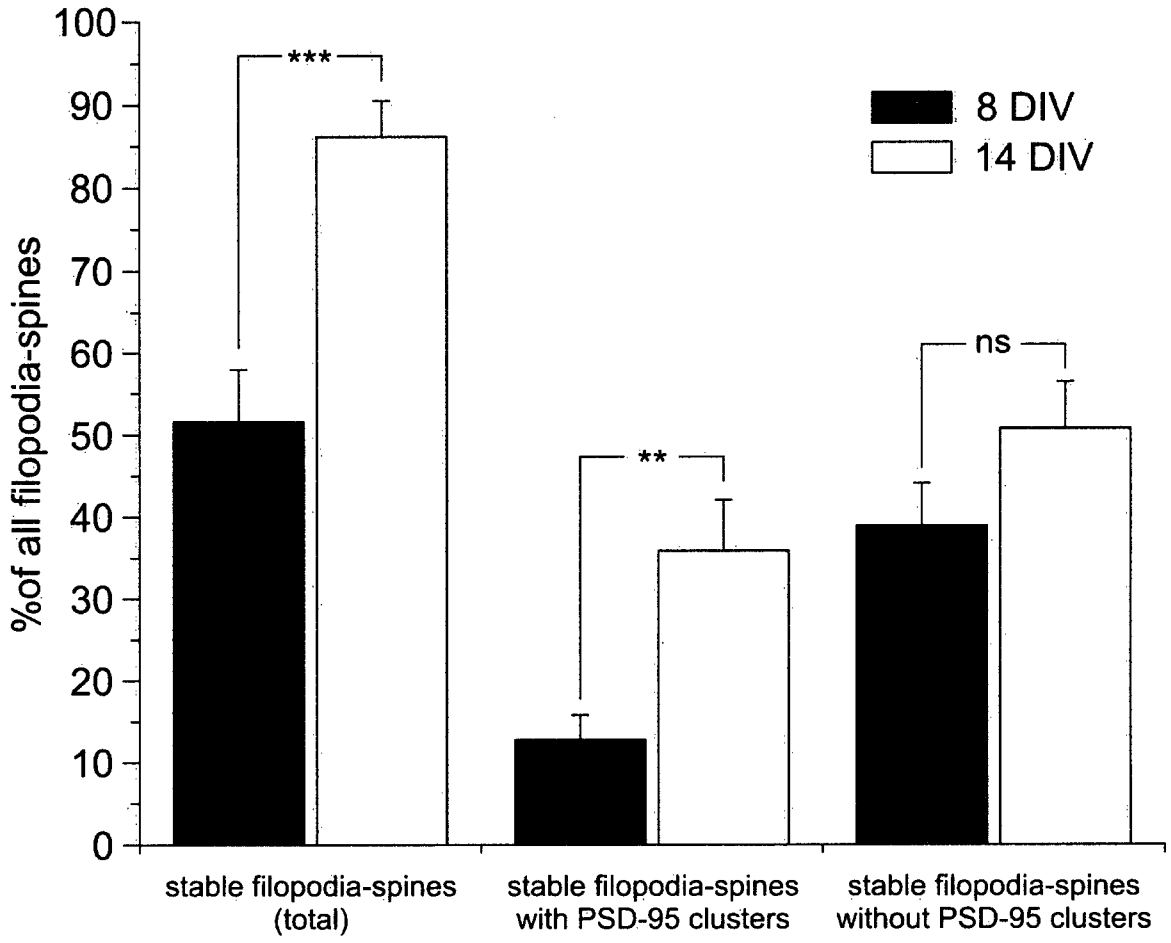

Fig. 21 Developmental stabilization of the filopodium-spine population can be attributed to an increase in filopodia-spines with PSD-95 clusters

In neurons expressing WT PSD-95/GFP the fraction of stable filopodia-spines increases by 68 % (***$p < 0.005$) between 8 DIV and 14 DIV. Over the same time period the fraction of stable filopodia-spines with PSD-95/GFP clusters largely increases (by 281 %; **$p < 0.01$). No significant (ns; $p>0.1$) increase in the fraction of stable filopodia-spines that lack PSD-95/GFP clusters was observed.

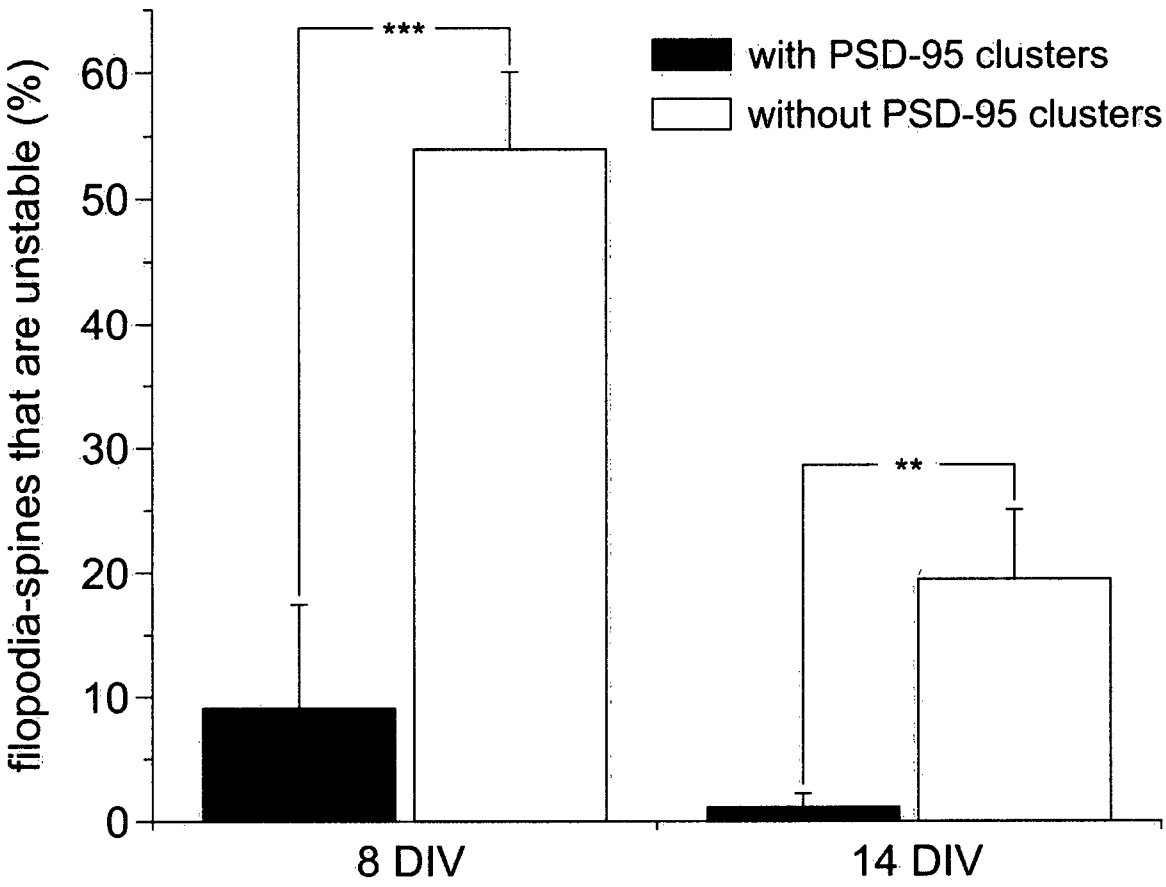

Fig. 22 Filopodia-spines with PSD-95/GFP clusters are more stable than filopodia-spines without clusters

The stability of filopodia-spines was compared between filopodia-spines with PSD-95/GFP clusters, and filopodia-spines devoid of clusters. Neurons expressing the WT PSD95/GFP construct matured, on average, for either 8 DIV (n = 13; 303 filopodia-spines) or for 12 - 18 DIV (n = 10 cells; 440 filopodia-spines). Filopodia-spines without PSD-95/GFP clusters are significantly more unstable at 8 DIV (***$p < 0.001$) and 14 DIV (**$p < 0.005$) compared to filopodia-spines with PSD-95/GFP clusters.

cases in which PSD-95 clusters either exited (n = 7) and/or entered a filopodium-spine (n = 2), usually within less than 20 min. (Fig. 23). Seven of these cases were found in neurons at within the younger age group (8 DIV), representing 13 % of all filopodia-spines with PSD-95 clusters. In the older age group (14 DIV) we observed this phenomenon in only 2 cases (1 %) of filopodia-spines with PSD-95 clusters. In some cases in which a PSD-95 cluster exited a filopodium-spine (Fig. 23), the process subsequently underwent a significant structural change (see Fig. 23 for examples). This data indicates the existence of two distinct mechanisms: one for pre-assembling PSD-95 into clusters, and one for subsequently localizing PSD-95 complexes into emerging filopodia-spines, which is reversible.

To assess whether the developmental changes in filopodium-spine stability and PSD-95 localization were accompanied by presynaptic changes we used an immunostaining approach. A primary antibody against the presynaptic marker synaptophysin and a secondary Texas Red-conjugated antibody were used in cultures transfected with WT PSD-95/GFP at 8 and 14 DIV (Fig. 24). Analysis of co-localization between PSD-95/GFP and synaptophysin demonstrated a significant increase ($p < 0.0001$) between 8 DIV (37 ± 2 % of all PSD-95 clusters co-localizing with synaptophysin; n = 9 cells) and 14 DIV (75 ± 5 % ; n = 9 cells) (Fig. 24). However, even at the younger age (8 DIV) when PSD-95/GFP was present in filopodia-spines (rather than dendrite shafts) co-localization with synaptophysin was significantly higher than the overall rate (71 ± 9 % ; $p < 0.01$) (Fig. 24). The same trend was apparent of older cultures (14 DIV) where co-localization of PSD-95 and synaptophysin increased significantly to 93 ± 2 % ($p < 0.001$) when only filopodia-spine clusters were considered and shaft clusters were excluded (Fig. 24).

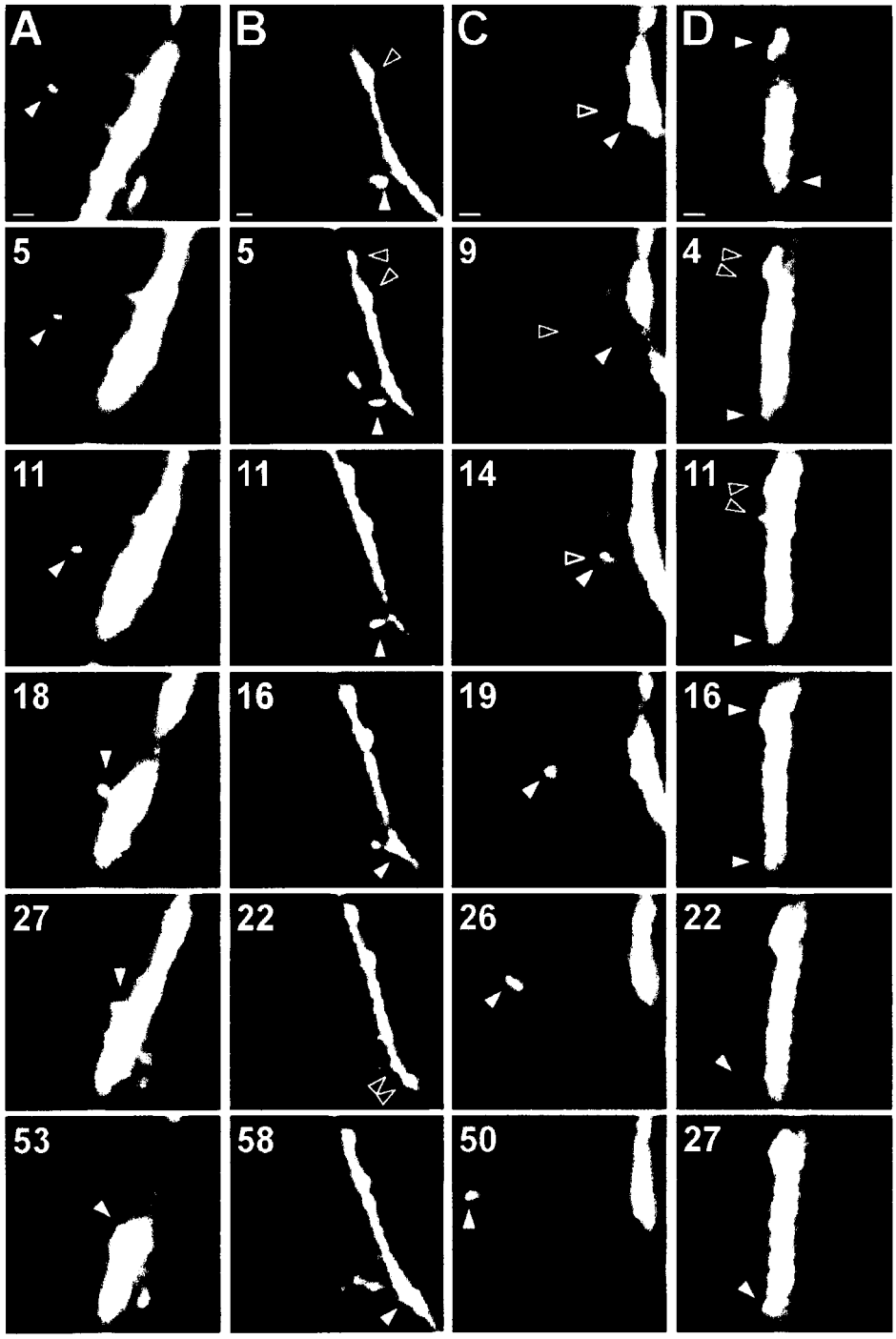

Fig. 23 Dynamic properties of PSD-95 clusters within developing neurons. Rapid translocation of PSD-95/GFP clusters into and/or out of developing filopodia-spines

Partial time-lapse series of dendrites of cells transfected with WT PSD-95/GFP (green) and filled with sulforhodamine (red) to assess structure. Areas of dye co-localization appear in yellow. Images in respective columns were taken consecutively, with the

exception of the last time-point in A-C which represents the last data point of the series. Time stamps in min; all series start at 0 min. Bars = 1 μm. **A)** 10 DIV neuron in which a PSD-95 cluster (white arrow head) moves out of a filopodium-spine. Spine splitting at 27 min. **B)** 6 DIV neuron in which a shaft cluster splits into 2 domains (0 - 5 min; top, black arrowheads). A cluster (bottom) leaves a filopodium-spine (between 11 and 16 min time points; white arrowhead), and transiently splits (22 min; black arrowhead). Filopodium-spine consecutively undergoes rapid outgrowth (22 min) and retraction (58 min). **C)** A 8 DIV neuron in which filopodium-spine outgrowth (0 - 9 min; black arrowhead) precedes localization of cluster into its tip (14 - 19 min; white arrowhead) and further elongation of the structure with arrested cluster in its tip (26 - 50 min). **D)** An 8 DIV neuron in which a small PSD-95/GFP labeled structure reversibly protrudes from a large shaft cluster (top). Another small filopodium reversible protrudes (bottom) from the dendritic shaft carrying a PSD-95 cluster from the dendritic shaft with it.

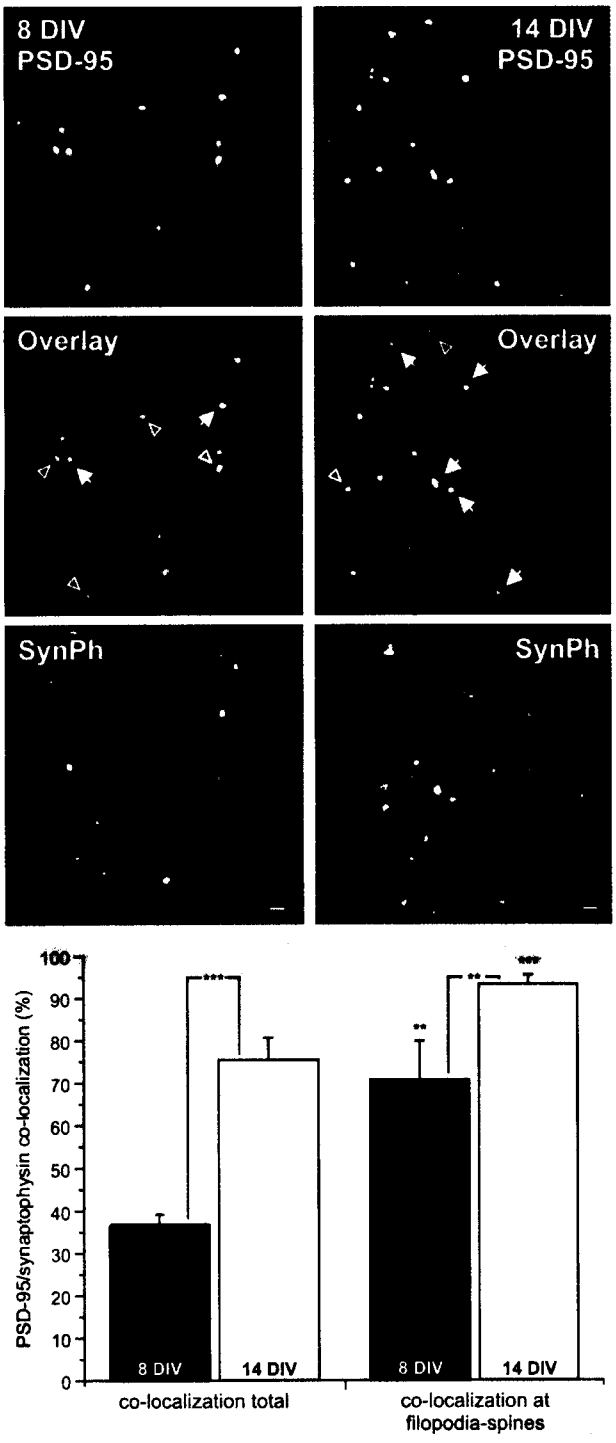

Fig. 24 Developmental increase in the co-localization of PSD-95 and a presynaptic marker

Neurons were transfected with the WT PSD-95/GFP (PSD-95, upper panels) construct and were immunostained for the presynaptic marker synaptophysin (SynPh, lower panels) using a Texas Red-conjugated 2° antibody. The left and right columns depict representative confocal images from dendritic regions immunostained at 8 DIV and 14 DIV, respectively. Center panels: Composites of the PSD-95 (green) and SynPh (red) images. White arrows depict examples of PSD-95 and SynPh co-localization; black arrowheads indicate examples of PSD-95 clusters without corresponding SynPh clusters. Scale bar = 2 µm. Bar graph: Co-localization of PSD-95 and SynPh increases significantly between 8 DIV (37 ± 2 % of all PSD-95 clusters are co-localized with SynPh; n = 9 cells) and 14 DIV (75 ± 5 %; n = 9 cells) (left column). A significantly higher rate of co-localization when PSD-95/GFP clusters are localized in filopodia-spines (compare between same age group of left and right column). ** $p < 0.01$, *** $p < 0.001$

DISCUSSION

Dendritic filopodia are highly motile transient processes that move in an actin dependent manner (Fischer et al., 1998). During early development, it is proposed that these processes continuously probe the extracellular environment for potential presynaptic partners (Saito et al., 1992; Dailey and Smith, 1996; Ziv and Smith, 1996; Fiala et al., 1998; Halpain, 2000). Recent data suggests a model for excitatory synapse development in which initial motile filopodial structures become stabilized in a partially activity-dependent manner leading to the formation of mature dendritic spines (Jontes and Smith, 2000; Lee and Sheng, 2000; Segal, 2001). In fact, time-lapse experiments have indicated that a functional synapse can develop from a motile filopodium within about one hour (Friedman et al., 2000). This observation has placed new time constraints on synaptogenesis and now focuses attention on the regulatory role that synaptic proteins play in this process (Jontes and Smith, 2000; Rao and Craig, 2000; Segal, 2001). The integral postsynaptic density protein PSD-95 represents a conceivably good candidate protein for such a function as it can tether receptors and signal transduction proteins into complexes and crosslink them to structural protein arrays using its protein-protein interaction domains (Garner et al., 2000; Scannevin and Huganir, 2000). Clustering of PSD-95 into filopodia and the consequent scaffolding of the postsynaptic signal transduction machinery may therefore provide an important step in the proper assembly of functional synapses.

Accordingly, we have performed time-lapse imaging experiments with GFP-tagged PSD-95 to simultaneously monitor filopodial-spine stability and PSD-95 localization during a time period of *in vitro* development believed to be critical for synaptogenesis and stabilization of dendritic processes. Although previous time-lapse studies of PSD-95 have been done (Okabe et al., 1999), they were performed on considerably older neurons that lacked filopodia. Furthermore this study used relatively low-resolution wide field microscopy and focused on PSD-95 dynamics over much longer time periods (up to 8 h) with much lower sampling rates. We have extended this work by using higher resolution confocal imaging with considerably shorter time intervals (5 min). An additional advantage of our study was that we took multiple optical sections that spanned the vertical extent of the dendrite of interest to ensure that all filopodia-spine processes were indeed captured and that changes in

process disposition did not reflect changes in optical planes sampled. Finally, we have introduced a second fluorescent marker into PSD-95/GFP expressing neurons, which allowed us to label dendritic structure and analyze filopodial-spine dynamics independently of PSD-95/GFP disposition. During the early developmental period of neurons used in the present study it was often not possible to clearly classify a dendritic protrusion as either a filopodium or a spine. Hence, we have grouped all dendritic protrusions matching the criteria outlined above (see Methods) into one category (filopodia-spines). This was done to prevent the introduction of an additional level of potential observer bias into our analysis. However, applying categorizing criteria for spines and filopodia established by others (Parnass et al., 2000; Sorra and Harris, 2000) most cautiously to our system, we can conservatively estimate that even within the relatively older developmental group (14 DIV) more than 50 % of all protrusions show characteristics typical for filopodia, with lengths usually exceeding 2 - 3 μm, and poorly defined heads (diameter not larger than that of the "neck") (Parnass et al., 2000; Sorra and Harris, 2000). Yet many of these processes contained PSD-95 clusters (see Results). Within the younger group (8 DIV), the protrusions exhibit almost exclusively (>90 %) filopodial features and most were mostly devoid of PSD-95 clusters (see Results).

Consistent with previous data (Ziv and Smith, 1996; Fiala et al., 1998; Dunaevsky et al., 1999) we show that dendritic filopodia-spines are transient structures present during early development. Interestingly, recent data suggests that *in vivo*, developing cortical neurons have active dendritic filopodia that extend and turnover with kinetics similar to what we have reported (Lendvai et al., 2000). Furthermore, motile dendritic filopodia become considerably arrested at an *in vitro* age similar to their *in vivo* counterparts (Fiala et al., 1998; Dunaevsky et al., 1999), suggesting that important parallels between *in vitro* and *in vivo* development exist. Since overexpression of PSD-95 has been demonstrated to have a permissive role on spine development and transmitter release probability (El-Husseini et al., 2000b) we have overexpressed wild type (WT) PSD-95 or a palmitoylation mutant (MUT) PSD-95, that lacks synaptic targeting and fails to form clusters, and determined whether correlates of this might be observed in developing filopodial-spine dynamics. We hypothesized that if PSD-95 levels were limiting, we would be able to possibly drive the development of new filopodia-spines by overexpressing the wild type protein

and/or alter the dynamic development of existing ones. However, no significant change in either the number of filopodia-spines or their stability was observed when overexpression of either wild type PSD-95 or mutant (non-clustering) forms were compared. This result suggested that under the conditions we have used endogenous PSD-95 cluster levels were sufficient to promote synapse development and stability. Therefore, it is likely that clustered PSD-95 is a marker for stable filopodia-spines, but by itself is not sufficient to induce stabilization. Alternatively longer periods of PSD-95/GFP expression may be required to promote spine development. Interestingly, previous reports of PSD-95 stimulation of spine maturation were from cultures that were considerably older and more developed than the ones that we used (El-Husseini et al., 2000b).

The fact that PSD-95/GFP overexpression does not affect spine development in our system importantly indicates that we were not perturbing the system and altering the properties or number of filopodia-spines that we study with time-lapse imaging. It was under these conditions that within WT PSD-95/GFP expressing neurons we observed a profound increase in the stability of filopodia-spines with PSD-95 clusters compared to filopodia-spines that lack PSD-95 clusters at both developmental stages studied. These findings suggest that events associated with the presence of clusters lead to the development of stable filopodia-spines, which, over longer time periods, may transform into functional postsynaptic spines with their typical morphological features (Lee and Sheng, 2000; Wong and Wong, 2000). However, at both developmental stages a considerable fraction of stable filopodia-spines (38 and 52 % for young and old neurons, respectively) did not contain detectable PSD-95/GFP clusters. Spines lacking PSD-95 have also been reported by others (Friedman et al., 2000). These filopodia-spines may represent a subpopulation that develop more slowly (Rao et al., 1998), or alternatively constitute precursors of inhibitory synapses (Benson and Cohen, 1996; Rao et al., 2000). Thus, it is unclear whether these synapses possess a different phenotype from those that contain PSD-95 clusters. Nevertheless, this result does suggest that PSD-95 clustering is not the only factor that can lead to dendritic filopodium and spine stability.

Consistent with the relative stability of the PSD (Allison et al., 1998; Passafaro et al., 1999; Allison et al., 2000), we observe that clusters of PSD-95 were generally stable over a 1 h period. Although the PSD-95 clusters themselves were stable, we did

observe a considerable number of clusters exhibiting at times substantial lateral movement over short periods of time (~ 1 μm per min). Most interestingly, in a few cases dendritic shaft PSD-95 clusters were able to move from the shaft or into a spine-filopodium or vice versa. In general, structures into which the cluster moved appeared to be quite stable. We proposed that the PSD-95 cluster might be moving with a group of associated postsynaptic proteins consistent with the proteomic analysis data (Husi et al., 2000; Walikonis et al., 2000). Recently it has been shown that rapid presynaptic development occurs through the use of prefabricated protein complexes (Ahmari et al., 2000). Analogously, a mechanism for translocating modular, prefabricated core components of the postsynaptic signal transduction machinery may be required to achieve rapid development of functional spines. Conceivably translocation of PSD-95 protein complexes may be triggered through an initial contact between filopodia and presynaptic partners (Ziv and Smith, 1996; Fiala et al., 1998), resulting in filopodial stabilization, maturation, and development into spines.

In a few examples, filopodia-spines exhibited significant structural changes after a PSD-95 cluster retracted as if the cluster was part of a structural element, which needed to be removed before the filopodium-spine could undergo this change (see Fig. 23). In other cases, PSD-95 clusters were within a filopodium-spine in which the process would grow or morph around the cluster. That is, the cluster appeared to remain stable despite the surrounding process changing in shape. This provides additional functional evidence that the PSD-95 cluster is a rather stable structural element.

By performing synaptophysin immunocytochemistry in combination with localization of PSD-95/GFP, we observed that in young cultures (that have more dynamic dendritic processes) many of the clusters (> 60 %) were not associated with presynaptic terminals. Perhaps these non-synaptic clusters are reserve materials for building new synapses from prefabricated structural elements. Consistent with this idea, we found a robust increase (by ~ 2X) of PSD-95/synaptophysin co-localization when analysis was restricted to PSD-95 clusters that were located in filopodia-spines. Clearly a better understanding of the molecular events associated with the formation and maintenance of PSD-95 cluster and its role in will be crucial to understanding its role in stabilizing dendritic filopodia and spines.

V. GENERAL DISCUSSION

Since first characterized by Santiago Raymon y Cajal (Raymon y Cajal, 1888) and Charles Sherrington (Sherrington, 1897), the synapse has arguably become one of the major focuses in the field of neuroscience and related fields such as neuropharmacology and neuropsychiatry. Highly modifiable synaptic transmission taken together with parallel information processing has been suggested to account for the computational power of the brain (Brunel, 1996; Buonomano and Merzenich, 1998; Merzenich, 1998; Poon and Shah, 1998; Holthausen and Breidbach, 1999; Compte et al., 2000). Furthermore, all of today's known psychopharmaca (Breier et al., 1999; Carlsson et al., 1999) as well as recreational drugs, such as cannabinoids (Auclair et al., 2000; Hoffman and Lupica, 2000; review in Montgomery and Madison, 2001), cocaine (review in Kreek, 1996; Blakely and Bauman, 2000), and amphetamines (Amara and Sonders, 1998; Blakely and Bauman, 2000) act by directly modulating aspects of synaptic transmission. As these drugs significantly influence cognitive capabilities, it has become increasingly clear that synaptic processing is directly involved in the generation of cognition and may therefore underlie the development and expression of the individual's personality (Eccles, 1992; Honer, 1999; Kandel and Squire, 2000). Our understanding of how the synergy of nerve impulse propagation and synaptic modulation encodes for the properties of the brain, however, is still in its infancies. Neurobiological strategies to tackle this problem include top-down approaches, such as functional MRI (Foster, 1999; Shulman, 2001; Wickelgren, 2001) as well as bottom-up approaches including molecular (Sanes and Lichtman, 1999; Yuste and Sur, 1999; Benson et al., 2000), genetic (Mayford and Kandel, 1999; Tsien, 2000) and electrophysiological (Kreiman et al., 2000) experiments. In addition, there is ongoing development of computational models to understand the complexity of neural coding and synaptic signaling (Tsodyks et al., 1998; Johnson, 2000).

Even though neuroscience is still far from developing an encompassing model of information processing in the brain, the rapid advances in molecular, physiological and imaging techniques has enabled the field to unravel structure and function of many key players involved in the regulation of signal propagation and synaptic transmission.

Yet incomplete, we now have a principal understanding how electrical signals are propagated and integrated in neurons (Magee, 2000; Poirazi and Mel, 2001), how cells control neurotransmission (Lin and Scheller, 2000; Fon and Edwards, 2001), and how chemical signals arising from this transmission can be translated into molecular events that can alter structure and function of the neuron (Walton et al., 1999; Luscher et al., 2000; Muller et al., 2000; Soderling and Derkach, 2000). Much of this knowledge has come from studies on the anatomy, molecular composition and physiology of the synapse itself (see **INTRODUCTION**). Hence, the research projects presented in this thesis have focused on mechanisms of synaptic transmitter release (**CHAPTER II & III**) as well as synaptic development (**CHAPTER IV**) to contribute to our understanding of synaptic physiology.

A hallmark of synaptic structure and function is that it is extremely modifiable (Jan and Stevens, 2000; Martin et al., 2000). The continuing structural and functional plasticity after the embryonic development of the CNS may enable the brain to preserve its adaptational capabilities throughout life (Roman et al., 1999; Alvarado and Bachevalier, 2000; Martin et al., 2000). Importantly, during development and adulthood synaptic plasticity is rendered by neuronal activity and therefore directly modifiable by experience (Morris and Frey, 1997; Buonomano and Merzenich, 1998; Feldman and Knudsen, 1998; Gilbert, 1998; Kolb and Whishaw, 1998; Berardi et al., 2000; Sanes and Donoghue, 2000). Hence, to understand how synaptic events are triggered by and/or translate into behavior, the molecular machinery and physiological processes coding for these synaptic mechanisms have to be examined.

Among many characterized forms of synaptic plasticity, long-term potentiation (LTP) at the hippocampal CA3 - CA1 synapse represents the most widely studied form of long-lasting synaptic modification (review in Tsien, 2000). Synaptic changes associated with LTP can occur either on the presynaptic or the postsynaptic side, but is most likely to involve both synaptic compartments (see below and Malenka and Nicoll, 1999). However, the field of Neuroscience has, based on different experimental approaches, become somewhat polarized in favoring (the importance of) one form of plasticity (pre- or postsynaptic) over the other (see e.g. Kullmann and Siegelbaum, 1995). For a long time a number of groups had favored the presynaptic site as the primary locus for LTP expression. Arguments for this were mostly based on an enhancement of release probability ($P_{rel.}$) (Bekkers and Stevens, 1990; Liao et al.,

1992; Stevens and Wang, 1994; Bolshakov and Siegelbaum, 1995a; Kullmann and Siegelbaum, 1995; Clark and Collingridge, 1996) and of miniature synaptic activity (Minota et al., 1991; Malgaroli and Tsien, 1992; Arancio et al., 1995; Tong et al., 1996; Chen and Regehr, 1997; review in Malenka and Nicoll, 1999) associated with the expression of LTP. However, since postsynaptic activity was used as a proxy to estimate both miniature and evoked presynaptic release, the conclusion of these studies was subject to a potentially fundamental flaw.

It is now widely accepted that AMPA receptors can be rapidly (within minutes) inserted into and/or removed out of synaptic membranes (Carroll et al., 1999b; Lissin et al., 1999; Shi et al., 1999; review in Luscher et al., 2000). The cycling of latent AMPA receptor clusters is continuous (Luscher et al., 1999), but can be regulated by NMDA receptor activation (Carroll et al., 1999b; Heynen et al., 2000; Lu et al., 2001). AMPA receptor cycling is dependent on an intact SNARE fusion protein complex (AMPA exocytosis) (Lledo et al., 1998; Luscher et al., 1999), and dynamin (AMPA endocytosis) (Carroll et al., 1999a) as well as on Ca^{2+} mediated actin dynamics (Zhou et al., 2001). Importantly, it has been demonstrated that endocytosis of AMPA receptors into endosomal vesicles is associated with the expression of LTD (Carroll et al., 1999b), and conversely that AMPA receptor exocytosis into active zones contributes to LTP expression (Lu et al., 2001). The dynamic and activity-dependent AMPA receptor distribution may help to solve the dispute over the site (pre- or postsynaptic) of LTP expression (Kullmann and Siegelbaum, 1995; Malinow, 1998; Malenka and Nicoll, 1999): AMPA receptor insertion into synapses which were previously only expressing NMDA receptors (i.e. "silent synapses" at resting membrane potentials) (Carroll et al., 1999b; Shi et al., 1999; Lu et al., 2001) provides a powerful alternative explanation for the observation of enhanced miniature activity and "release probability" ($P_{rel.}$) independently of presynaptic changes (Gomperts et al., 1998; Heynen et al., 2000; review in Luscher et al., 2000). In this model, LTP-induced "un-silencing" of NMDA-only synapses results in additional synaptic receptor fields which, at resting membrane potential, can sense transmitter released from presynaptic terminals during evoked and spontaneous activity (review in Malinow, 1998; Atwood and Wojtowicz, 1999; Malenka and Nicoll, 1999; Malinow et al., 2000).

Hence, at least for the hippocampal CA3 - CA1 synapse it is now mostly agreed that the primary locus for expression of LTP occurs at the postsynaptic site (Malinow,

1998; Rumpel et al., 1998; Malenka and Nicoll, 1999; Reid and Clements, 1999; Malinow et al., 2000; Soderling and Derkach, 2000). However, there is a small number of studies showing that after LTP induction $P_{rel.}$, but not in the average size of the postsynaptic current, is increased (Stevens and Wang, 1994; Bolshakov and Siegelbaum, 1995b). These Authors monitored synaptic transmission from single synaptic connections of hippocampal pyramidal cells, hence occluding the potential involvement of additional synapses after LTP induction (Stevens and Wang, 1994; Bolshakov and Siegelbaum, 1995b). These findings seem hard to reconcile with a purely postsynaptic expression of LTP and may indicate different mechanisms for LTP expression under varying experimental conditions (Malenka and Nicoll, 1999). Alternatively they may simply suggest an involvement of the presynaptic release machinery in the expression of LTP in addition to the postsynaptic changes. Further evidence for this possibility comes from a study by Ryan and Smith (Ryan et al., 1996) who used imaging of stimulated presynaptic FM1-43 turnover as a measure for release probability, thereby eliminating the need to use postsynaptic recordings as an indicator for presynaptic activity. The authors found a long-lasting (> 1 hour) enhancement of presynaptic release after LTP induction (Ryan et al., 1996).

There are other potential mechanisms to regulate synaptic efficacy on the presynaptic side. As studied in **CHAPTER II,** multivesicular release could represent one such mechanism. Initial studies using quantal analysis in CNS neurons have indicated that the number of quantal peaks in amplitude distributions equal to the number of presynaptic release sites (review in Redman, 1990). These findings together with electron microscopy (EM) data have been interpreted as indicating that an AP can at maximum trigger the release of one vesicle per release site ("one site-one vesicle" hypothesis) (Triller and Korn, 1982). Most support for this theory has come from studies on the hippocampal CA3 - CA1 synapse; a connection that has been shown to involve mostly a single release sites between two connected neurons (Shepherd and Harris, 1998). To study synaptic transmission at these sites Stevens and co-workers used "minimal stimulation" of the hippocampal CA1 afferents (Stevens and Wang, 1994; Stevens and Wang, 1995; Dobrunz and Stevens, 1997) while recording from CA3 neurons, and Bolshakov and Siegelbaum used paired CA3 - CA1 recordings (Bolshakov and Siegelbaum, 1995b). Both groups found that postsynaptic responses to presynaptic stimulation were either 0 (no presynaptic release) or 1 (release of one

transmitter quantum), but unlike at the NMJ (Fatt and Katz, 1952) never multiples of 1, which would indicate the release of more than one transmitter quantum per stimulus (Stevens and Wang, 1994; Bolshakov and Siegelbaum, 1995b; Stevens and Wang, 1995). These findings were further substantiated by an elegant study by Forti et al. who first used lose patch-clamping on single cultured hippocampal terminals and corresponding postsynaptic sites, and then subsequently showed (by EM techniques) the involvement of only single release sites (Forti et al., 1997). These authors found that the positively skewed distribution of postsynaptic miniature currents from whole-cell recordings was reduced to a normal distribution when recording was performed at single release site synapses (Forti et al., 1997), indicating no occurrence of multivesicular release. The interpretation of these data led Stevens to propose a mechanism of presynaptic "lateral inhibition" by which release of one vesicle inhibits the release competence of another vesicle at the same release site within a certain time window (Dobrunz and Stevens, 1997; Stevens and Sullivan, 1998a). However, there is still lack of experimental data to sufficiently support this hypothesis. Moreover, it is not clear if the phenomenon of "all-or-none" release is limited by the experimental approach and/or restricted to CA3 - CA1 synapses. Other studies, using a similar electrophysiological approach clearly indicate that the postsynaptic responses to single presynaptic stimuli can be multiquantal, corresponding to the concurrent release of more than one transmitter vesicle (review in Auger and Marty, 2000). Examples of multivesicular release have been found in cerebellar stellate, basket and Purkinje cells (Vincent and Marty, 1996; Auger et al., 1998), the goldfish Mauthner cell (Korn et al., 1993), the Calyx of Held (Trussell et al., 1993), as well as in cultured hippocampal neurons (Tong and Jahr, 1994). Yet, common to all of the studies mentioned above is their use of postsynaptic recordings to infer about presynaptic release. Hence the conclusions of these studies are limited in that the results are subject to postsynaptic signal contamination, such as receptor desensitization, receptor saturation, dendritic cable properties, or yet unidentified mechanisms that potentially modulate postsynaptic channel properties. Moreover, unambiguous postsynaptic detection of multivesicular release is only possible if < 50 % of postsynaptic receptors are saturated by the content of a single vesicle (Auger and Marty, 2000). To circumvent this problem, it seems advantageous to directly monitor presynaptic release, rather than its postsynaptic response. We have done that by using activity-dependent FM1-43 staining and de-staining of synaptic vesicles in single

cortical presynaptic terminals (**CHAPTER II**). Using this approach, our results indicate that multivesicular release occurs at about 13 -17 % of cortical synapses *in vitro* (Prange and Murphy, 1999). Our conclusion is limited by two factors: first, we were not able to determine the phenotype of the imaged synapses, and second, due to the lower sensitivity of FM1-43 imaging as compared to electrophysiological recordings, we had to integrate presynaptic release over a number of AP-stimuli. However, by restricting our analysis to synapses with high $P_{rel.}$ we have aimed to minimize these limitations (see **Results** and **Discussion** in **CHAPTER II**).

It is possible to reconcile both the "lateral inhibition" hypothesis (above) and the occurrence of multivesicular release, if one assumes that the latter is mostly restricted to synapses with more than one active zone. Support for this assumption in cortical neurons comes from ultrastructural studies showing the existence of multiple active zone terminals in the hippocampus (Harris et al., 1992; Harris, 1995; Shepherd and Harris, 1998) at a fraction that is comparable to the one we have found multivesicular release to occur at (see above and **CHAPTER II**). Furthermore electrophysiological approaches in the hippocampus have indicated that multivesicular release occurs after LTP induction, and that it originates from multiple release zones on the same terminal (Bolshakov et al., 1997). Multivesicular release as a means of presynaptic plasticity may only be biologically useful if postsynaptic receptors are not saturated by the content of a single vesicle. In fact, there is now accumulating evidence that this holds true at least for AMPA- and NMDA receptors on glutamatergic CNS synapses (Mainen et al., 1999b; Umemiya et al., 1999; McAllister and Stevens, 2000; Chen et al., 2001; Hanse and Gustafsson, 2001).

Another fascinating form of presynaptic plasticity is the AP-independent spontaneous release of transmitter quanta, termed miniature synaptic activity. This terminology is based on initial studies at the NMJ where the miniature postsynaptic response was found to be the smallest unit of recorded activity and therefore concluded to correspond to the transmitter content of a single vesicle (Fatt and Katz, 1952). It has been shown that miniature release can be regulated at the level of the single synapses in response to AP-stimulation (Kamiya and Zucker, 1994; Cummings et al., 1996; review in Zucker, 1996; Fisher et al., 1997). However, some findings including studies on the correlation between miniature activity and LTP and/or LTD expression (Minota et al., 1991; Arancio et al., 1995; Tong et al., 1996; Chen and

Regehr, 1997) will have to be re-evaluated in light of the now generally accepted silent-synapses hypothesis (see above). Our results in **CHAPTER III** indicate that miniature release in cortical synapses *in vitro* can vary greatly between neighboring synaptic terminals. Furthermore, we find that miniature synaptic release is directly proportional to the $P_{rel.}$ of the synaptic terminal. These findings indicate that the sensitivity of the presynaptic release machinery can be tuned, and its efficiency is reflected by the frequency of spontaneously released vesicles. In other words, the more likely an AP is to trigger vesicle release, the higher the chances are that this release can occur spontaneously. A molecular basis for this is likely to be found in the array of release machinery proteins (Lin and Scheller, 2000) which operate on a highly sensitive thermodynamic threshold to balance release readiness of docked vesicles with inhibition of spontaneous fusion.

If spontaneous release is viewed as inadvertent, the concept of co-regulated $P_{rel.}$ and miniature release may seem somewhat paradoxical in that up-regulation of a synapse's release efficacy (e.g. after STE or LTP) would have the "side-effect" of increased "accidental" releases. However, an alternative explanation is that up-regulated miniature synaptic activity can ensure ongoing release at synapses that have received (STE- or LTP-) priming, even in the absence of subsequent AP-dependent activity. A certain level of synaptic activity may be important to sustain longer-lasting forms of synaptic enhancement (Okabe et al., 1999; Segal and Andersen, 2000; Zhu et al., 2000). Support for such a "trophic effect" of miniature synaptic activity comes from a study of Thompson and co-workers, who used the hippocampal slice culture preparation (McKinney et al., 1999). The authors found that, after de-afferentation, spine-loss on dendrites is prevented by miniature synaptic activity, but is independent of AP-dependent release (McKinney et al., 1999). In addition, it has been indicated that early in brain development, before the onset of electrical activity, miniature activity can facilitate synaptic development (Gottmann et al., 1994; Ali et al., 2000). However, the view that synaptic activity is necessary for proper development of synaptic structure has been challenged by surprising findings from Thomas Südhof's group. Their results show that a genetic *knock-out* of the presynaptic protein Munc-18 results in complete abolishment of (AP-dependent and spontaneous) transmitter release, but does not affect synaptic assembly in the brain (Verhage et al., 2000). Hence, rather than initiating synaptic formation during development, spontaneous

neurotransmitter secretion may function to validate already established synaptic connections (see below and **INTRODUCTION**).

During the development of the CNS the assembly of pre- and postsynaptic elements has to be orchestrated in a spatio-temporal coordinated fashion to guarantee proper formation of synaptic junctions. Extensive studies on *in vitro* development of hippocampal pyramidal neurons have utilized simultaneous immunocytochemical labeling of multiple of pre- and postsynaptic proteins, such as glutamate receptors, postsynaptic density proteins, and proteins of the presynaptic release machinery (O'Brien et al., 1997; Allison et al., 1998; Gomperts et al., 1998; Rao et al., 1998; review in Scannevin and Huganir, 2000). These studies indicate that during early development there is an initial production and targeting of postsynaptic density (PSD) proteins such as PSD-95 and GKAP into dendrites which precedes dendritic localization of NMDA receptors, and later AMPA receptors (Gomperts et al., 1998; Rao et al., 1998). Initially, targeting of these - and possibly other - designated postsynaptic core components (Garner et al., 2000) is mostly restricted to "non-synaptic" sites, that is locations that are not apposed to presynaptic markers, such as synaptophysin or SV2 (Rao et al., 1998). Formation of these protein clusters together with the observation that release competent vesicle clusters occur in the axon before dendritic contact (Kraszewski et al., 1995; Zhang et al., 1998) indicates the initial formation of independent "protosynapses" in both axonal and dendritic compartments. During the same time period there is a accumulation of the actin bundling protein alpha-actinin in highly motile dendritic protrusions (Allison et al., 1998; Rao and Craig, 2000), so-called filopodia (Dunaevsky et al., 1999; Harris, 1999; Parnass et al., 2000; Segal, 2001). There is now evidence from real-time imaging (Ziv and Smith, 1996; Friedman et al., 2000) and EM studies (Fiala et al., 1998) indicating that filopodia can initiate contacts with presynaptic sites. These findings prompted a model by which filopodial motility serves to establish synaptic contact formation (Jontes and Smith, 2000; Parnass et al., 2000; Segal, 2001). However, the chronology of as well as the cellular control over molecular events underlying the synaptogenesis are still not well understood. As synaptic activity does not seem to be necessary to trigger synaptic contact formation (Rao et al., 1998; Verhage et al., 2000), a likely mechanism for contact initiation is structural interaction between pre- and postsynapse mediated by membrane spanning cell adhesion molecules such as neurexins/neuroligins (Cantallops

and Cline, 2000; Scheiffele et al., 2000), cadherins (Kaibuchi et al., 1999; Obst-Pernberg and Redies, 1999; Bruses, 2000), immunoglobulins and integrins (Benson et al., 2000) (see also **INTRODUCTION**). Once a contact is formed, cadherin- and/or neuroligin- associated signaling cascades can conceivably arrest the filopodial movement and trigger its maturation into a functional spine (Kaibuchi et al., 1999; Rao and Craig, 2000). As this maturation period can be vary rapid - within tens of minutes - (Friedman et al., 2000) there is likely a need for pre-assembled synaptic machineries that can be inserted into the rapidly developing synaptic compartments. Targeting of such pre-assembled protein complexes to presynaptic sites have been shown to occur in hippocampal axons (Ahmari et al., 2000). Our study in **CHAPTER IV** confirms that an analogous process may exist also for the postsynaptic site. We find preformed, non-synaptic PSD-95 clusters, which often are located on the base of dendritic protrusion, can rapidly move into and/or out of developing filopodia (see Fig. 23). It is likely that these PSD-95 clusters also contain additional postsynaptic proteins, such as GKAP (Rao et al., 1998). Hence, initial contact formation with a potential presynaptic partner might trigger a signaling cascade to recruit PSD-95 based potentially multimeric protein complexes into the developing spine. This may serve to establish a fundamental postsynaptic matrix, stabilize the filopodial structure and subsequently localize NMDA receptors into these sites (Rao et al., 1998). Accordingly, we find that once PSD-95 clusters are localized into filopodia these structures are significantly more stable, i.e. less likely to turn-over during the time course of 1 hour (see Fig. 22). Finally, spontaneous miniature, or AP-dependent activity might serve to consolidate the newly formed synaptic connection or, the lack of either might lead to its recession. Consistent with this model we have found an example in which PSD-95 departure out of a filopodium is associated with massive morphological changes of the structure, including splitting and retraction (see Fig. 23).

Future experiments will have to fill many holes that still reside in our current theory about synaptogenesis and synaptic plasticity. However, with ever increasing precision of scientific approaches, including high-resolution live imaging of cellular events in living animals (Helmchen et al., 1999; Svoboda et al., 1999; Lendvai et al., 2000) and proteomic approaches such as mass spectroscopy (Walikonis et al., 2000; Walikonis et al., 2001), neuroscientists are well equipped to tackle these future challenges. A key point in advancing our understanding of synaptic function may be

contained in the close association of the still somewhat divided fields of "synaptic development" and adult "synaptic plasticity". As it has become increasingly clear now that many of the fundamental mechanisms and molecules are shared between both processes (Cramer and Sur, 1995; Rauschecker, 1995; Katz and Shatz, 1996; Lewin and Barde, 1996; Lu and Figurov, 1997; Aamodt and Constantine-Paton, 1999), neuroscientists may strive to prove that synaptic plasticity is indeed a specialized form of lifelong ongoing synaptic development. In addition, harnessing the power of our understanding about synaptic development and plasticity may prove to be our most valuable weapon in fighting many neurological and neurodevelopmental disorders we are challenged with today. Ultimately, neuroscience will have to attempt to solve our inherent questions about the fundaments of our minds, thoughts, and emotions. If this quest can ever be completed, or even be started, remains to be seen. However, as the decade of the brain has ended, neuroscience is ready to begin another the century of the synapse.

VI. REFERENCES

Aamodt SM, Constantine-Paton M (1999) The role of neural activity in synaptic development and its implications for adult brain function. Adv Neurol 79:133-144.

Ahmari SE, Buchanan J, Smith SJ (2000) Assembly of presynaptic active zones from cytoplasmic transport packets. Nat Neurosci 3:445-451.

Ali DW, Drapeau P, Legendre P (2000) Development of spontaneous glycinergic currents in the Mauthner neuron of the zebrafish embryo. J Neurophysiol 84:1726-1736.

Allen C, Stevens CF (1994) An evaluation of causes for unreliability of synaptic transmission. Proc Natl Acad Sci U S A 91:10380-10383.

Allison DW, Chervin AS, Gelfand VI, Craig AM (2000) Postsynaptic scaffolds of excitatory and inhibitory synapses in hippocampal neurons: maintenance of core components independent of actin filaments and microtubules. J Neurosci 20:4545-4554.

Allison DW, Gelfand VI, Spector I, Craig AM (1998) Role of actin in anchoring postsynaptic receptors in cultured hippocampal neurons: differential attachment of NMDA versus AMPA receptors. J Neurosci 18:2423-2436.

Alvarado MC, Bachevalier J (2000) Revisiting the maturation of medial temporal lobe memory functions in primates. Learn Mem 7:244-256.

Amara SG, Sonders MS (1998) Neurotransmitter transporters as molecular targets for addictive drugs. Drug Alcohol Depend 51:87-96.

Arancio O, Kandel ER, Hawkins RD (1995) Activity-dependent long-term enhancement of transmitter release by presynaptic 3',5'-cyclic GMP in cultured hippocampal neurons. Nature 376:74-80.

Atwood HL, Wojtowicz JM (1999) Silent synapses in neural plasticity: current evidence. Learn Mem 6:542-571.

Auclair N, Otani S, Soubrie P, Crepel F (2000) Cannabinoids modulate synaptic strength and plasticity at glutamatergic synapses of rat prefrontal cortex pyramidal neurons. J Neurophysiol 83:3287-3293.

Auger C, Kondo S, Marty A (1998) Multivesicular release at single functional synaptic sites in cerebellar stellate and basket cells. J Neurosci 18:4532-4547.

Auger C, Marty A (2000) Quantal currents at single-site central synapses. J Physiol 526 Pt 1:3-11.

Baba H, Kohno T, Okamoto M, Goldstein PA, Shimoji K, Yoshimura M (1998) Muscarinic facilitation of GABA release in substantia gelatinosa of the rat spinal dorsal horn. J Physiol 508:83-93.

Bailey CH, Kandel ER (1993) Structural changes accompanying memory storage. Annu Rev Physiol 55:397-426.

Bajjalieh SM (1999) Synaptic vesicle docking and fusion. Curr Opin Neurobiol 9:321-328.

Bao J, Li JJ, Perl ER (1998) Differences in Ca2+ channels governing generation of miniature and evoked excitatory synaptic currents in spinal laminae I and II. J Neurosci 18:8740-8750.

Bartsch D, Ghirardi M, Casadio A, Giustetto M, Karl KA, Zhu H, Kandel ER (2000) Enhancement of memory-related long-term facilitation by ApAF, a novel transcription factor that acts downstream from both CREB1 and CREB2. Cell 103:595-608.

Bear MF (1999) Homosynaptic long-term depression: a mechanism for memory? Proc Natl Acad Sci U S A 96:9457-9458.

Bear MF, Malenka RC (1994) Synaptic plasticity: LTP and LTD. Curr Opin Neurobiol 4:389-399.

Bekkers JM, Stevens CF (1990) Presynaptic mechanism for long-term potentiation in the hippocampus. Nature 346:724-729.

Benson DL, Cohen PA (1996) Activity-independent segregation of excitatory and inhibitory synaptic terminals in cultured hippocampal neurons. J Neurosci 16:6424-6432.

Benson DL, Schnapp LM, Shapiro L, Huntley GW (2000) Making memories stick: cell-adhesion molecules in synaptic plasticity. Trends Cell Biol 10:473-482.

Berardi N, Pizzorusso T, Maffei L (2000) Critical periods during sensory development. Curr Opin Neurobiol 10:138-145.

Betz WJ, Angleson JK (1998) The synaptic vesicle cycle. Annu Rev Physiol 60:347-363.

Betz WJ, Bewick GS (1992) Optical analysis of synaptic vesicle recycling at the frog neuromuscular junction. Science 255:200-203.

Betz WJ, Bewick GS (1993) Optical monitoring of transmitter release and synaptic vesicle recycling at the frog neuromuscular junction. J Physiol 460:287-309.

Betz WJ, Mao F, Bewick GS (1992) Activity-dependent fluorescent staining and destaining of living vertebrate motor nerve terminals. J Neurosci 12:363-375.

Betz WJ, Mao F, Smith CB (1996) Imaging exocytosis and endocytosis. Curr Opin Neurobiol 6:365-371.

Beutner D, Voets T, Neher E, Moser T (2001) Calcium dependence of exocytosis and endocytosis at the cochlear inner hair cell afferent synapse. Neuron 29:681-690.

Bi G, Poo M (2001) Synaptic modification by correlated activity: hebb's postulate revisited. Annu Rev Neurosci 24:139-166.

Blakely RD, Bauman AL (2000) Biogenic amine transporters: regulation in flux. Curr Opin Neurobiol 10:328-336.

Bliss TV, Lomo T (1973) Long-lasting potentiation of synaptic transmission in the dentate area of the anaesthetized rabbit following stimulation of the perforant path. J Physiol 232:331-356.

Bolshakov VY, Golan H, Kandel ER, Siegelbaum SA (1997) Recruitment of new sites of synaptic transmission during the cAMP- dependent late phase of LTP at CA3-CA1 synapses in the hippocampus. Neuron 19:635-651.

Bolshakov VY, Siegelbaum SA (1995a) Hippocampal long-term depression: arachidonic acid as a potential retrograde messenger. Neuropharmacology 34:1581-1587.

Bolshakov VY, Siegelbaum SA (1995b) Regulation of hippocampal transmitter release during development and long-term potentiation. Science 269:1730-1734.

Breier A, Su TP, Malhotra AK, Elman I, Adler CM, Weisenfeld NI, Pickar D (1999) Effects of atypical antipsychotic drug treatment on amphetamine-induced striatal dopamine release in patients with psychotic disorders. Neuropsychopharmacology 20:340-345.

Brunel N (1996) Hebbian learning of context in recurrent neural networks. Neural Comput 8:1677-1710.

Brunger AT (2001) Structural insights into the molecular mechanism of calcium-dependent vesicle-membrane fusion. Curr Opin Struct Biol 11:163-173.

Bruses JL (2000) Cadherin-mediated adhesion at the interneuronal synapse. Curr Opin Cell Biol 12:593-597.

Buchs PA, Muller D (1996) Induction of long-term potentiation is associated with major ultrastructural changes of activated synapses. Proc Natl Acad Sci U S A 93:8040-8045.

Buonomano DV, Merzenich MM (1998) Cortical plasticity: from synapses to maps. Annu Rev Neurosci 21:149-186.

Burger MM, Schaefer T (1998) Regulation of intracellular membrane interactions: recent progress in the field of neurotransmitter release. J Cell Biochem Suppl 31:103-110.

Byrne JH, Kandel ER (1996) Presynaptic facilitation revisited: state and time dependence. J Neurosci 16:425-435.

Calverley RK, Jones DG (1990) Contributions of dendritic spines and perforated synapses to synaptic plasticity. Brain Res Brain Res Rev 15:215-249.

Cantallops I, Cline HT (2000) Synapse formation: if it looks like a duck and quacks like a duck. Curr Biol 10:R620-623.

Capogna M, Gahwiler BH, Thompson SM (1995) Presynaptic enhancement of inhibitory synaptic transmission by protein kinases A and C in the rat hippocampus in vitro. J Neurosci 15:1249-1260.

Capogna M, Gahwiler BH, Thompson SM (1996a) Calcium-independent actions of alpha-latrotoxin on spontaneous and evoked synaptic transmission in the hippocampus. J Neurophysiol 76:3149-3158.

Capogna M, Gahwiler BH, Thompson SM (1996b) Presynaptic inhibition of calcium-dependent and -independent release elicited with ionomycin, gadolinium, and alpha-latrotoxin in the hippocampus. J Neurophysiol 75:2017-2028.

Capogna M, McKinney RA, O'Connor V, Gahwiler BH, Thompson SM (1997) Ca2+ or Sr2+ partially rescues synaptic transmission in hippocampal cultures treated with botulinum toxin A and C, but not tetanus toxin. J Neurosci 17:7190-7202.

Carlsson A, Waters N, Carlsson ML (1999) Neurotransmitter interactions in schizophrenia-therapeutic implications. Eur Arch Psychiatry Clin Neurosci 249:37-43.

Carroll RC, Beattie EC, Xia H, Luscher C, Altschuler Y, Nicoll RA, Malenka RC, von Zastrow M (1999a) Dynamin-dependent endocytosis of ionotropic glutamate receptors. Proc Natl Acad Sci U S A 96:14112-14117.

Carroll RC, Lissin DV, von Zastrow M, Nicoll RA, Malenka RC (1999b) Rapid redistribution of glutamate receptors contributes to long-term depression in hippocampal cultures. Nat Neurosci 2:454-460.

Carroll RC, Nicoll RA, Malenka RC (1998) Effects of PKA and PKC on miniature excitatory postsynaptic currents in CA1 pyramidal cells. J Neurophysiol 80:2797-2800.

Castro-Alamancos MA, Connors BW (1997) Distinct forms of short-term plasticity at excitatory synapses of hippocampus and neocortex. Proc Natl Acad Sci U S A 94:4161-4166.

Catterall WA (1999) Interactions of presynaptic Ca2+ channels and snare proteins in neurotransmitter release. Ann N Y Acad Sci 868:144-159.

Ceccarelli B, Hurlbut WP, Iezzi N (1988) Effect of alpha-latrotoxin on the frog neuromuscular junction at low temperature. J Physiol 402:195-217.

Chavez-Noriega LE, Stevens CF (1994) Increased transmitter release at excitatory synapses produced by direct activation of adenylate cyclase in rat hippocampal slices. J Neurosci 14:310-317.

Chavis P, Mollard P, Bockaert J, Manzoni O (1998) Visualization of cyclic AMP-regulated presynaptic activity at cerebellar granule cells. Neuron 20:773-781.

Chen C, Regehr WG (1997) The mechanism of cAMP-mediated enhancement at a cerebellar synapse. J Neurosci 17:8687-8694.

Chen N, Ren J, Raymond LA, Murphy TH (2001) Changes in agonist concentration dependence that are a function of duration of exposure suggest N-methyl-D-aspartate receptor nonsaturation during synaptic stimulation. Mol Pharmacol 59:212-219.

Clark KA, Collingridge GL (1996) Evidence that presynaptic changes are involved in the expression of LTP and LTD of NMDA receptor-mediated EPSCs in area CA1 of the hippocampus. J Physiol Paris 90:311.

Cline HT (2001) Dendritic arbor development and synaptogenesis. Curr Opin Neurobiol 11:118-126.

Collin C, Vicario-Abejon C, Rubio ME, Wenthold RJ, McKay RD, Segal M (2001) Neurotrophins act at presynaptic terminals to activate synapses among cultured hippocampal neurons. Eur J Neurosci 13:1273-1282.

Compte A, Brunel N, Goldman-Rakic PS, Wang XJ (2000) Synaptic mechanisms and network dynamics underlying spatial working memory in a cortical network model. Cereb Cortex 10:910-923.

Connor JA, Petrozzino J, Pozzo-Miller LD, Otani S (1999) Calcium signals in long-term potentiation and long-term depression. Can J Physiol Pharmacol 77:722-734.

Connor JA, Wadman WJ, Hockberger PE, Wong RK (1988) Sustained dendritic gradients of Ca2+ induced by excitatory amino acids in CA1 hippocampal neurons. Science 240:649-653.

Cormier RJ, Greenwood AC, Connor JA (2001) Bidirectional synaptic plasticity correlated with the magnitude of dendritic calcium transients above a threshold. J Neurophysiol 85:399-406.

Cormier RJ, Kelly PT (1996) Glutamate-induced long-term potentiation enhances spontaneous EPSC amplitude but not frequency. J Neurophysiol 75:1909-1918.

Craig AM, Blackstone CD, Huganir RL, Banker G (1994) Selective clustering of glutamate and gamma-aminobutyric acid receptors opposite terminals releasing the corresponding neurotransmitters. Proc Natl Acad Sci U S A 91:12373-12377.

Cramer KS, Sur M (1995) Activity-dependent remodeling of connections in the mammalian visual system. Curr Opin Neurobiol 5:106-111.

Craven SE, Bredt DS (1998) PDZ proteins organize synaptic signaling pathways. Cell 93:495-498.

Craven SE, El-Husseini AE, Bredt DS (1999) Synaptic targeting of the postsynaptic density protein PSD-95 mediated by lipid and protein motifs. Neuron 22:497-509.

Cummings DD, Wilcox KS, Dichter MA (1996) Calcium-dependent paired-pulse facilitation of miniature EPSC frequency accompanies depression of EPSCs at hippocampal synapses in culture. J Neurosci 16:5312-5323.

Dailey ME, Smith SJ (1996) The dynamics of dendritic structure in developing hippocampal slices. J Neurosci 16:2983-2994.

Dalva MB, Takasu MA, Lin MZ, Shamah SM, Hu L, Gale NW, Greenberg ME (2000) EphB receptors interact with NMDA receptors and regulate excitatory synapse formation. Cell 103:945-956.

Daniel H, Levenes C, Crepel F (1998) Cellular mechanisms of cerebellar LTD. Trends Neurosci 21:401-407.

Davis S, Vanhoutte P, Pages C, Caboche J, Laroche S (2000) The MAPK/ERK cascade targets both Elk-1 and cAMP response element- binding protein to control long-term potentiation-dependent gene expression in the dentate gyrus in vivo. J Neurosci 20:4563-4572.

Debanne D, Guerineau NC, Gahwiler BH, Thompson SM (1996) Paired-pulse facilitation and depression at unitary synapses in rat hippocampus: quantal fluctuation affects subsequent release. J Physiol 491:163-176.

Deitcher DL, Ueda A, Stewart BA, Burgess RW, Kidokoro Y, Schwarz TL (1998) Distinct requirements for evoked and spontaneous release of neurotransmitter are revealed by mutations in the Drosophila gene neuronal-synaptobrevin. J Neurosci 18:2028-2039.

Delaney KR (2000) Calcium and Neurotransmitter Release. In: Encyclopedia of Life Sciences. London: Nature Publishing Group.

Delaney KR, Tank DW (1994) A quantitative measurement of the dependence of short-term synaptic enhancement on presynaptic residual calcium. J Neurosci 14:5885-5902.

Derkach V, Barria A, Soderling TR (1999) Ca2+/calmodulin-kinase II enhances channel conductance of alpha-amino-3- hydroxy-5-methyl-4-isoxazolepropionate type glutamate receptors. Proc Natl Acad Sci U S A 96:3269-3274.

Desai RC, Vyas B, Earles CA, Littleton JT, Kowalchyck JA, Martin TF, Chapman ER (2000) The C2B domain of synaptotagmin is a Ca(2+)-sensing module essential for exocytosis. J Cell Biol 150:1125-1136.

Dittman JS, Regehr WG (1996) Contributions of calcium-dependent and calcium-independent mechanisms to presynaptic inhibition at a cerebellar synapse. J Neurosci 16:1623-1633.

Dobrunz LE, Huang EP, Stevens CF (1997) Very short-term plasticity in hippocampal synapses. Proc Natl Acad Sci U S A 94:14843-14847.

Dobrunz LE, Stevens CF (1997) Heterogeneity of release probability, facilitation, and depletion at central synapses. Neuron 18:995-1008.

Dodge FA, Jr., Rahamimoff R (1967) Co-operative action a calcium ions in transmitter release at the neuromuscular junction. J Physiol 193:419-432.

Doze VA, Cohen GA, Madison DV (1995) Calcium channel involvement in GABAB receptor-mediated inhibition of GABA release in area CA1 of the rat hippocampus. J Neurophysiol 74:43-53.

Drescher U (2000) Excitation at the synapse: Eph receptors team up with NMDA receptors. Cell 103:1005-1008.

Dunaevsky A, Tashiro A, Majewska A, Mason C, Yuste R (1999) Developmental regulation of spine motility in the mammalian central nervous system. Proc Natl Acad Sci U S A 96:13438-13443.

Eccles JC (1992) Evolution of consciousness. Proc Natl Acad Sci U S A 89:7320-7324.

Eccles JC, Katz B, Kuffler SW (1941) Nature of the 'endplate potential' in curarized muscle. 4:362-387.

Edwards FA (1995) Anatomy and electrophysiology of fast central synapses lead to a structural model for long-term potentiation. Physiol Rev 75:759-787.

El-Husseini AE, Craven SE, Chetkovich DM, Firestein BL, Schnell E, Aoki C, Bredt DS (2000a) Dual palmitoylation of PSD-95 mediates its vesiculotubular sorting, postsynaptic targeting, and ion channel clustering. J Cell Biol 148:159-172.

El-Husseini AE, Schnell E, Chetkovich DM, Nicoll RA, Bredt DS (2000b) PSD-95 involvement in maturation of excitatory synapses. Science 290:1364-1368.

Ellitot TR (1904) On the action of adrenaline. J. Physiol. (London) 31:20-21.

Emptage NJ, Reid CA, Fine A (2001) Calcium stores in hippocampal synaptic boutons mediate short-term plasticity, store-operated Ca2+ entry, and spontaneous transmitter release. Neuron 29:197-208.

Engert F, Bonhoeffer T (1999) Dendritic spine changes associated with hippocampal long-term synaptic plasticity. Nature 399:66-70.

Fanning AS, Anderson JM (1999) Protein modules as organizers of membrane structure. Curr Opin Cell Biol 11:432-439.

Fatt P, Katz B (1950) J. Physiol. 46p-47p.

Fatt P, Katz B (1952) Spontaneous subthreshold activity at motor nerve endings. J. Physiol. 117:109-128.

Feldman DE, Knudsen EI (1998) Experience-dependent plasticity and the maturation of glutamatergic synapses. Neuron 20:1067-1071.

Fernandez-Chacon R, Konigstorfer A, Gerber SH, Garcia J, Matos MF, Stevens CF, Brose N, Rizo J, Rosenmund C, Sudhof TC (2001) Synaptotagmin I functions as a calcium regulator of release probability. Nature 410:41-49.

Fiala JC, Feinberg M, Popov V, Harris KM (1998) Synaptogenesis via dendritic filopodia in developing hippocampal area CA1. J Neurosci 18:8900-8911.

Fischer M, Kaech S, Knutti D, Matus A (1998) Rapid actin-based plasticity in dendritic spines. Neuron 20:847-854.

Fischer M, Kaech S, Wagner U, Brinkhaus H, Matus A (2000) Glutamate receptors regulate actin-based plasticity in dendritic spines. Nat Neurosci 3:887-894.

Fisher SA, Fischer TM, Carew TJ (1997) Multiple overlapping processes underlying short-term synaptic enhancement. Trends Neurosci 20:170-177.

Fon EA, Edwards RH (2001) Molecular mechanisms of neurotransmitter release. Muscle Nerve 24:581-601.

Forti L, Bossi M, Bergamaschi A, Villa A, Malgaroli A (1997) Loose-patch recordings of single quanta at individual hippocampal synapses. Nature 388:874-878.

Foster JK (1999) Memory, imaging, and the mind-brain: in conclusion. Memory 7:733-740.

Frerking M, Borges S, Wilson M (1997) Are some minis multiquantal? J Neurophysiol 78:1293-1304.

Frey S, Bergado-Rosado J, Seidenbecher T, Pape HC, Frey JU (2001) Reinforcement of early long-term potentiation (early-LTP) in dentate gyrus by stimulation of the basolateral amygdala: heterosynaptic induction mechanisms of late-LTP. J Neurosci 21:3697-3703.

Friedman HV, Bresler T, Garner CC, Ziv NE (2000) Assembly of new individual excitatory synapses: time course and temporal order of synaptic molecule recruitment [see comments]. Neuron 27:57-69.

Froc DJ, Chapman CA, Trepel C, Racine RJ (2000) Long-term depression and depotentiation in the sensorimotor cortex of the freely moving rat. J Neurosci 20:438-445.

Gad H, Low P, Zotova E, Brodin L, Shupliakov O (1998) Dissociation between Ca2+-triggered synaptic vesicle exocytosis and clathrin-mediated endocytosis at a central synapse. Neuron 21:607-616.

Garcia R, Vouimba RM, Jaffard R (1993) Spatial discrimination learning induces LTP-like changes in the lateral septum of mice. Neuroreport 5:329-332.

Garner CC, Nash J, Huganir RL (2000) PDZ domains in synapse assembly and signalling. Trends Cell Biol 10:274-280.

Geinisman Y (2000) Structural synaptic modifications associated with hippocampal LTP and behavioral learning. Cereb Cortex 10:952-962.

Ghirardi M, Braha O, Hochner B, Montarolo PG, Kandel ER, Dale N (1992) Roles of PKA and PKC in facilitation of evoked and spontaneous transmitter release at depressed and nondepressed synapses in Aplysia sensory neurons. Neuron 9:479-489.

Gilbert CD (1998) Adult cortical dynamics. Physiol Rev 78:467-485.

Golgi C (1873) Sulla struttura della sostanza grigia del cervello. Gazzetta Medica Italiana - Lombardia 33:244-246.

Gomperts SN, Rao A, Craig AM, Malenka RC, Nicoll RA (1998) Postsynaptically silent synapses in single neuron cultures. Neuron 21:1443-1451.

Goodman CS, Shatz CJ (1993) Developmental mechanisms that generate precise patterns of neuronal connectivity. Cell 72 Suppl:77-98.

Gottmann K, Pfrieger FW, Lux HD (1994) The formation of glutamatergic synapses in cultured central neurons: selective increase in miniature synaptic currents. Brain Res Dev Brain Res 81:77-88.

Haage D, Karlsson U, Johansson S (1998) Heterogeneous presynaptic Ca2+ channel types triggering GABA release onto medial preoptic neurons from rat. J Physiol 507:77-91.

Halpain S (2000) Actin and the agile spine: how and why do dendritic spines dance? Trends Neurosci 23:141-146.

Hamill OP, Marty A, Neher E, Sakmann B, Sigworth FJ (1981) Improved patch-clamp techniques for high-resolution current recording from cells and cell-free membrane patches. Pflugers Arch 391:85-100.

Hamori J, Takacs J, Petrusz P (1990) Immunogold electron microscopic demonstration of glutamate and GABA in normal and deafferented cerebellar cortex: correlation between transmitter content and synaptic vesicle size. J Histochem Cytochem 38:1767-1777.

Hanse E, Gustafsson B (2001) Quantal variability at glutamatergic synapses in area CA1 of the rat neonatal hippocampus. J Physiol 531:467-480.

Hansel C, Linden DJ, D'Angelo E (2001) Beyond parallel fiber LTD: the diversity of synaptic and non-synaptic plasticity in the cerebellum. Nat Neurosci 4:467-475.

Hardingham GE, Arnold FJ, Bading H (2001) Nuclear calcium signaling controls CREB-mediated gene expression triggered by synaptic activity. Nat Neurosci 4:261-267.

Harris EW, Ganong AH, Cotman CW (1984) Long-term potentiation in the hippocampus involves activation of N- methyl-D-aspartate receptors. Brain Res 323:132-137.

Harris KM (1995) How multiple-synapse boutons could preserve input specificity during an interneuronal spread of LTP. Trends Neurosci 18:365-369.

Harris KM (1999) Structure, development, and plasticity of dendritic spines. Curr Opin Neurobiol 9:343-348.

Harris KM, Jensen FE, Tsao B (1992) Three-dimensional structure of dendritic spines and synapses in rat hippocampus (CA1) at postnatal day 15 and adult ages: implications for the maturation of synaptic physiology and long-term potentiation. J Neurosci 12:2685-2705.

Harris KM, Sultan P (1995) Variation in the number, location and size of synaptic vesicles provides an anatomical basis for the nonuniform probability of release at hippocampal CA1 synapses. Neuropharmacology 34:1387-1395.

Hata Y, Takai Y (1999) Roles of postsynaptic density-95/synapse-associated protein 90 and its interacting proteins in the organization of synapses. Cell Mol Life Sci 56:461-472.

Hebb DO (1949) The organization of behavior; a neuropsychological theory. New York: Wiley-Interscience.

Heemskerk FM, Schrama LH, de Graan PN, Gispen WH (1987) 4-Aminopyridine inhibits synaptosomal plasma membrane protein phosphorylation in vitro: effect of the selective NMDA-antagonist 2- amino-5-phosphonovalerate. Biochem Biophys Res Commun 147:94-99.

Hell JW, Yokoyama CT, Breeze LJ, Chavkin C, Catterall WA (1995) Phosphorylation of presynaptic and postsynaptic calcium channels by cAMP-dependent protein kinase in hippocampal neurons. Embo J 14:3036-3044.

Helmchen F, Svoboda K, Denk W, Tank DW (1999) In vivo dendritic calcium dynamics in deep-layer cortical pyramidal neurons. Nat Neurosci 2:989-996.

Henkel AW, Lubke J, Betz WJ (1996) FM1-43 dye ultrastructural localization in and release from frog motor nerve terminals. Proc Natl Acad Sci U S A 93:1918-1923.

Herron CE, Lester RA, Coan EJ, Collingridge GL (1985) Intracellular demonstration of an N-methyl-D-aspartate receptor mediated component of synaptic transmission in the rat hippocampus. Neurosci Lett 60:19-23.

Herron CE, Lester RA, Coan EJ, Collingridge GL (1986) Frequency-dependent involvement of NMDA receptors in the hippocampus: a novel synaptic mechanism. Nature 322:265-268.

Hessler NA, Shirke AM, Malinow R (1993) The probability of transmitter release at a mammalian central synapse. Nature 366:569-572.

Heuser JE, Reese TS (1973) Evidence for recycling of synaptic vesicle membrane during transmitter release at the frog neuromuscular junction. J Cell Biol 57:315-344.

Heynen AJ, Quinlan EM, Bae DC, Bear MF (2000) Bidirectional, activity-dependent regulation of glutamate receptors in the adult hippocampus in vivo. Neuron 28:527-536.

Hoffman AF, Lupica CR (2000) Mechanisms of cannabinoid inhibition of GABA(A) synaptic transmission in the hippocampus. J Neurosci 20:2470-2479.

Holthausen K, Breidbach O (1999) Analytical description of the evolution of neural networks: learning rules and complexity. Biol Cybern 81:169-175.

Honer WG (1999) Assessing the machinery of mind: synapses in neuropsychiatric disorders. J Psychiatry Neurosci 24:116-121.

Hua SY, Raciborska DA, Trimble WS, Charlton MP (1998) Different VAMP/synaptobrevin complexes for spontaneous and evoked transmitter release at the crayfish neuromuscular junction. J Neurophysiol 80:3233-3246.

Husi H, Ward MA, Choudhary JS, Blackstock WP, Grant SG (2000) Proteomic analysis of NMDA receptor-adhesion protein signaling complexes. Nat Neurosci 3:661-669.

Isaacson JS, Hille B (1997) GABA(B)-mediated presynaptic inhibition of excitatory transmission and synaptic vesicle dynamics in cultured hippocampal neurons. Neuron 18:143-152.

Jan LY, Stevens CF (2000) Signalling mechanisms: a decade of signalling. Curr Opin Neurobiol 10:625-630.

Johnson KO (2000) Neural coding. Neuron 26:563-566.

Jones MW, Errington ML, French PJ, Fine A, Bliss TV, Garel S, Charnay P, Bozon B, Laroche S, Davis S (2001) A requirement for the immediate early gene Zif268 in the expression of late LTP and long-term memories. Nat Neurosci 4:289-296.

Jontes JD, Smith SJ (2000) Filopodia, spines, and the generation of synaptic diversity. Neuron 27:11-14.

Josselyn SA, Shi C, Carlezon WA, Jr., Neve RL, Nestler EJ, Davis M (2001) Long-Term Memory Is Facilitated by cAMP Response Element-Binding Protein Overexpression in the Amygdala. J Neurosci 21:2404-2412.

Kaibuchi K, Kuroda S, Fukata M, Nakagawa M (1999) Regulation of cadherin-mediated cell-cell adhesion by the Rho family GTPases. Curr Opin Cell Biol 11:591-596.

Kamiya H, Zucker RS (1994) Residual Ca2+ and short-term synaptic plasticity. Nature 371:603-606.

Kandel ER, Squire LR (2000) Neuroscience: Breaking Down Scientific Barriers to the Study of Brain and Mind. Science 290:1113-1120.

Katz B, Miledi R (1968) The role of calcium in neuromuscular facilitation. J Physiol 195:481-492.

Katz E, Ferro PA, Cherksey BD, Sugimori M, Llinas R, Uchitel OD (1995) Effects of Ca2+ channel blockers on transmitter release and presynaptic currents at the frog neuromuscular junction. J Physiol 486:695-706.

Katz LC, Shatz CJ (1996) Synaptic activity and the construction of cortical circuits. Science 274:1133-1138.

Kauer JA, Malenka RC, Nicoll RA (1988) NMDA application potentiates synaptic transmission in the hippocampus. Nature 334:250-252.

Kolb B, Whishaw IQ (1998) Brain plasticity and behavior. Annu Rev Psychol 49:43-64.

Kombian SB, Hirasawa M, Mouginot D, Chen X, Pittman QJ (2000) Short-term potentiation of miniature excitatory synaptic currents causes excitation of supraoptic neurons. J Neurophysiol 83:2542-2553.

Kondo S, Marty A (1997) Protein kinase A-mediated enhancement of miniature IPSC frequency by noradrenaline in rat cerebellar stellate cells. J Physiol 498:165-176.

Kondo S, Marty A (1998) Differential effects of noradrenaline on evoked, spontaneous and miniature IPSCs in rat cerebellar stellate cells. J Physiol 509:233-243.

Korn H, Bausela F, Charpier S, Faber DS (1993) Synaptic noise and multiquantal release at dendritic synapses. J Neurophysiol 70:1249-1254.

Kraszewski K, Mundigl O, Daniell L, Verderio C, Matteoli M, De Camilli P (1995) Synaptic vesicle dynamics in living cultured hippocampal neurons visualized with CY3-conjugated antibodies directed against the lumenal domain of synaptotagmin. J Neurosci 15:4328-4342.

Kreek MJ (1996) Cocaine, dopamine and the endogenous opioid system. J Addict Dis 15:73-96.

Kreiman G, Koch C, Fried I (2000) Imagery neurons in the human brain. Nature 408:357-361.

Kullmann DM, Siegelbaum SA (1995) The site of expression of NMDA receptor-dependent LTP: new fuel for an old fire. Neuron 15:997-1002.

Lashley KS (1929) Brain mechanisms and intelligence: a quantative study of injuries of the brain. Chicago: Chicago University Press.

Leahy JC, Luo Y, Kent CS, Meiri KF, Vallano ML (1993) Demonstration of presynaptic protein kinase C activation following long- term potentiation in rat hippocampal slices. Neuroscience 52:563-574.

Lee SH, Sheng M (2000) Development of neuron-neuron synapses. Curr Opin Neurobiol 10:125-131.

Lendvai B, Stern EA, Chen B, Svoboda K (2000) Experience-dependent plasticity of dendritic spines in the developing rat barrel cortex in vivo. Nature 404:876-881.

Levenes C, Daniel H, Soubrie P, Crepel F (1998) Cannabinoids decrease excitatory synaptic transmission and impair long- term depression in rat cerebellar Purkinje cells. J Physiol 510:867-879.

Lewin GR, Barde YA (1996) Physiology of the neurotrophins. Annu Rev Neurosci 19:289-317.

Li YX, Zhang Y, Lester HA, Schuman EM, Davidson N (1998) Enhancement of neurotransmitter release induced by brain-derived neurotrophic factor in cultured hippocampal neurons. J Neurosci 18:10231-10240.

Liao D, Jones A, Malinow R (1992) Direct measurement of quantal changes underlying long-term potentiation in CA1 hippocampus. Neuron 9:1089-1097.

Lin RC, Scheller RH (2000) Mechanisms of synaptic vesicle exocytosis. Annu Rev Cell Dev Biol 16:19-49.

Lisman JE (1997) Bursts as a unit of neural information: making unreliable synapses reliable. Trends Neurosci 20:38-43.

Lisman JE, Harris KM (1993) Quantal analysis and synaptic anatomy--integrating two views of hippocampal plasticity. Trends Neurosci 16:141-147.

Lissin DV, Carroll RC, Nicoll RA, Malenka RC, von Zastrow M (1999) Rapid, activation-induced redistribution of ionotropic glutamate receptors in cultured hippocampal neurons. J Neurosci 19:1263-1272.

Littleton JT, Bai J, Vyas B, Desai R, Baltus AE, Garment MB, Carlson SD, Ganetzky B, Chapman ER (2001) synaptotagmin mutants reveal essential functions for the C2B domain in Ca2+-triggered fusion and recycling of synaptic vesicles in vivo. J Neurosci 21:1421-1433.

Liu G, Tsien RW (1995) Properties of synaptic transmission at single hippocampal synaptic boutons. Nature 375:404-408.

Lledo PM, Zhang X, Sudhof TC, Malenka RC, Nicoll RA (1998) Postsynaptic membrane fusion and long-term potentiation. Science 279:399-403.

Lonart G, Sudhof TC (1998) Region-specific phosphorylation of rabphilin in mossy fiber nerve terminals of the hippocampus. J Neurosci 18:634-640.

Lu B, Figurov A (1997) Role of neurotrophins in synapse development and plasticity. Rev Neurosci 8:1-12.

Lu W, Man H, Ju W, Trimble WS, MacDonald JF, Wang YT (2001) Activation of synaptic NMDA receptors induces membrane insertion of new AMPA receptors and LTP in cultured hippocampal neurons. Neuron 29:243-254.

Luscher C, Nicoll RA, Malenka RC, Muller D (2000) Synaptic plasticity and dynamic modulation of the postsynaptic membrane. Nat Neurosci 3:545-550.

Luscher C, Xia H, Beattie EC, Carroll RC, von Zastrow M, Malenka RC, Nicoll RA (1999) Role of AMPA receptor cycling in synaptic transmission and plasticity. Neuron 24:649-658.

Ma L, Zablow L, Kandel ER, Siegelbaum SA (1999) Cyclic AMP induces functional presynaptic boutons in hippocampal CA3- CA1 neuronal cultures. Nat Neurosci 2:24-30.

Mackenzie PJ, Umemiya M, Murphy TH (1996) Ca2+ imaging of CNS Axons in culture indicates reliable coupling between single action potentials and distal functional release sites. Neuron 16:783-795.

Magee JC (2000) Dendritic integration of excitatory synaptic input. Nat Rev Neurosci 1:181-190.

Mainen ZF, Maletic-Savatic M, Shi SH, Hayashi Y, Malinow R, Svoboda K (1999a) Two-photon imaging in living brain slices. Methods 18:231-239, 181.

Mainen ZF, Malinow R, Svoboda K (1999b) Synaptic calcium transients in single spines indicate that NMDA receptors are not saturated. Nature 399:151-155.

Majewski H, Iannazzo L (1998) Protein kinase C: a physiological mediator of enhanced transmitter output. Prog Neurobiol 55:463-475.

Malenka RC, Madison DV, Nicoll RA (1986) Potentiation of synaptic transmission in the hippocampus by phorbol esters. Nature 321:175-177.

Malenka RC, Nicoll RA (1999) Long-term potentiation--a decade of progress? Science 285:1870-1874.

Maletic-Savatic M, Malinow R, Svoboda K (1999) Rapid dendritic morphogenesis in CA1 hippocampal dendrites induced by synaptic activity. Science 283:1923-1927.

Malgaroli A, Tsien RW (1992) Glutamate-induced long-term potentiation of the frequency of miniature synaptic currents in cultured hippocampal neurons. Nature 357:134-139.

Malinow R (1998) Silencing the controversy in LTP? Neuron 21:1226-1227.

Malinow R, Madison DV, Tsien RW (1988) Persistent protein kinase activity underlying long-term potentiation. Nature 335:820-824.

Malinow R, Mainen ZF, Hayashi Y (2000) LTP mechanisms: from silence to four-lane traffic. Curr Opin Neurobiol 10:352-357.

Manahan-Vaughan D, Braunewell KH (1999) Novelty acquisition is associated with induction of hippocampal long- term depression. Proc Natl Acad Sci U S A 96:8739-8744.

Marcus DS, Kriebel ME, Hanna RB (1992) Effects of calcium on the dynamic process of transmitter release which generates either skew- or bell-MEPPS. Brain Res 593:185-196.

Martin SJ, Grimwood PD, Morris RG (2000) Synaptic plasticity and memory: an evaluation of the hypothesis. Annu Rev Neurosci 23:649-711.

Matthews G, Wickelgren WO (1977) On the effect of calcium on the frequency of miniature end-plate potentials at the frog neuromuscular junction. J Physiol 266:91-101.

Matus A, Brinkhaus H, Wagner U (2000) Actin dynamics in dendritic spines: a form of regulated plasticity at excitatory synapses. Hippocampus 10:555-560.

Mayer ML, Westbrook GL, Guthrie PB (1984) Voltage-dependent block by Mg2+ of NMDA responses in spinal cord neurones. Nature 309:261-263.

Mayford M, Kandel ER (1999) Genetic approaches to memory storage. Trends Genet 15:463-470.

McAllister AK, Stevens CF (2000) Nonsaturation of AMPA and NMDA receptors at hippocampal synapses. Proc Natl Acad Sci U S A 97:6173-6178.

McGaugh JL (2000) Memory--a century of consolidation. Science 287:248-251.

McKinney RA, Capogna M, Durr R, Gahwiler BH, Thompson SM (1999) Miniature synaptic events maintain dendritic spines via AMPA receptor activation. Nat Neurosci 2:44-49.

Merzenich M (1998) Long-term change of mind. Science 282:1062-1063.

Milner B, Squire LR, Kandel ER (1998) Cognitive neuroscience and the study of memory. Neuron 20:445-468.

Minota S, Kumamoto E, Kitakoga O, Kuba K (1991) Long-term potentiation induced by a sustained rise in the intraterminal Ca2+ in bull-frog sympathetic ganglia. J Physiol 435:421-438.

Mintz IM, Sabatini BL, Regehr WG (1995) Calcium control of transmitter release at a cerebellar synapse. Neuron 15:675-688.

Mitsuno K, Sasa M, Ishihara K, Ishikawa M, Kikuchi H (1994) LTP of mossy fiber-stimulated potentials in CA3 during learning in rats. Physiol Behav 55:633-638.

Mochida S, Fukuda M, Niinobe M, Kobayashi H, Mikoshiba K (1997) Roles of synaptotagmin C2 domains in neurotransmitter secretion and inositol high-polyphosphate binding at mammalian cholinergic synapses. Neuroscience 77:937-943.

Mochida S, Yokoyama CT, Kim DK, Itoh K, Catterall WA (1998) Evidence for a voltage-dependent enhancement of neurotransmitter release mediated via the synaptic protein interaction site of N-type Ca2+ channels. PNAS 95:14523-14528.

Momiyama A, Takahashi T (1994) Calcium channels responsible for potassium-induced transmitter release at rat cerebellar synapses. J Physiol 476:197-202.

Montgomery JM, Madison DV (2001) The grass roots of synapse suppression. Neuron 29:567-570.

Morgan JR, Lafer EM, Augustine GJ (2001) Rapid-fire synaptic vesicle exocytosis. Neuron 30:5-7.

Morris RG, Anderson E, Lynch GS, Baudry M (1986) Selective impairment of learning and blockade of long-term potentiation by an N-methyl-D-aspartate receptor antagonist, AP5. Nature 319:774-776.

Morris RG, Frey U (1997) Hippocampal synaptic plasticity: role in spatial learning or the automatic recording of attended experience? Philos Trans R Soc Lond B Biol Sci 352:1489-1503.

Muller D, Toni N, Buchs PA (2000) Spine changes associated with long-term potentiation. Hippocampus 10:596-604.

Murphy TH, Baraban JM, Wier WG (1995) Mapping miniature synaptic currents to single synapses using calcium imaging reveals heterogeneity in postsynaptic output. Neuron 15:159-168.

Murphy TH, Baraban JM, Wier WG, Blatter LA (1994) Visualization of quantal synaptic transmission by dendritic calcium imaging. Science 263:529-532.

Murthy VN, Sejnowski TJ, Stevens CF (1997) Heterogeneous release properties of visualized individual hippocampal synapses. Neuron 18:599-612.

Murthy VN, Stevens CF (1998) Synaptic vesicles retain their identity through the endocytic cycle. Nature 392:497-501.

Nakayama AY, Luo L (2000) Intracellular signaling pathways that regulate dendritic spine morphogenesis. Hippocampus 10:582-586.

Ngezahayo A, Schachner M, Artola A (2000) Synaptic activity modulates the induction of bidirectional synaptic changes in adult mouse hippocampus. J Neurosci 20:2451-2458.

Nowak L, Bregestovski P, Ascher P, Herbet A, Prochiantz A (1984) Magnesium gates glutamate-activated channels in mouse central neurones. Nature 307:462-465.

O'Brien RJ, Mammen AL, Blackshaw S, Ehlers MD, Rothstein JD, Huganir RL (1997) The development of excitatory synapses in cultured spinal neurons. J Neurosci 17:7339-7350.

Obst-Pernberg K, Redies C (1999) Cadherins and synaptic specificity. J Neurosci Res 58:130-138.

Okabe S, Kim HD, Miwa A, Kuriu T, Okado H (1999) Continual remodeling of postsynaptic density and its regulation by synaptic activity. Nat Neurosci 2:804-811.

Olney JW, Labruyere J, Collins JF, Curry K (1981) D-aminophosphonovalerate is 100-fold more powerful than D-alpha- aminoadipate in blocking N-methylaspartate neurotoxicity. Brain Res 221:207-210.

Palay SL (1956) J. Biophys. Biochem. Cytol. 2:193-202.

Parfitt KD, Madison DV (1993) Phorbol esters enhance synaptic transmission by a presynaptic, calcium- dependent mechanism in rat hippocampus. J Physiol 471:245-268.

Parnass Z, Tashiro A, Yuste R (2000) Analysis of spine morphological plasticity in developing hippocampal pyramidal neurons. Hippocampus 10:561-568.

Passafaro M, Sala C, Niethammer M, Sheng M (1999) Microtubule binding by CRIPT and its potential role in the synaptic clustering of PSD-95. Nat Neurosci 2:1063-1069.

Paulsen O, Sejnowski TJ (2000) Natural patterns of activity and long-term synaptic plasticity. Curr Opin Neurobiol 10:172-179.

Poirazi P, Mel BW (2001) Impact of active dendrites and structural plasticity on the memory capacity of neural tissue. Neuron 29:779-796.

Poisbeau P, Rene F, Egles C, Felix JM, Feltz P, Schlichter R (1996) Characterization of functional GABAergic synapses formed between rat hypothalamic neurons and pituitary intermediate lobe cells in coculture: Ca2+ dependence of spontaneous IPSCs. J Neurosci 16:4835-4845.

Poon CS, Shah JV (1998) Hebbian learning in parallel and modular memories. Biol Cybern 78:79-86.

Prange O, Murphy TH (1997) FM1-43 as an indicator for miniature synaptic activity at single synapses of cortical neurons. In: Soc Neurosci Abst, p 2272.

Prange O, Murphy TH (1998) Comparison of evoked and miniature release at single CNS synapses in culture. In: Soc Neurosci Abst, p 226.

Prange O, Murphy TH (1999) Analysis of multiquantal transmitter release from single cultured cortical neuron terminals. J Neurophysiol 81:1810-1817.

Ramakers GM, Pasinelli P, Hens JJ, Gispen WH, De Graan PN (1997) Protein kinase C in synaptic plasticity: changes in the in situ phosphorylation state of identified

pre- and postsynaptic substrates. Prog Neuropsychopharmacol Biol Psychiatry 21:455-486.

Rao A, Cha EM, Craig AM (2000) Mismatched appositions of presynaptic and postsynaptic components in isolated hippocampal neurons. J Neurosci 20:8344-8353.

Rao A, Craig AM (2000) Signaling between the actin cytoskeleton and the postsynaptic density of dendritic spines. Hippocampus 10:527-541.

Rao A, Kim E, Sheng M, Craig AM (1998) Heterogeneity in the molecular composition of excitatory postsynaptic sites during development of hippocampal neurons in culture. Journal of Neuroscience 18:1217-1229.

Rauschecker JP (1995) Developmental plasticity and memory. Behav Brain Res 66:7-12.

Raymon y Cajal S (1888) Rev. Trim. Histol. Norm. Patol. 1:1-10.

Redman S (1990) Quantal analysis of synaptic potentials in neurons of the central nervous system. Physiol Rev 70:165-198.

Redmond L, Ghosh A (2001) The role of Notch and Rho GTPase signaling in the control of dendritic development. Curr Opin Neurobiol 11:111-117.

Reid CA, Clements JD (1999) Postsynaptic expression of long-term potentiation in the rat dentate gyrus demonstrated by variance-mean analysis. J Physiol 518:121-130.

Roberts WM, Jacobs RA, Hudspeth AJ (1990) Colocalization of ion channels involved in frequency selectivity and synaptic transmission at presynaptic active zones of hair cells. J Neurosci 10:3664-3684.

Roman FS, Truchet B, Marchetti E, Chaillan FA, Soumireu-Mourat B (1999) Correlations between electrophysiological observations of synaptic plasticity modifications and behavioral performance in mammals. Prog Neurobiol 58:61-87.

Rosenmund C, Clements JD, Westbrook GL (1993) Nonuniform probability of glutamate release at a hippocampal synapse. Science 262:754-757.

Rosenmund C, Stevens CF (1996) Definition of the readily releasable pool of vesicles at hippocampal synapses. Neuron 16:1197-1207.

Rouze NC, Schwartz EA (1998) Continuous and transient vesicle cycling at a ribbon synapse. J Neurosci 18:8614-8624.

Rumpel S, Hatt H, Gottmann K (1998) Silent synapses in the developing rat visual cortex: evidence for postsynaptic expression of synaptic plasticity. J Neurosci 18:8863-8874.

Rusakov DA, Davies HA, Harrison E, Diana G, Richter-Levin G, Bliss TV, Stewart MG (1997) Ultrastructural synaptic correlates of spatial learning in rat hippocampus. Neuroscience 80:69-77.

Ryan TA, Reuter H, Smith SJ (1997) Optical detection of a quantal presynaptic membrane turnover. Nature 388:478-482.

Ryan TA, Reuter H, Wendland B, Schweizer FE, Tsien RW, Smith SJ (1993) The kinetics of synaptic vesicle recycling measured at single presynaptic boutons. Neuron 11:713-724.

Ryan TA, Smith SJ (1995) Vesicle pool mobilization during action potential firing at hippocampal synapses. Neuron 14:983-989.

Ryan TA, Ziv NE, Smith SJ (1996) Potentiation of evoked vesicle turnover at individually resolved synaptic boutons. Neuron 17:125-134.

Sabatini BL, Regehr WG (1999) Timing of synaptic transmission. Annu Rev Physiol 61:521-542.

Saito Y, Murakami F, Song WJ, Okawa K, Shimono K, Katsumaru H (1992) Developing corticorubral axons of the cat form synapses on filopodial dendritic protrusions. Neurosci Lett 147:81-84.

Sampo B, Tricaud N, Leveque C, Seagar M, Couraud F, Dargent B (2000) Direct interaction between synaptotagmin and the intracellular loop I-II of neuronal voltage-sensitive sodium channels. PNAS 97:3666-3671.

Sanes JN, Donoghue JP (2000) Plasticity and primary motor cortex. Annu Rev Neurosci 23:393-415.

Sanes JR, Lichtman JW (1999) Can molecules explain long-term potentiation? Nat Neurosci 2:597-604.

Scannevin RH, Huganir RL (2000) Postsynaptic organization and regulation of excitatory synapses. Nature Rev Neurosci 1:133-141.

Scanziani M, Gahwiler BH, Thompson SM (1995) Presynaptic inhibition of excitatory synaptic transmission by muscarinic and metabotropic glutamate receptor activation in the hippocampus: are Ca2+ channels involved? Neuropharmacology 34:1549-1557.

Scheiffele P, Fan J, Choih J, Fetter R, Serafini T (2000) Neuroligin expressed in nonneuronal cells triggers presynaptic development in contacting axons. Cell 101:657-669.

Schikorski T, Stevens CF (1997) Quantitative ultrastructural analysis of hippocampal excitatory synapses. J Neurosci 17:5858-5867.

Schikorski T, Stevens CF (2001) Morphological correlates of functionally defined synaptic vesicle populations. Nat Neurosci 4:391-395.

Schneggenburger R, Neher E (2000) Intracellular calcium dependence of transmitter release rates at a fast central synapse. Nature 406:889-893.

Schoppa NE, Westbrook GL (1997) Modulation of mEPSCs in olfactory bulb mitral cells by metabotropic glutamate receptors. J Neurophysiol 78:1468-1475.

Segal M (2001) Rapid plasticity of dendritic spine: hints to possible functions? Prog Neurobiol 63:61-70.

Segal M, Andersen P (2000) Dendritic spines shaped by synaptic activity. Curr Opin Neurobiol 10:582-586.

Sejnowski TJ (1999) The book of Hebb. Neuron 24:773-776.

Shepherd GM, Erulkar SD (1997) Centenary of the synapse: from Sherrington to the molecular biology of the synapse and beyond. Trends Neurosci 20:385-392.

Shepherd GM, Harris KM (1998) Three-dimensional structure and composition of CA3-->CA1 axons in rat hippocampal slices: implications for presynaptic connectivity and compartmentalization. J Neurosci 18:8300-8310.

Sherrington CS (1897) The Central Nervous System. In: A Textbook of Physiology (Foster M, ed), p 60. London: MacMillan.

Shi SH, Hayashi Y, Petralia RS, Zaman SH, Wenthold RJ, Svoboda K, Malinow R (1999) Rapid spine delivery and redistribution of AMPA receptors after synaptic NMDA receptor activation. Science 284:1811-1816.

Shulman RG (2001) Functional imaging studies: linking mind and basic neuroscience. Am J Psychiatry 158:11-20.

Skelton RW, Scarth AS, Wilkie DM, Miller JJ, Phillips AG (1987) Long-term increases in dentate granule cell responsivity accompany operant conditioning. J Neurosci 7:3081-3087.

Slepnev VI, De Camilli P (2000) Accessory factors in clathrin-dependent synaptic vesicle endocytosis. Nat Rev Neurosci 1:161-172.

Smart FM, Halpain S (2000) Regulation of dendritic spine stability. Hippocampus 10:542-554.

Smith CB, Betz WJ (1996) Simultaneous independent measurement of endocytosis and exocytosis. Nature 380:531-534.

Soderling TR, Derkach VA (2000) Postsynaptic protein phosphorylation and LTP. Trends Neurosci 23:75-80.

Sorra KE, Harris KM (2000) Overview on the structure, composition, function, development, and plasticity of hippocampal dendritic spines. Hippocampus 10:501-511.

Stevens CF (1998) A million dollar question: does LTP = memory? Neuron 20:1-2.

Stevens CF, Sullivan J (1998a) Synaptic plasticity. Curr Biol 8:R151-153.

Stevens CF, Sullivan JM (1998b) Regulation of the readily releasable vesicle pool by protein kinase C. Neuron 21:885-893.

Stevens CF, Tsujimoto T (1995) Estimates for the pool size of releasable quanta at a single central synapse and for the time required to refill the pool. Proc Natl Acad Sci U S A 92:846-849.

Stevens CF, Wang Y (1994) Changes in reliability of synaptic function as a mechanism for plasticity. Nature 371:704-707.

Stevens CF, Wang Y (1995) Facilitation and depression at single central synapses. Neuron 14:795-802.

Stevens CF, Wesseling JF (1999a) Augmentation is a potentiation of the exocytotic process. Neuron 22:139-146.

Stevens CF, Wesseling JF (1999b) Identification of a novel process limiting the rate of synaptic vesicle cycling at hippocampal synapses. Neuron 24:1017-1028.

Sudhof TC (2000) The synaptic vesicle cycle revisited. Neuron 28:317-320.

Sun J, Wu L (2001) Fast kinetics of exocytosis revealed by simultaneous measurements of presynaptic capacitance and postsynaptic currents at a central synapse. Neuron 30:171-182.

Svoboda K, Helmchen F, Denk W, Tank DW (1999) Spread of dendritic excitation in layer 2/3 pyramidal neurons in rat barrel cortex in vivo. Nat Neurosci 2:65-73.

Tang Y, Zucker RS (1997) Mitochondrial involvement in post-tetanic potentiation of synaptic transmission. Neuron 18:483-491.

Tang YP, Shimizu E, Dube GR, Rampon C, Kerchner GA, Zhuo M, Liu G, Tsien JZ (1999) Genetic enhancement of learning and memory in mice. Nature 401:63-69.

Thompson SM (2000) Synaptic plasticity: Building memories to last. Curr Biol 10:R218-221.

Thomson AM (1986) A magnesium-sensitive post-synaptic potential in rat cerebral cortex resembles neuronal responses to N-methylaspartate. J Physiol 370:531-549.

Tong G, Jahr CE (1994) Multivesicular release from excitatory synapses of cultured hippocampal neurons. Neuron 12:51-59.

Tong G, Malenka RC, Nicoll RA (1996) Long-term potentiation in cultures of single hippocampal granule cells: a presynaptic form of plasticity. Neuron 16:1147-1157.

Toni N, Buchs PA, Nikonenko I, Bron CR, Muller D (1999) LTP promotes formation of multiple spine synapses between a single axon terminal and a dendrite. Nature 402:421-425.

Topinka JR, Bredt DS (1998) N-terminal palmitoylation of PSD-95 regulates association with cell membranes and interaction with K+ channel Kv1.4. Neuron 20:125-134.

Triller A, Korn H (1982) Transmission at a central inhibitory synapse. III. Ultrastructure of physiologically identified and stained terminals. J Neurophysiol 48:708-736.

Trudeau LE, Doyle RT, Emery DG, Haydon PG (1996) Calcium-independent activation of the secretory apparatus by ruthenium red in hippocampal neurons: a new tool to assess modulation of presynaptic function. J Neurosci 16:46-54.

Trussell LO, Zhang S, Raman IM (1993) Desensitization of AMPA receptors upon multiquantal neurotransmitter release. Neuron 10:1185-1196.

Tsien JZ (2000) Linking Hebb's coincidence-detection to memory formation. Curr Opin Neurobiol 10:266-273.

Tsodyks M, Pawelzik K, Markram H (1998) Neural networks with dynamic synapses. Neural Comput 10:821-835.

Umemiya M, Senda M, Murphy TH (1999) Behaviour of NMDA and AMPA receptor-mediated miniature EPSCs at rat cortical neuron synapses identified by calcium imaging. J Physiol 521 Pt 1:113-122.

Vautrin J, Barker JL (1995) How can exocytosis account for the actual properties of miniature synaptic signals? Synapse 19:144-149.

Verhage M, Maia AS, Plomp JJ, Brussaard AB, Heeroma JH, Vermeer H, Toonen RF, Hammer RE, van den Berg TK, Missler M, Geuze HJ, Sudhof TC (2000) Synaptic assembly of the brain in the absence of neurotransmitter secretion. Science 287:864-869.

Villacres EC, Wong ST, Chavkin C, Storm DR (1998) Type I adenylyl cyclase mutant mice have impaired mossy fiber long-term potentiation. J Neurosci 18:3186-3194.

Vincent P, Marty A (1996) Fluctuations of inhibitory postsynaptic currents in Purkinje cells from rat cerebellar slices. J Physiol 494:183-199.

Walikonis R, Oguni A, Khorosheva E, Jeng C, Asuncion F, Kennedy M (2001) Densin-180 forms a ternary complex with the (alpha)-subunit of Ca2+/calmodulin-dependent protein kinase II and (alpha)-actinin. J Neurosci 21:423-433.

Walikonis RS, Jensen ON, Mann M, Provance DW, Jr., Mercer JA, Kennedy MB (2000) Identification of proteins in the postsynaptic density fraction by mass spectrometry. J Neurosci 20:4069-4080.

Wall MJ, Usowicz MM (1998) Development of the quantal properties of evoked and spontaneous synaptic currents at a brain synapse. Nat Neurosci 1:675-682.

Walton M, Henderson C, Mason-Parker S, Lawlor P, Abraham WC, Bilkey D, Dragunow M (1999) Immediate early gene transcription and synaptic modulation. J Neurosci Res 58:96-106.

Wang S, Prange O, Murphy TH (1999) Amplification of calcium signals at dendritic spines provides a method for CNS quantal analysis. Can J Physiol Pharmacol 77:651-659.

Wang SS, Denk W, Hausser M (2000) Coincidence detection in single dendritic spines mediated by calcium release. Nat Neurosci 3:1266-1273.

Wickelgren I (2001) NEUROBIOLOGY: Working Memory Helps the Mind Focus. Science 291:1684-1685.

Wigstrom H, Gustafsson B (1986) Postsynaptic control of hippocampal long-term potentiation. J Physiol 81:228-236.

Wong WT, Wong RO (2000) Rapid dendritic movements during synapse formation and rearrangement. Curr Opin Neurobiol 10:118-124.

Wong WT, Wong RO (2001) Changing specificity of neurotransmitter regulation of rapid dendritic remodeling during synaptogenesis. Nat Neurosci 4:351-352.

Xia Z, Zhou Q, Lin J, Liu Y (2001) Stable SNARE complex prior to evoked synaptic vesicle fusion revealed by fluorescence resonance energy transfer. J Biol Chem 276:1766-1771.

Xu L, Anwyl R, Rowan MJ (1998) Spatial exploration induces a persistent reversal of long-term potentiation in rat hippocampus. Nature 394:891-894.

Yang SN, Tang YG, Zucker RS (1999) Selective induction of LTP and LTD by postsynaptic [Ca2+]i elevation. J Neurophysiol 81:781-787.

Yuste R, Majewska A, Cash SS, Denk W (1999) Mechanisms of calcium influx into hippocampal spines: heterogeneity among spines, coincidence detection by NMDA receptors, and optical quantal analysis. J Neurosci 19:1976-1987.

Yuste R, Sur M (1999) Development and plasticity of the cerebral cortex: from molecules to maps. J Neurobiol 41:1-6.

Zhang S, Ehlers MD, Bernhardt JP, Su CT, Huganir RL (1998) Calmodulin mediates calcium-dependent inactivation of N-methyl-D- aspartate receptors. Neuron 21:443-453.

Zhang W, Benson DL (2000) Development and molecular organization of dendritic spines and their synapses. Hippocampus 10:512-526.

Zhou Q, Xiao M, Nicoll RA (2001) Contribution of cytoskeleton to the internalization of AMPA receptors. Proc Natl Acad Sci U S A 98:1261-1266.

Zhu JJ, Esteban JA, Hayashi Y, Malinow R (2000) Postnatal synaptic potentiation: delivery of GluR4-containing AMPA receptors by spontaneous activity. Nat Neurosci 3:1098-1106.

Ziv NE, Smith SJ (1996) Evidence for a role of dendritic filopodia in synaptogenesis and spine formation. Neuron 17:91-102.

Zucker RS (1996) Exocytosis: a molecular and physiological perspective. Neuron 17:1049-1055.

Zucker RS (1999) Calcium- and activity-dependent synaptic plasticity. Curr Opin Neurobiol 9:305-313.